

CHAPTER 9

Methods for Numerical Conformal Mapping

Dedicated to the memory of Dieter Gaier

Rudolf Wegmann

Max-Planck-Institut für Astrophysik, D-85748 Garching, Germany
E-mail: ruw@mpa-garching.mpg.de

Contents

1. Introduction	353
2. Auxiliary material	354
2.1. Spaces	354
2.2. Conformal mapping	355
2.3. Corners	358
2.4. Crowding	359
2.5. Function theoretic boundary value problems	362
2.6. The operator \mathbf{R}	367
3. Mapping from the region to the disk	369
3.1. Potential theoretic methods	369
3.2. Extremum principles	377
3.3. Osculation methods	385
3.4. Accuracy	386
4. Mapping from the disk to the region	387
4.1. Mapping to nearby regions	388
4.2. Projection	389
4.3. Newton methods	401
4.4. Interpolation	408
4.5. Accuracy	415
5. Mapping from an ellipse to the region	416
6. Waves	418
7. Mapping from a quadrilateral to a rectangle	419
8. Mapping of exterior regions	421
8.1. Mapping from the exterior region to the exterior of the disk	421
8.2. Mapping from the exterior of the disk to the exterior region	424
9. Mapping to Riemann surfaces	432

HANDBOOK OF COMPLEX ANALYSIS: GEOMETRIC FUNCTION THEORY,
VOLUME 2

Edited by R. Kühnau

© 2005 Elsevier B.V. All rights reserved

10. Mapping of a doubly-connected region to an annulus	437
10.1. Potential theoretic methods	437
10.2. Extremum principles	439
11. Mapping from an annulus to a doubly-connected region	440
11.1. Boundary value problems	441
11.2. Projection	443
11.3. The Newton method	446
11.4. Other methods	450
12. Multiply-connected regions	450
12.1. Potential theoretic methods	452
12.2. Osculation methods	453
12.3. Projection	455
12.4. Riemann–Hilbert problems	458
12.5. The Newton method	461
12.6. Other methods	464
References	467

1. Introduction

Riemann formulated in his famous thesis [235] a remarkable mapping theorem which in modern language reads:

THEOREM 1. *Each simply connected region G in the extended complex plane $\overline{\mathbb{C}}$ with at least two boundary points can be mapped conformally to the unit disk D .*

Riemann left us with the problem of how to determine for a given region G such a conformal mapping from G to D , or the inverse mapping from D to G . There are many well-studied classes of analytic functions: polynomials, rational functions, the elementary transcendental functions, such as the exponential, the logarithm and the trigonometric functions, and the higher-transcendental functions, such as elliptic integrals and hypergeometric functions. One can find the known mapping properties of these functions collected in dictionaries, like those of Kober [137] or von Koppenfels and Stallmann [145]. Nehari gives an extensive collection of mapping properties of special functions in Chapter VI of his book [189]. The book of Lavrik and Savenkov [157] contains a catalog of 115 conformal mappings, accompanied by diagrams. Ivanov and Trubetskov [128] offer computer-aided visualization of numerous mapping functions.

When suitable explicit functions cannot be found the only means to determine a conformal mapping is by numerical calculation. The main textbook for numerical conformal mapping was for a long time Gaier's book [65], which is still an excellent source. One must not be discouraged by Gaier's reports on numerical experiments, where computing times of several hours are reported. Since 1964, computers have been improved, the Fast Fourier Transform has been (re)invented by Cooley and Tukey [30] and fast mapping methods have been developed such as, e.g., Wegmann's method [283]. Thus, a mapping problem can now be solved numerically in seconds – even on a small computer. The statement of Symm [253]: “When a conformal mapping, purporting to simplify solution of some problem of applied mathematics, can be obtained only by numerical means, it is often considered to have outlived its usefulness” is no longer true.

The third volume of Henrici's monumental work on *Applied and Computational Complex Analysis* [107] is now one of the main sources for theoretical and computational aspects of numerical conformal mapping.

In 1986 Trefethen edited a collection of articles about numerical conformal mapping [265]. Recent books about computational conformal mapping are those of Kythe [152] and of Schinzinger and Laura [240]. Articles by Anderson et al. [4], Opfer [199], Gutknecht [95] and DeLillo [34] give overviews of available methods. Much work on conformal mapping has been done in the former Soviet Union. Some of it is summarized in the book of Fil'čakov [57].

Conformal mapping is frequently applied for the solution of problems of fluid mechanics (see, e.g., the classic book of Lamb [153]). But it is also a useful tool in grid generation for numerical calculations (see, e.g., Thompson et al. [261,262]).

This review covers mainly the recent literature. For some of the older literature we refer to Gaier's book [65]. Interest in numerical conformal mapping began again to grow in the late seventies and culminated in 1986 in Trefethen's collection [265] of 15 articles. In the

same year Henrici's book [107] appeared. Numerical conformal mapping is still an active field.

A review article about numerical conformal mapping must discuss many (if not all) available methods with the unavoidable consequence that the bewildered reader at the end will not know what to do when he really feels the need to map a region of his choice to some standard region. Authors give, in general, an evaluation biased in favor of their own methods. Therefore, it is important to report also some experimental experience, in particular, about test calculations for the same problem with different methods.

2. Auxiliary material

2.1. Spaces

Functional analytic methods are very powerful for proving convergence of some iterative methods. Function spaces are also convenient for describing certain properties of functions, such as smoothness of various degrees, and properties of some associated functions, such as the harmonic conjugate.

We consider only spaces of (complex or real) 2π -periodic functions. The Lebesgue space L^2 consists of all functions f which are square integrable over the interval $[0, 2\pi]$; it becomes a Hilbert space with norm

$$\|f\|_2 := \left(\frac{1}{2\pi} \int_0^{2\pi} |f(t)|^2 dt \right)^{1/2}. \quad (1)$$

Each function $f \in L^2$ can be represented by a Fourier series

$$f(t) \sim \sum_{l=-\infty}^{\infty} A_l e^{ilt} \quad (2)$$

(the sign \sim denotes that the series converges in the L^2 norm but in general not pointwise). The norm (1) can be expressed in terms of the Fourier coefficients by

$$\|f\|_2 = \left(\sum_{l=-\infty}^{\infty} |A_l|^2 \right)^{1/2}. \quad (3)$$

Related to L^2 there is the *Sobolev space* W (to be precise, $W^{1,2}$) which consists of absolutely continuous functions with derivative f' in L^2 . It becomes a Banach space when provided with the norm

$$\|f\|_W := \|f\|_2 + \|f'\|_2. \quad (4)$$

The supremum norm

$$\|f\|_{\infty} := \sup_t |f(t)| \quad (5)$$

is defined for bounded functions. The space $C^{(n)}$ of n times differentiable functions with continuous n th derivative $f^{(n)}$ is a Banach space when normed by

$$\|f\|_{C^{(n)}} = \|f\|_\infty + \|f^{(n)}\|_\infty. \quad (6)$$

For α in the interval $0 < \alpha \leq 1$, the *Hölder space* C^α consists of all functions f which are uniformly Hölder continuous with exponent α . Then the *Hölder coefficient*

$$[f]_\alpha := \sup_{s \neq t} \frac{|f(s) - f(t)|}{|s - t|^\alpha} \quad (7)$$

is finite. With the norm

$$\|f\|_\alpha := \|f\|_\infty + [f]_\alpha, \quad (8)$$

C^α is a Banach space. When f is Hölder continuous with exponent $\alpha = 1$, it is also called *Lipschitz continuous*.

More generally, for an integer $n \geq 0$ the Hölder space $C^{n,\alpha}$ consists of all functions f which are n times differentiable with derivative $f^{(n)} \in C^\alpha$. With the norm

$$\|f\|_{n,\alpha} := \|f\|_\infty + [f^{(n)}]_\alpha, \quad (9)$$

$C^{n,\alpha}$ is a Banach space.

2.2. Conformal mapping

The typical domain G dealt by numerical conformal mapping is bounded by finitely many smooth arcs that may form corners. Parts of the boundary may be run through twice; different parts of the boundary may touch each other.

This is described by the following situation. Let G be a bounded simply connected region. Without loss of generality we assume that G contains the origin 0. The boundary Γ of G is parameterized by a 2π -periodic complex function $\eta(s)$ such that $\eta(s)$ surrounds G once in the counterclockwise direction when s increases from 0 to 2π . The function $\eta(s)$ is differentiable for all s with the exception of finitely many values s_j in the interval $[0, 2\pi]$, and the derivative $\dot{\eta}(s)$ does not vanish. (We denote by a dot always the derivative with respect to the parameter s . A prime denotes derivatives with respect to other variables t, z, \dots) The function η is not assumed to be one-to-one. So it can also describe cuts in the region such as shown in the example of Figure 1.

One considers two types of conformal mappings: The mapping F from a region G to a canonical region, which, in general, is the unit disk D , and the inverse mapping Φ from the disk to the region. We will consistently use F and Φ for these two types of mappings. The geometry is illustrated in Figure 2.

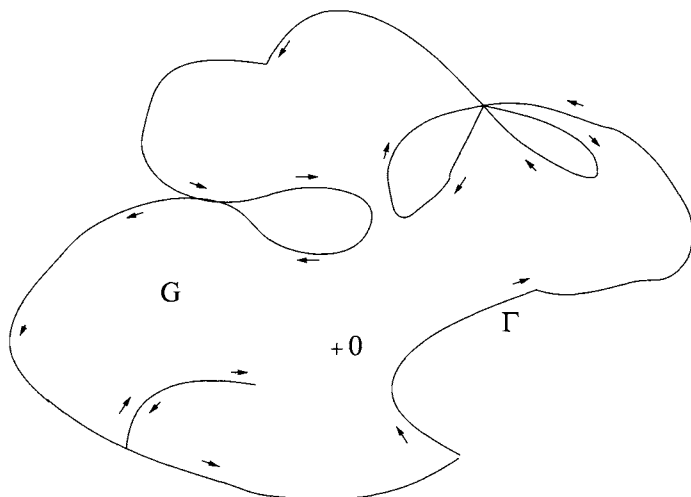


Fig. 1. A typical region G for conformal mapping. The arrows indicate the orientation of the boundary curve.

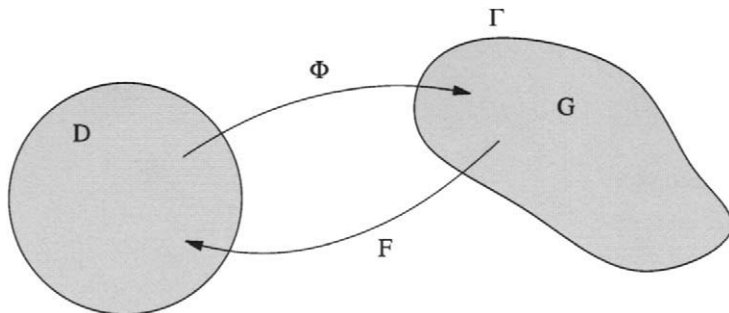


Fig. 2. The conformal mapping F from the region G to the disk and its inverse Φ .

The mapping $\Phi : D \rightarrow G$ is unique only up to conformal automorphisms of D . These are of the form

$$\Psi(z) = e^{i\theta} \frac{z - z_0}{1 - z\bar{z}_0} \quad (10)$$

with $\theta \in \mathbb{R}$ and $z_0 \in D$. These parameters are fixed when Φ is constrained by the conditions

$$\Phi(0) = 0, \quad \Phi'(0) > 0. \quad (11)$$

Instead of the second condition (11) one can also prescribe $\Phi(1) = w_0$ for some w_0 on the boundary $\Gamma := \partial G$. One can also replace both conditions (11) by the prescription of three boundary values $\Phi(e^{it_j}) = w_j$ for $0 \leq t_1 < t_2 < t_3 < 2\pi$ and counterclockwise ordered points w_1, w_2, w_3 on Γ .

It is very helpful to know in advance something about the mapping function. To this aim we collect here some properties of the mapping which can be inferred from the properties of the boundary Γ . For details we refer to the book of Pommerenke [224].

A homeomorphic image of the unit circle is called a *Jordan curve*. A *Jordan region* is the interior of a Jordan curve.

THEOREM 2 (Osgood, Carathéodory; see also [224, p. 18]). *The conformal mapping $\Phi : D \rightarrow G$ can be extended to a homeomorphism $\Phi : \bar{D} \rightarrow \bar{G}$ of the closed disk to the closure \bar{G} of G if and only if G is a Jordan region.*

It follows, in particular, that the extended function Φ restricted to the boundary is a homeomorphism $\Phi : \partial D \rightarrow \partial G$ of the boundaries. Theorem 2 implies that for Jordan regions the inverse mapping $F : G \rightarrow D$ can also be extended to a homeomorphism $F : \bar{G} \rightarrow \bar{D}$.

Numerical conformal mappers have to deal with regions whose boundaries consist of one (or several) closed curves, i.e., of the continuous (not necessarily one-to-one) images of circles. Therefore, the following result is very useful.

THEOREM 3 [224, p. 20]. *The conformal mapping $\Phi : D \rightarrow G$ can be extended to a continuous mapping $\Phi : \bar{D} \rightarrow \bar{G}$ if and only if the boundary of G consists of a closed curve.*

Since the values of Φ in D can be constructed from the values on ∂D by Cauchy's formula

$$\Phi(z) = \frac{1}{2\pi i} \int_{\partial D} \frac{\Phi(\zeta)}{\zeta - z} d\zeta \quad \text{for } z \in D, \quad (12)$$

it is sufficient to determine only the boundary values of Φ . This reduces the two-dimensional problem to a one-dimensional one.

The next theorem guarantees that under certain circumstances the mapping function is just as smooth as the boundary curve.

THEOREM 4 (Warschawski–Kellogg [273]). *When the boundary Γ of the simply connected region G is parameterized by a function $\eta \in C^{k,\alpha}$ for some $k \geq 1$ and $0 < \alpha < 1$ then the boundary values $\Phi(e^{it})$ of the conformal mapping Φ of the unit disk D to G as a function of t are also in $C^{k,\alpha}$.*

Theorem 4 does not hold for $\alpha = 1$. It does not hold for $k = 0$ either, as the mappings to regions with corners show (see Section 2.3). When the boundary curve Γ is rectifiable and satisfies the condition that for any two points $z_1, z_2 \in \Gamma$, the length Δs of the shorter arc of Γ between z_1, z_2 satisfies $\Delta s \leq C|z_1 - z_2|$ with a constant C independent of z_1, z_2 , then the conformal mapping $F : G \rightarrow D$ is Hölder continuous with a certain exponent α which depends on C (Warschawski [278]; see also Lesley [162]).

One can assign to each complex 2π -periodic function η which parameterizes the boundary of a region G , the boundary values $\Phi(e^{is})$ of the conformal mapping $\Phi : D \rightarrow G$. The

continuity of this mapping $\eta \rightarrow \Phi(e^{i\eta})$ in certain Hölder and Sobolev spaces is investigated by Warschawski [274] and Lanza de Cristoforis [155].

A theorem of Coifman and Meyer (see Semmes [242]) says that the conformal mapping function $F : G \rightarrow U$ from the region to the upper half-plane U depends (in suitable topologies) in a real-analytic way on the boundary curve of G .

2.3. Corners

Regions with corners are beyond the range of many mapping methods. Corners deserve special attention since in any case they deteriorate the accuracy of the result. Therefore, it is often advisable to give the corners a special treatment using a priori information about the behavior of the mapping function near corners.

It is generally assumed that a corner is formed by analytic arcs. Recall that an *analytic arc* is the image of an interval $[a, b]$ by a function f which is analytic in a neighborhood of $[a, b]$. The function $f(z) = z^\alpha$, $0 < \alpha \leq 2$, maps the upper half-plane U to a wedge region with opening angle $\alpha\pi$. This mapping is representative for mappings to regions with corners, since the following theorem holds. We consider mappings to U and assume that $0 \in \Gamma$, and Γ has a corner at 0.

THEOREM 5 (Lichtenstein, Warschawski; see Henrici [107]). *Assume that the boundary Γ of G has a corner of opening angle $\alpha\pi$ at $z = 0$ formed by two analytic arcs. If F maps G conformally to the upper half-plane U so that $F(0) = 0$, then the limit*

$$c := \lim_{z \rightarrow 0} (z^{-1/\alpha} F(z)) \quad (13)$$

exists and is not equal to 0. For $n = 1, 2, \dots$,

$$\lim_{z \rightarrow 0} (z^{n-1/\alpha} F^{(n)}(z)) = c \frac{1}{\alpha} \left(\frac{1}{\alpha} - 1 \right) \cdots \left(\frac{1}{\alpha} - n + 1 \right) \quad (14)$$

holds for unrestricted approach $z \rightarrow 0$ in G .

Therefore, at a corner the conformal mapping $F : G \rightarrow U$ behaves locally like the function $cz^{1/\alpha}$ which straightens the corner at 0. The condition that the corner is formed by analytic arcs has been somewhat relaxed by Gaier [74].

Let G and F be defined as in Theorem 5. Since the corner at 0 is formed by two analytic arcs, F can be extended by reflection to a function defined on a Riemann surface covering a neighborhood of the origin. Lehman [160] has shown that for irrational α there is an asymptotic expansion of F in the neighborhood of the origin, valid in any sector, in integral powers of z and $z^{1/\alpha}$. If α is rational there is an asymptotic expansion of F in integral powers of z , $z^{1/\alpha}$ and $\log z$. In both cases the term $z^{1/\alpha}$ occurs with nonzero coefficient. The inverse mapping $\Phi := F^{-1}$ from the upper half-plane to the region G admits near the origin an asymptotic expansion in integral powers of z , z^α and $\log z$ for rational α ,

and in integral powers of z and z^α for irrational α . In both cases the term z^α has nonzero coefficient.

The accuracy of the numerically calculated mapping depends on the smoothness of the boundary. For general regions with corners it is sometimes advisable to remove the corners by some auxiliary mappings of the type $f(z) = (z - z_0)^\alpha$ (see, e.g., Carey and Muleshkov [25]). Landweber and Miloh [154] consider a transformation which removes all corners of a simple closed curve at the same time.

Several of the methods discussed in the next sections work only for sufficiently smooth boundaries. Some methods can be adapted to treat corners. For polygons a Schwarz–Christoffel mapping is advisable (see Trefethen [264], Henrici [107], Driscoll and Trefethen [47]).

2.4. Crowding

The behavior of a conformal mapping depends on the local property of smoothness – and on the global property of shape.

On small scales a conformal mapping maps disks to disks, but on large scales a disk can be mapped to any simply-connected bounded region, however elongated and distorted it may be. But it takes some effort for a mapping which has such a strong tendency to map disks to disks, to map a disk to an elongated region. The mapping suffers, lying on a Procrustean bed, and the numerical conformal mapper must share the pains.

It was first noted by Grassman [86] that the numerical calculation of the mapping from the disk to an elongated region becomes laborious due to an effect which is now called *crowding*. The images of equidistributed points on the unit circle become very unevenly distributed on the boundary of the region.

This is nicely illustrated by the inverse hyperbolic tangent function

$$\Phi(z) = \operatorname{Arctanh}(rz) \quad (15)$$

which, for $0 < r < 1$, maps the unit disk to an elongated region G with axes $a := 2\Phi(1) = 2\operatorname{Arctanh}r$, $b := 2|\Phi(i)| = 2\arctan r$ (see DeLillo [37]). The aspect ratio of G is

$$\tau := \frac{b}{a} = \frac{\arctan r}{\operatorname{Arctanh} r}. \quad (16)$$

The supremum norm of the derivative

$$\|\Phi'\|_D = \sup_{|z|<1} |\Phi'(z)| \quad (17)$$

measures the distortion of the mapping. The distortion $|\Phi'(z)|$ is maximal on the boundary.

For the inverse hyperbolic tangent function (15) the distortion can be calculated and expressed in terms of the aspect ratio

$$\|\Phi'\|_D = |\Phi'(1)| = \frac{r}{1-r^2} \approx \frac{b}{2\pi} \exp\left(\frac{\pi}{2\tau}\right). \quad (18)$$

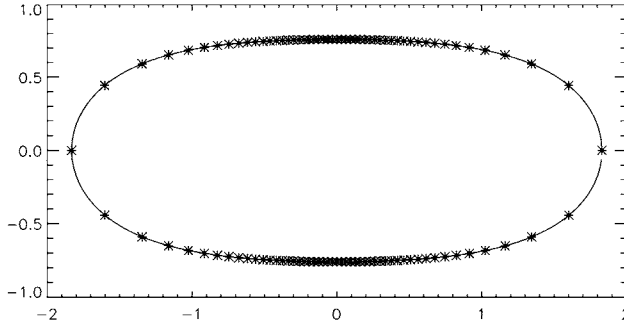


Fig. 3. The images (stars) of 100 equidistributed points on the unit circle mapped by the inverse hyperbolic tangent (15) with parameter $r = 0.95$.

The sign \approx in this section means that the ratio of the left-hand and right-hand sides tends to 1 as $\tau \rightarrow 0$. Equation (18) means that the distortion increases exponentially when the image region becomes more and more elongated. Figure 3 shows the images of 100 equidistributed points on the unit circle for $r = 0.95$. These points assemble in the flat part of the boundary curve while the ends are only poorly covered by the image points.

A sort of crowding was already detected by Gaier [66] in the mapping to a rectangle. When the unit disk is mapped to a rectangle with sides $a > b$ in such a way that the corners correspond to the points $\pm \exp(\pm i\theta)$ then (see DeLillo [37])

$$\theta \approx 4 \exp\left(-\frac{\pi}{2\tau}\right) \quad \text{with } \tau = \frac{b}{a}. \quad (19)$$

This means that the preimages of the small sides of the rectangle become exponentially small when the aspect ratio τ of the rectangle tends to 0. One might suspect that this behavior is caused by the corners of the image region where the derivative Φ' becomes unbounded. Crowding occurs however also for regions with analytic boundaries, such as ellipses. Numerical experiments indicate that it depends only on the aspect ratio τ and increases exponentially with $1/\tau$.

The example of the inverse hyperbolic tangent function is typical for the distortion of conformal maps of the disk to elongated regions. Wegmann [289,290] proved the following result.

THEOREM 6. *When the region G can be enclosed in a rectangle with sides a and b , $b \leq a$, such that G touches both small sides (see Figure 4) then the conformal mapping $\Phi : D \rightarrow G$ satisfies*

$$\|\Phi'\|_D \geq b\psi(b/a) \quad (20)$$

with a function $\psi(\tau)$ which behaves for small τ like

$$\psi(\tau) \approx \frac{1}{2\pi\sqrt{e}} \exp\left(\frac{\pi}{2\tau}\right). \quad (21)$$

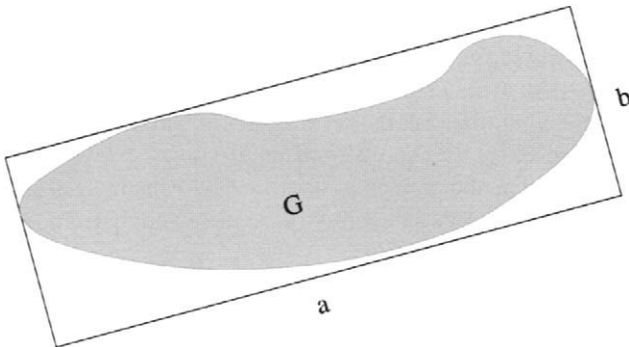


Fig. 4. The aspect ratio $b:a$ of the region G for Theorem 6.

The constant in (21) is best possible. Equality in (20) for $\tau \rightarrow 0$ is asymptotically attained by sportgrounds bounded by two long straight lines connected by two nearly circular arcs.

To give an impression of how crowding disturbs conformal mapping procedures, consider a region G of breadth $b = 1$ and length $a = 10$. Let $\zeta_j := \exp(2\pi ji/N)$ be N equidistributed points on the unit circle. The maximum distance of adjacent image points $\Phi(\zeta_j)$ by a conformal map is then about $2\pi \|\Phi'\|_D/N \geq 4 \times 10^6/N$. For a good resolution of the boundary of G one needs therefore a grid with several millions of points. The problems connected with the mapping of the disk to an ellipse with axis ratio 1 : 5 are nicely illustrated in Figure 7.5 and Table 7.4 of Gutknecht's paper [94].

Crowding is cumbersome for all methods which work with grid points. On the other hand, methods which approximate the mapping functions by polynomials also face severe problems when the target region is elongated. Szegö [257] proved the following sharp estimate:

THEOREM 7. *If P is a polynomial of degree n such that $P(0)$ is real and $|\operatorname{Re} P(z)| \leq 1$ for $|z| \leq 1$, then the imaginary part is estimated by*

$$|\operatorname{Im} P(z)| \leq \frac{2}{n+1} \sum_{k=1}^{[(n+1)/2]} \cot\left(\frac{(2k-1)\pi}{2n+2}\right). \quad (22)$$

The right-hand side of (22) is asymptotically equal to $(2/\pi) \ln n$ for $n \rightarrow \infty$. This means that the aspect ratio of the image $P(D)$ of the unit disk by a polynomial of degree n is asymptotically

$$\tau \geq \frac{\pi}{2 \ln n}. \quad (23)$$

It follows that, for the mapping of the disk to a region of aspect ratio 1 : 10 by a polynomial, the degree must be of several millions.

In any case, the number of grid points and the degree of the approximating polynomials increase both like $\exp(\pi/2\tau)$ as the aspect ratio, τ , tends to zero.

One can to some extent avoid or reduce the adverse effects of crowding by choosing as the fundamental domain not the disk but an ellipse with similar aspect ratio as the target region (see DeLillo and Elcrat [39] and Wegmann [291]).

Domain decomposition methods, such as described by Papamichael and Stylianopoulos [214], cut the region G into pieces and approximate the mapping from G to a rectangle by means of the mappings of the subregions.

DeLillo [35] used an inequality of Rengel to relate the crowding for elongated regions to the crowding (19) for rectangles. DeLillo and Pfaltzgraff [43] gave estimates for crowding in terms of harmonic measure and extremal distance. These estimates also show the exponential increase. They are more complicated than those of Theorem 6, but are more generally applicable.

DeLillo [37] has shown how crowding affects the accuracy of numerical computations. Crowding also limits the practical usefulness of conformal maps. This was demonstrated by DeLillo [36] for the Laplace equation.

Crowding has also been observed for regions with elongated sections (“fingers”). For “pinched” regions, such as the interior of an inverted ellipse, ill conditioning occurs of a less severe, algebraic nature (DeLillo [37]).

2.5. Function theoretic boundary value problems

Riemann considered in his thesis [235] conformal mapping as a special case of a more general class of boundary value problems for analytic functions, which are now called nonlinear *Riemann–Hilbert* (RH) problems (see Wegert [281]). One of the most effective strategies for dealing with the conformal mapping problem solves the nonlinear RH problem by a Newton iteration using in each iterative step a linear RH problem.

We consider here mainly boundary value problems for analytic functions in the unit disk D or in the exterior of the disk $D^- := \{z: |z| > 1\}$. By saying that a function is analytic in D^- we tacitly assume that it is also analytic at ∞ .

Let us start with the simplest and most basic problem.

For a given real Hölder continuous 2π -periodic function ψ , a function Ψ is to be determined as analytic in D , continuous in \bar{D} and satisfying on the boundary,

$$\operatorname{Re} \Psi(e^{it}) = \psi(t). \quad (24)$$

It is well known that this problem has a solution which is unique up to an imaginary constant. The imaginary part of Ψ can be constructed by means of the operator \mathbf{K} of *conjugation*, which can be defined in several equivalent ways. Usually it is defined as a singular integral operator

$$\mathbf{K}\psi(s) := \frac{1}{2\pi} \int_0^{2\pi} \psi(t) \cot \frac{s-t}{2} dt, \quad (25)$$

where the integral is understood as a Cauchy principal value integral. The operator \mathbf{K} is sometimes also called *Hilbert transform* (see, e.g., Henrici [107, p. 103]).

For numerical calculations the representation in terms of Fourier series is most convenient, since it can be evaluated numerically in a very efficient way using Fast Fourier Transforms (FFT).

When the right-hand side of (24) is represented by a (real or complex) Fourier series

$$\psi(t) = \sum_{l=-\infty}^{\infty} A_l e^{ilt} = a_0 + \sum_{l=1}^{\infty} (a_l \cos lt + b_l \sin lt) \quad (26)$$

then the conjugate function $\mathbf{K}\psi$ has the (real or complex) Fourier series representation

$$\mathbf{K}\psi(s) = \sum_{l=1}^{\infty} (-iA_l e^{ils} + iA_{-l} e^{-ils}) = \sum_{l=1}^{\infty} (-b_l \cos ls + a_l \sin ls). \quad (27)$$

This means that conjugation is done in the complex Fourier series simply by multiplication of the complex Fourier coefficients by $\pm i$, and in the real trigonometric series by interchange of the coefficients and multiplication by ± 1 .

The operator \mathbf{K} of conjugation maps each of the spaces L^2 , W , $C^{n,\alpha}$, $0 < \alpha < 1$, into itself and is a bounded operator in each of these spaces.

A theorem of Plessner says something about pointwise convergence: When the series (26) converges everywhere on a measurable subset E of $[0, 2\pi]$ then the series (27) converges almost everywhere on E .

Jumps in ψ generate logarithmic singularities in $\mathbf{K}\psi$. To take care of these explicitly, sometimes the representation as a Stieltjes integral

$$\mathbf{K}\psi(s) := \frac{1}{\pi} \int_0^{2\pi} \log \left| \sin \frac{s-t}{2} \right| d\psi(t) \quad (28)$$

is used which is obtained by integrating (25) by parts (see DeLillo [34]).

The property of conjugate functions most important for what follows is contained in the following theorem.

THEOREM 8. (a) *For each function $\psi \in W$, there is a unique function Ψ , which is analytic in D , continuous in \bar{D} and satisfies (24) and $\operatorname{Im} \Psi(0) = 0$. This function has the boundary values*

$$\Psi(e^{it}) = (\mathbf{I} + i\mathbf{K})\psi(t) \quad (29)$$

with the identity operator \mathbf{I} .

(b) *There is also a unique function Ψ , which is analytic in the exterior D^- of the unit disk (including ∞), and continuous in $|z| \geq 1$ and satisfies (24) and $\operatorname{Im} \Psi(\infty) = 0$. This function has the boundary values*

$$\Psi(e^{it}) = (\mathbf{I} - i\mathbf{K})\psi(t). \quad (30)$$

This means that the operator \mathbf{K} constructs from the boundary values of the real part of an analytic function Ψ in D (or D^-) the boundary values of the imaginary part up to a constant.

For numerical calculations ψ is represented on a grid of $N = 2n$ equidistant points $t_j = (j - 1)2\pi/N$ by the interpolating trigonometric polynomial of degree n

$$\psi(t_j) = \sum_{l=-n+1}^n \tilde{A}_l e^{ilt_j} = \sum_{l=0}^n \tilde{a}_l \cos lt_j + \sum_{l=1}^{n-1} \tilde{b}_l \sin lt_j \quad (31)$$

for $j = 1, \dots, N$. The conjugate function $\mathbf{K}_N \psi$ has the representation by a (real or complex) Fourier polynomial

$$\mathbf{K}_N \psi(s) = \sum_{l=1}^{n-1} (-i\tilde{A}_l e^{ils} + i\tilde{A}_{-l} e^{-ils}) = \sum_{l=1}^{n-1} (-\tilde{b}_l \cos ls + \tilde{a}_l \sin ls). \quad (32)$$

Conjugation is thus reduced to forward and inverse Fourier transform. This can be evaluated very fast by FFT (Cooley and Tukey [30]). The representation (32) is equivalent to Wittich's method which evaluates discrete conjugation by multiplication by a matrix with checkerboard structure (see Gaier [65, p. 75]). But while this matrix multiplication needs $O(N^2)$ operations, the Fourier transform with FFT needs only $O(N \log N)$ operations, and therefore is much faster (Henrici [103, 104], Gutknecht [91]).

There is a qualitative difference between \mathbf{K} and \mathbf{K}_N which becomes important at some places. The operator \mathbf{K} has defect 1. It maps the constant functions to 0. The operator \mathbf{K}_N has defect 2. It maps the constant functions to 0, but also the function $\cos nt$ which on the grid is simply a sequence of alternating +1 and -1.

The function $\mathbf{K}_N \psi$ is defined for all t by the trigonometric polynomial on the right-hand side of (32) with coefficients which are calculated by trigonometric interpolation (31) of ψ at the grid points. The accuracy measured by the maximum norm can be estimated in terms of the Fourier coefficients of ψ (see Gaier [67], Henrici [105])

$$\|\mathbf{K}\psi - \mathbf{K}_N \psi\|_\infty \leq |A_n| + |A_{-n}| + 2 \sum_{|l|>n} |A_l|. \quad (33)$$

With well-known estimates for the Fourier coefficients of smooth functions one obtains from (33) the following estimates: If ψ is analytic and bounded by $|\psi(z)| \leq M$ in a strip $S_a := \{z : |\operatorname{Im} z| < a\}$ around the real axis, then

$$\|\mathbf{K}\psi - \mathbf{K}_N \psi\|_\infty = 2M \operatorname{Coth} \frac{a}{2} e^{-an}, \quad (34)$$

i.e., the error is $O(e^{-an})$ as $n \rightarrow \infty$ (Gaier [67], Kreß [148]). Gaier [67] shows that

$$\|\mathbf{K}\psi - \mathbf{K}_N \psi\|_\infty = O(n^{-\alpha+1/2}) \quad (35)$$

if ψ is in the Hölder class C^α for some $\alpha > 1/2$.

For $(k - 1)$ -times differentiable functions ψ whose derivative $\psi^{(k-1)}$ is absolutely continuous and $\psi^{(k)}$ is bounded, the estimate

$$\|\mathbf{K}\psi - \mathbf{K}_N\psi\|_\infty = O(n^{-k} \log n \|\psi^{(k)}\|_\infty) \quad (36)$$

holds. The O order in (36) is best possible, in the sense that it cannot be improved by using different methods of numerical conjugation based on the same grid (Braß [22]). When ψ is in $C^{k,\alpha}$ then (36) can be improved to

$$\|\mathbf{K}\psi - \mathbf{K}_N\psi\|_\infty = O(n^{-(k+\alpha)} \log n [\psi^{(k)}]_\alpha). \quad (37)$$

These estimates are important, since the accuracy of several mapping methods which are based on function conjugation, is determined by the accuracy of the approximation \mathbf{K}_N of the conjugation operator \mathbf{K} .

In some cases it may be a disadvantage that FFT require equidistant grid points, since some effects (e.g., crowding, see Section 2.4) may make a nonequidistant grid preferable. There have been several attempts to develop fast Fourier transform on nonequidistant grids (see, e.g., Luchini and Manzo [169], Sugiura and Torii [251], Dutt and Rokhlin [49], Beylkin [19], Anderson and Dillon Daleh [5], Steidl [249]). According to Steidl, the most efficient algorithms for the fast direct and indirect Fourier transform are those proposed by Dutt and Rokhlin [49] and by Beylkin [19].

One could instead of trigonometric interpolation (31) use another interpolation procedure, e.g., by periodic splines. The conjugate of such an interpolating function can still be calculated by FFT, but the coefficients in (32) have to be multiplied by suitable *attenuation factors* (Gautschi [82]). The calculation of the conjugate of a rational trigonometric function has been discussed by Gutknecht [93]. Li and Syngellakis [165] evaluate conjugation by a boundary element method. They introduce a *generalized conjugation* which satisfies the property $\mathbf{K}^2\psi = -\psi + \text{const}$ of the conjugation operator \mathbf{K} only approximately.

One can solve the boundary value problem (24) directly by solving the Cauchy–Riemann equations in polar coordinates by difference methods. For this purpose it is convenient to use a staggered grid (see Chakravarty and Anderson [27]).

Let $A(t) \neq 0$ be a complex and $\psi(t)$ a real function, both Hölder continuous and 2π -periodic. The (linear) RH problem asks for a function Ψ analytic in D , continuous in \bar{D} , such that the boundary values satisfy the relation

$$\operatorname{Re}(\overline{A(t)}\Psi(e^{it})) = \psi(t). \quad (38)$$

The function A can be represented in the form

$$A(t) = r(t)e^{i\theta(t)} \quad (39)$$

with Hölder continuous functions θ and $r > 0$. Linear RH problems are studied in full generality in the book of Muskhelishvili [187]. We consider here only the case where the function A has *winding number*

$$m := \frac{1}{2\pi} (\theta(2\pi) - \theta(0)) \geq 0. \quad (40)$$

The RH problem can be solved in closed form using the operator of conjugation. The function

$$v(t) := \theta(t) - mt \quad (41)$$

is 2π -periodic. Let $w := \mathbf{K}v$ be its conjugate.

THEOREM 9. *The general solution of (38) is obtained by*

$$\Psi(e^{it}) = \frac{e^{i\theta}}{e^w} \left[(\mathbf{I} + i\mathbf{K}) \left(\frac{e^w}{r} \psi \right) + P_m(e^{it}) \right] \quad (42)$$

with a Laurent polynomial

$$P_m(z) = ip_0 + \sum_{j=1}^m (p_j z^j - \overline{p_j} z^{-j}) \quad (43)$$

with a real number p_0 and complex coefficients p_j .

Hence the general solution of (38) contains $2m + 1$ free real parameters $p_0, \operatorname{Re} p_j, \operatorname{Im} p_j$, $j = 1, \dots, m$.

We note the special case which is most important for conformal mapping in the following corollary. We define the averaging operator

$$\mathbf{J}\psi := \frac{1}{2\pi} \int_0^{2\pi} \psi(t) dt. \quad (44)$$

COROLLARY 1. *When $m = 1$ and the angle $\alpha := \mathbf{J}(v)$ is not congruent $\pi/2$ modulo π then the RH problem*

$$\operatorname{Im}(\overline{A(t)}\Psi(e^{it})) = \psi(t) \quad (45)$$

with the constraints

$$\Psi(0) = 0, \quad \operatorname{Im} \Psi'(0) = 0 \quad (46)$$

has a unique solution Ψ . The solution is given by

$$\Psi(e^{it}) = \frac{e^{i\theta}}{e^w} \left[(\mathbf{I} + i\mathbf{K} + \cot \alpha \cdot \mathbf{J}) \left(\frac{e^w}{r} \psi \right) \right]. \quad (47)$$

For the exterior problem we note only the following special result:

There is a function Ψ analytic in D^- except for a pole of order m at ∞ which satisfies the boundary condition (38) on the unit circle. The function is unique up to a real parameter. The general form of this function is given by

$$\Psi(e^{it}) = e^{w+i\theta} \left[(\mathbf{I} - i\mathbf{K}) \left(\frac{\psi}{e^w r} \right) + ip_0 \right] \quad (48)$$

with a real number p_0 .

2.6. The operator \mathbf{R}

In some conformal mapping methods, boundary value problems

$$\Psi(e^{it}) = B(t) + A(t)U(t) \quad (49)$$

occur with given complex functions A, B . The real function U and the analytic function Ψ in D must be determined so that (49) is satisfied. By multiplication by \bar{A} the real function U can be eliminated from (49) and an RH problem

$$\operatorname{Im}(\bar{A}(t)\Psi(e^{it})) = \operatorname{Im}(\bar{A}(t)B(t)), \quad (50)$$

for the analytic function Ψ , remains.

Iterative methods need the function U in the first place, not Ψ . Therefore, it is desirable to eliminate Ψ from (49) in order to get an equation for U instead. We will show in this section that U must satisfy a second kind Fredholm integral equation. Since the kernel of this equation has very nice properties, methods based on this equation are very efficient (see Section 4.4).

In the conformal mapping problem the function A has winding number 1. Therefore, we consider functions of the form

$$A(t) = \exp(i\beta(t)) \quad (51)$$

with a Hölder continuous real function β such that $\beta(t) - t$ is 2π -periodic. We define the integral operator

$$\mathbf{R}_\beta f(t) := \int_0^{2\pi} R_\beta(t, s) f(s) ds \quad (52)$$

with the symmetric kernel

$$R_\beta(t, s) := -\frac{1}{2\pi} \frac{\sin(\beta(t) - \beta(s) - (t-s)/2)}{\sin((t-s)/2)}. \quad (53)$$

The operator can be expressed by

$$\mathbf{R}_\beta U = \operatorname{Re}(e^{-i\beta} (\mathbf{J} - i\mathbf{K})(e^{i\beta} U)) \quad (54)$$

in terms of the conjugation operator \mathbf{K} and the averaging operator \mathbf{J} defined in (44).

The operator \mathbf{R}_β plays a role in the solution of the problem (49) due to the following fact (Wegmann [284]):

THEOREM 10. *There exists a function Ψ analytic in D with $\Psi(0) = 0$ satisfying the boundary problem (49) if and only if U is a solution of the Fredholm integral equation of the second kind*

$$(\mathbf{I} + \mathbf{R}_\beta)U = g \quad (55)$$

with the right-hand side

$$g := -\operatorname{Re}(e^{-i\beta} (\mathbf{I} - i\mathbf{K} + \mathbf{J})B). \quad (56)$$

Multiplication of (55) from the left by $\mathbf{I} - \mathbf{R}_\beta$ yields the equation

$$(\mathbf{I} - \mathbf{R}_\beta^2)U = (\mathbf{I} - \mathbf{R}_\beta)g. \quad (57)$$

We first note that both the equations (55) and (57) have a solution when the function g on the right-hand side is given by (56). The general solution is given by

$$U = U_0 + c \exp(-w) \quad (58)$$

with a particular solution U_0 , the conjugate $w := \mathbf{K}v$ of the function $v(t) := \beta(t) - t$ and an arbitrary real number c . Therefore, uniqueness of the solution can be enforced by prescribing the value $U(t_0) = a_0$ of U at a specified point t_0 .

When β is Hölder continuous with exponent μ , the kernel has along the diagonal a weak singularity of order $|t - s|^{\mu-1}$. Hence, for $\mu > \frac{1}{2}$, the operator \mathbf{R}_β is compact in L^2 . Since the kernel R_β is symmetric, all eigenvalues of \mathbf{R}_β are real. It follows from (54) that the norm of \mathbf{R}_β in L^2 is ≤ 1 . Hence, all eigenvalues of \mathbf{R}_β are in the interval $[-1, +1]$. Therefore, the symmetric operator $\mathbf{I} - \mathbf{R}_\beta^2$ is positive semidefinite. This makes equation (57) amenable to conjugate gradient methods. These are very efficient due to the favorable eigenvalue distribution of \mathbf{R}_β . This was noted in numerical experiments by Fornberg [62], and proved by Wegmann [284].

THEOREM 11. (a) $\lambda_0 = -1$ is a simple eigenvalue of \mathbf{R}_β . All other eigenvalues λ satisfy $|\lambda| < 1$.

(b) If 0 is an eigenvalue of \mathbf{R}_β , then its multiplicity is either an even number or infinity.

(c) If $\lambda \in (0, 1)$ is an eigenvalue of \mathbf{R}_β , then $-\lambda$ is also an eigenvalue with the same multiplicity as λ .

(d) When the k th derivative of β is in C^α then at most $2n + 1$ eigenvalues λ of \mathbf{R}_β satisfy

$$|\lambda| > C \|A\|_{k,\alpha} n^{-k-\alpha}. \quad (59)$$

(e) When $A(s) = F(e^{is})$ with a function F analytic in the annulus $1/r < |z| < r$ and bounded by $|F(z)| \leq M$ then at most $2n + 1$ eigenvalues of \mathbf{R}_β satisfy

$$|\lambda| > CMr^{-n}. \quad (60)$$

In (d) and (e) the constant C is independent of n and A .

The eigenvalue -1 has the corresponding eigenfunction $\exp(-w)$ which occurs in (58). The properties (d) and (e) say that the eigenvalues of $\mathbf{I} - \mathbf{R}_\beta^2$ cluster at 1 when A is sufficiently smooth, and that only very few differ from 1 by an appreciable amount. Therefore, conjugate gradient methods converge very fast. Their efficiency is also due to the fact that in view of the representation (54) $\mathbf{R}_\beta U$ can be evaluated by FFT. Also, the function g in (56) and the right-hand side of (57) can be calculated by FFT.

3. Mapping from the region to the disk

Let G be a simply-connected region as described in Section 2.2 with boundary parameterization $\eta(s)$, and let F be the conformal mapping from G to the unit disk D normalized by

$$F(0) = 0, \quad F'(0) > 0. \quad (61)$$

The number $1/F'(0)$ is called the *conformal radius* of G at 0 . It follows from Theorem 3 that there is a continuous function $T(s)$ such that $T(s) - s$ is 2π -periodic and

$$F(\eta(s)) = \exp(iT(s)). \quad (62)$$

The mapping is completely described by the function $T(s)$ which is called (*interior*) *boundary correspondence function*.

The values of $F(z)$ for interior points $z \in G$ can be calculated from the boundary values (62) by Cauchy's formula

$$F(z) = \frac{1}{2\pi i} \int_0^{2\pi} \frac{F(\eta(s))}{\eta(s) - z} \dot{\eta}(s) ds. \quad (63)$$

3.1. Potential theoretic methods

Several methods for conformal mapping of a region G to the unit disk D are based on the following simple observation. The function

$$H(z) := \log(F(z)/z) \quad (64)$$

is analytic in G and has boundary values

$$H(\eta(s)) = -\log|\eta(s)| + i[T(s) - \arg \eta(s)]. \quad (65)$$

Its real part $u := \operatorname{Re} H$ is a harmonic function in G with boundary values

$$u(\eta(s)) = -\log|\eta(s)| \quad (66)$$

on ∂G . This means that the harmonic function u solves a *Dirichlet problem*. A boundary problem of the kind (66) occurs in the construction of the *Green's function* $g(z, 0)$ of the region G with respect to the point 0. This gives the relation $u(z) = \log|F(z)| - \log|z| = -g(z, 0) - \log|z|$ (see, e.g., Nehari [189]). (Note that the singularity of the Green's function is sometimes defined with a factor $1/2\pi$.)

We assume for this section that G is a Jordan region and the boundary parameterization η is differentiable with continuous derivative $\dot{\eta}(s) \neq 0$. The Dirichlet problem of potential theory has a solution and this solution is unique. There are several methods for the calculation of the solution u .

An integral equation of the second kind can be derived starting from Cauchy's integral formula (63) restricted to the boundary

$$F(\eta(s)) = \frac{1}{\pi i} \int_0^{2\pi} \frac{F(\eta(t))\dot{\eta}(t)}{\eta(t) - \eta(s)} dt. \quad (67)$$

This integral with a singularity at $t = s$ must be interpreted as a Cauchy principal value integral.

The Cauchy kernel can be split into its real and imaginary parts

$$\frac{1}{\pi i} \frac{\dot{\eta}(t)}{\eta(t) - \eta(s)} = K_1(s, t) + iK_2(s, t). \quad (68)$$

Let \mathbf{K}_1 and \mathbf{K}_2 be the integral operators with kernels K_1 and K_2 , respectively.

With the components $\eta(s) = x(s) + iy(s)$ of η we get the explicit representation

$$K_1(s, t) = \frac{1}{\pi} \frac{(x(t) - x(s))\dot{y}(t) - (y(t) - y(s))\dot{x}(t)}{(x(t) - x(s))^2 + (y(t) - y(s))^2}, \quad (69)$$

$$K_2(s, t) = -\frac{1}{\pi} \frac{(x(t) - x(s))\dot{x}(t) + (y(t) - y(s))\dot{y}(t)}{(x(t) - x(s))^2 + (y(t) - y(s))^2}. \quad (70)$$

The representation (68) is very useful, since for sufficiently smooth curves, only the kernel K_2 is singular. If the second derivative of η at s exists, then it follows from Taylor's formula that

$$\lim_{t \rightarrow s} K_1(s, t) = \frac{1}{2\pi} \kappa(s) |\dot{\eta}(s)| \quad (71)$$

with the curvature $\kappa(s)$ of the curve Γ at the point $\eta(s)$. Hence the kernel K_1 is bounded. When η is only differentiable with $\dot{\eta} \in C^\alpha$ then it follows from $|K_1(s, t)| \leq C|s - t|^{\alpha-1}$ that K_1 has a weak singularity on the diagonal. This has the consequence that Fredholm's theorems are valid for the operator \mathbf{K}_1 (see, e.g., Mikhlin [181, p. 59]).

The kernel K_1 is well known in potential theory. This is due to the fact that the boundary values of a double layer potential with density μ and the normal derivative of a single layer potential with density σ can both be expressed in terms of the operator \mathbf{K}_1 and its adjoint.

It is well known, that all eigenvalues λ of \mathbf{K}_1 are real and contained in the interval $(-1, 1]$. The eigenvalue $\lambda_1 = +1$ is simple and the corresponding eigenfunction is $f_1 \equiv 1$. Let λ_2 be the eigenvalue $\neq 1$ of \mathbf{K}_1 with largest modulus $|\lambda_2|$. Ahlfors [1] gives an estimate for $|\lambda_2|$.

Integral equations with kernel K_1 were first studied by Carl Neumann in 1877 long before Fredholm theory was developed. Therefore, K_1 is called *Neumann kernel*, or to be more specific the *parametric Neumann kernel* (Henrici [107, p. 394], where the Neumann kernel is defined with s, t interchanged. The usual definition of the Neumann kernel is for curves with parameterization by arclength. In the general definition (69) the factor $|\dot{\eta}(t)|$ occurs).

By taking the real and imaginary parts of (67), the integral equations

$$(\mathbf{I} - \mathbf{K}_1)F_r = -\mathbf{K}_2 F_i \quad \text{and} \quad (\mathbf{I} - \mathbf{K}_1)F_i = \mathbf{K}_2 F_r \quad (72)$$

are obtained which connect the real and imaginary parts of the boundary values $F(\eta(s)) = F_r + iF_i$ of F . For Hölder continuously differentiable η , the equations (72) are Fredholm integral equations of the second kind for F_r when F_i is given, or for F_i , when F_r is known. The right-hand sides of (72) are calculated by applying the singular integral operator \mathbf{K}_2 to the known function F_i or F_r .

The second of the equations (72) applied to the boundary values (65) of the function H defined in (64) gives the *integral equation of Lichtenstein*

$$(\mathbf{I} - \mathbf{K}_1)g = \phi(s) := -\mathbf{K}_2(\log |\eta|) \quad (73)$$

for the difference $g(s) := T(s) - \arg \eta(s)$ of the arguments $T(s)$ of the image and $\arg \eta(s)$ of the preimage. Since a conformal mapping exists, it is clear that equation (73) has a solution. Since $+1$ is a simple eigenvalue of \mathbf{K}_1 with eigenfunction $g \equiv 1$, the solution of (73) is unique up to a constant. This constant corresponds to a rotation of the unit disk. It can be fixed by prescribing the boundary correspondence at a specified point

$$T(s_0) = t_0. \quad (74)$$

There are several ways to transform the right-hand side of (73) (see, e.g., Gaier [65, p. 11]). But in any case ϕ must be calculated by an integral transform.

Due to the eigenvalue distribution of \mathbf{K}_1 , integral equations with Neumann kernel, such as Lichtenstein's, can be conveniently solved by iteration. Starting with $g_0 := \phi$, the iterative step from g_k to g_{k+1} is performed by

$$g_{k+1}(s) = \int_0^{2\pi} K_1(s, t) g_k(t) dt + \phi(s). \quad (75)$$

The iterates g_k converge uniformly to a solution of (73). Convergence is geometric with a rate $|\lambda_2|$ (Warschawski [277], Gaier [65, p. 32]).

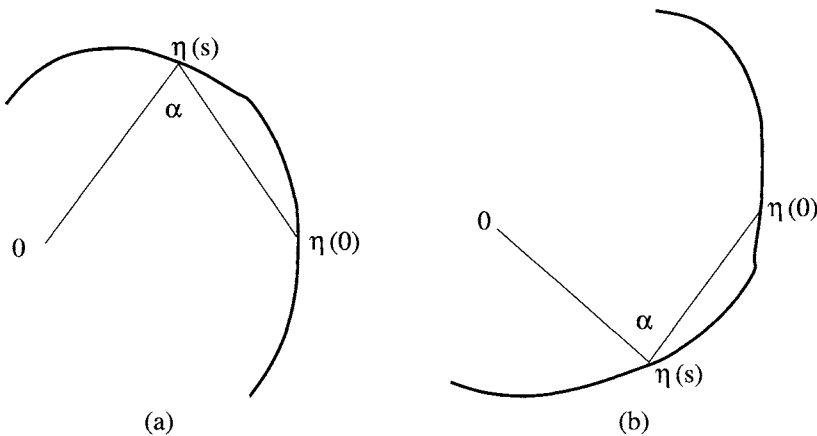


Fig. 5. Geometric interpretation of the right-hand side of Gershgorin's equation (76).

The *integral equation of Gershgorin* (see Gaier [65, p. 8] or Henrici [107, p. 395])

$$(\mathbf{I} - \mathbf{K}_1)T = \beta(s) := 2(\arg \eta(s) - \arg[\eta(s) - \eta(0)]) \quad (76)$$

gives directly the parameter mapping function $T(s)$. Equation (76) has the advantage that the right-hand side can be calculated very easily from the parameterization of the curve. A simple geometric consideration shows that $\beta(s) = \pm 2\alpha$, where α is the angle α at the corner $\eta(s)$ in the triangle formed by the points $0, \eta(s), \eta(0)$, counted negative (positive) when the points are in negative (positive) orientation (see Figures 5(a) and 5(b)).

One can represent the function H from (64) in a unique way as

$$H(z) = \frac{1}{2\pi i} \int_0^{2\pi} \frac{\mu(s)\dot{\eta}(s)}{\eta(s) - z} ds + Ci \quad (77)$$

with a real function μ and a real number C (see Muskhelishvili [187, p. 172]). After calculating the boundary values with (67), taking real parts and using the boundary condition (66), the *integral equation of Mikhlin*

$$(\mathbf{I} + \mathbf{K}_1)\mu = -2 \log |\eta(s)| \quad (78)$$

is obtained (Mikhlin [181], Mayo [173]). It is a Fredholm integral equation of the second kind with Neumann kernel.

The numerical solution of integral equations of the second kind in potential theory is a well-developed field (see, e.g., Atkinson [6] for an overview). For smooth boundary curves “essentially any numerical method will work well, and Nyström methods with the trapezoidal rule probably work best” [6, p. 229]. Stenger and Schmidlein [250] show that Mikhlin’s equation can be solved very efficiently by Sinc methods.

When for u an ansatz as a double-layer potential is made

$$u(z) = \frac{1}{2\pi} \int_0^{2\pi} \frac{\partial \log |z - \eta(s)|}{\partial n_s} \mu(s) ds \quad (79)$$

with density μ (n_s is the inner normal at the point $\eta(s)$) then u assumes the boundary values (66) if and only if Mikhlin's equation (78) is satisfied.

When instead u is represented as a single-layer potential

$$u(z) = -\frac{1}{2\pi} \int_0^{2\pi} \log |z - \eta(s)| \sigma(s) ds \quad (80)$$

with density σ then the boundary values $-\log |\eta|$ are attained when *Symm's integral equation*

$$\frac{1}{2\pi} \int_0^{2\pi} \log |\eta(t) - \eta(s)| \sigma(s) ds = \log |\eta(t)| \quad (81)$$

is satisfied (Symm [253]). With a solution σ of this equation, the function H can be evaluated

$$H(z) = -\frac{1}{2\pi} \int_0^{2\pi} \log(z - \eta(s)) \sigma(s) ds + i\alpha. \quad (82)$$

The real constant α effects a rotation by an angle α in the conformal mapping function $F(z) = z \exp(H(z))$. It can be fixed by prescribing the image $F(z_0)$ of a boundary point $z_0 \in \Gamma$.

Gaier [68] thoroughly investigated Symm's equation. We quote his main result:

THEOREM 12. (a) *If the boundary curve Γ has capacity $\gamma \neq 1$ (see definition in Section 8) then Symm's equation (81) has the unique solution*

$$\sigma(s) = T'(s), \quad (83)$$

where T' is the derivative of the (interior) boundary correspondence function T defined in (62).

(b) *If Γ has capacity $\gamma = 1$, then the general solution of (81) is*

$$T'(s) + c T'_e(s) \quad (84)$$

with the exterior boundary correspondence function T_e (defined by (222) in Section 8) and an arbitrary real number c .

In view of this theorem it is important to know when the derivative T' exists. We quote the result: If Γ is a rectifiable Jordan curve, then T is absolutely continuous (see Priwalow [226] or Gaier [68, p. 121]).

It is somewhat unexpected that the unique solvability of Symm's equation depends on the size of the region (measured by the capacity). This is a special feature of the logarithmic kernel which can be exemplified in the following way: For a circle of radius R the integral operator with logarithmic kernel on the left-hand side of (81) has eigenfunction $\sigma_0 \equiv 1$ to the eigenvalue $\lambda_0 = \log R$, which becomes 0 for the unit circle, $R = 1$, with capacity $\gamma = 1$.

One can easily remove the ambiguity by a suitable scaling of the curve Γ by a factor λ in such a way that the capacity $\lambda\gamma$ of $\lambda\Gamma$ is different from 1.

Equation (81) is more difficult than the more popular Fredholm equations of the second kind. This is due to the fact that the operator with logarithmic kernel has a smoothing effect. It maps a function space typically into a proper (dense) subspace and has no bounded inverse. As a result, analysis of this equation in a single function space will result in solutions failing to exist for some right-hand sides, and hence instability (see, e.g., Yan and Sloan [295, p. 550]).

There are standard methods available for the numerical solution of integral equations of the form (81) (see, e.g., Atkinson [6]). The logarithmic singularity in the integrals in formulas (81) and (82) requires special treatment. There is now an extensive literature about how to treat Symm's equation numerically. Symm [253] approximated σ by a step function. The convergence of the collocation solution can be improved by a simple postprocessing, the so-called *Sloan iteration* (Graham and Atkinson, [85]). Hayes et al. [101] represent σ by a piecewise quadratic polynomial, and Hough and Papamichael [115] by spline functions of various degrees.

Symm's method does not require the boundary of the region be smooth. If G has corners, however, the function σ may have singularities. In particular, at a re-entrant corner σ becomes unbounded, and this singularity has a serious damaging effect on the accuracy of the approximate mapping function (see Hough and Papamichael [115, p. 135]). To overcome this problem these authors approximate σ near corners by functions which reflect the main singular behavior. A priori information about the behavior of σ near a corner of a polygonal domain with interior angle α is detailed in [115, p. 136]. The experiments of [115] suggest that a reasonable strategy for solving Symm's equation is to use cubic splines with three singular terms for each corner. For the use of singular density functions see also Papamichael [220].

In a later paper Hough and Papamichael [116] give a unified treatment of Symm's equation for interior, exterior and doubly connected domains and again emphasize the importance of including appropriate "singular" functions to cope with corner singularities.

Hoidn [110] enforces by a reparameterization of the boundary curve that the boundary correspondence has certain required smoothness properties. McLean [174] uses a spectral Galerkin method suitable for smooth boundaries. There is rapid convergence of the approximate solution to the Dirichlet problem and all its derivatives uniformly up to the boundary. Hough et al. [114] and Levesley et al. [163] use expansion in terms of Chebyshev polynomials. This approach is also suitable for regions with corners. A convergence analysis is given.

All these methods need $O(N^3)$ operations when discretized with N boundary points. Henrici [104] and Reichel [234] use iteration procedures with FFT. This reduces the com-

putational cost to $O(N^2 \log N)$. Berrut and Trummer [18] show that the Fourier method is equivalent to the Nyström method.

Elschner and Stephan [52] propose a collocation method on curves with corners. When the corner singularities are smoothed by a mesh grading which accumulates grid points near the corners, fast convergence of the approximate solutions can be obtained. Graded meshes, however, produce ill-conditioned linear systems to be solved. This limits the achievable accuracy (see Monegato and Scuderi [183]).

Elschner and Graham [53] apply near corners a smoothing change of variables. A collocation method with splines on a uniform grid leads to optimal order of approximation. Monegato and Scuderi [183] approximate the solution of the transformed equation globally by algebraic polynomials. This leads to well-conditioned systems of equations.

Berrut [17] derived from Symm's equation a Fredholm integral equation of the second kind for the derivative T' of the parameter mapping function. A second kind integral equation for T' with Neumann kernel has been derived by Warschawski (see [107, p. 395]).

Ellacott [50] uses a more general form of the function H , namely $H(z) = \log(F(z)/g(z))$ with a function g satisfying $g'(0) > 0$, $g(0) = 0$ and $g(z) \neq 0$ elsewhere. Then $u = \operatorname{Re} H$ is a harmonic function with boundary values $-\log|g(\eta(s))|$. Ellacott approximates these boundary values in the uniform norm by the real part $\operatorname{Re} p_n(z)$ of polynomials of degree n . Then $F_n(z) = g(z) \exp(p_n(z))$ is an approximation for F .

Saranen and Vainikko [238] propose a two-grid method where inversions on a coarse grid and iterations on the fine grid are alternated. With appropriate solvers the computational cost varies between $O(N^2)$ and $O(N \log N)$ arithmetic operations with the number N of grid points.

Driscoll [46] proposes a domain decomposition method to solve Symm's equation on regions with a long narrow channel, or with structures on different scales.

For the calculation of conformal maps via Symm's equation the public-domain software package CONFPACK described by Hough [113] is available.

The methods discussed so far all solve the Dirichlet problem (66) by an integral equation. These methods are also called *integral equation methods*. These integral equations are linear but they must be solved on the (possibly complicated) boundary of the region G .

Hayes et al. [102] compared the integral equation methods of the first and of the second kind in a series of test calculations. Their conclusion is that Symm's method can compete with Lichtenstein's method. Symm's method is more robust in that it can deal with more distorted domains and with domains with corners. Lichtenstein's method "is clearly better if the domain to be mapped is not excessively distorted from the circle". Even if the domain is distorted Lichtenstein's method may be better if the mesh is sufficiently fine and special care is used in computing the right-hand side $\phi(s)$ of (73) ([102, p. 521]).

Closely related to Symm's method is the *charge simulation method* (Amano [2]). While in (80) or its discretized versions the harmonic function is represented as potential of charges distributed along the curve Γ , the charge simulation method approximates u as a linear combination of N charges Q_i at points ζ_i outside Γ . The charges Q_i are determined from the Dirichlet boundary condition $u(z_j) = -\log|z_j|$ at N collocation points $z_j \in \Gamma$. This resembles one of the methods discussed by Christiansen [28], where the Dirichlet problem is solved by an ansatz with charges outside the boundary. The results of [28, p. 383] indicate that the ensuing system of equations for the determination of the

charges has worse condition than for the discrete Symm's equation, where the charges lie on the boundary.

The charge simulation method has been used by Inoue [124] to calculate the inverse mapping Φ . It is still an open problem how to find the optimal arrangement of the charges. However, it is empirically known that the method can give numerical results of high accuracy if the charge point ζ_i is arranged on the outward normal of the boundary curve at the corresponding collocation point z_i and closer to the boundary where collocation points are dense (Amano [3, p. 1178]). Corners do not present severe difficulty if they are convex, but it seems difficult to obtain accurate results for domains with concave corners (Amano [2, p. 368]). In particular, for slit domains there is no space to place the charges outside the region but close to the boundary. For such difficult cases a premap is recommended (Okano et al. [196]).

Gillot [83] approximated directly F by a polynomial ansatz

$$F_n(z) = C_1 z + \cdots + C_n z^n \quad (85)$$

and determined the coefficients C_j from the condition $|F_n(z_j)|^2 = 1$ for n points $z_j \in \Gamma$. These conditions give quadratic equations for the coefficients, which are convenient to handle numerically. This is closely related to a method described by Kantorowitsch and Krylow [132, p. 360].

Curtiss [33] discusses the solution of the Dirichlet problem by interpolating harmonic polynomials (see also Gaier [65, p. 154]). Volkov [271] approximates the solution of the Dirichlet problem by means of the block method.

When the parameterization $\eta_\lambda(s)$ of the boundary curves of a family G_λ of regions depends analytically on a parameter λ , one may expect that the conformal mapping functions F_λ from G_λ onto the unit disk can be represented as a series

$$F_\lambda(z) = F_0(z) + \sum_{k=1}^{\infty} \lambda^k g_k(z) \quad (86)$$

in powers of λ . This approach is described by Kantorowitsch and Krylow [132, p. 359], where also hints are given on how to calculate the coefficient functions g_k .

The integral equation methods give only the boundary values of the mapping function. The values in the interior must be calculated by Cauchy's formula (77) or the integral (82). This may be a tedious task when the values at many points are required. Another difficulty arises from the fact that the kernels in (77) and (82) become unbounded as z approaches the boundary curve.

Mayo [172, 173] proposes the following procedure. The region G is embedded into a larger one, say a rectangle R , for which fast Poisson solvers are available. The double layer potential u of (79) is a harmonic function inside and outside Γ . The normal derivative is continuous on Γ , but the function u itself has a jump of μ on Γ . The idea is now to represent u as the solution of a Poisson equation

$$\Delta u = q \quad \text{in } R, \quad u = u_0 \quad \text{on } \partial R. \quad (87)$$

The boundary values u_0 are calculated with the integral (79). The volume source q is concentrated in a region of one-grid size width around Γ . It can be calculated from the density μ and the parameterization η of the curve. The complex conjugate function v can be calculated with the same method at little extra cost. It satisfies also a Poisson equation like u . The source term for v can also be calculated directly from μ and η and the boundary values are obtained from the Cauchy integral (77).

The harmonic measure is invariant under conformal mapping. It has a very simple structure in the unit disk: The level lines are segments of circles. Based on these observations one can construct the conformal mapping function F when only the harmonic measures of two segments of the boundary curve Γ are known (Hofmann [108]).

3.2. Extremum principles

The standard proof of the Riemann mapping theorem relies on the following extremum principle:

Among all functions f which are analytic and univalent in G and satisfy

$$f(0) = 0, \quad f'(0) = 1 \quad (88)$$

there is a unique function F which minimizes the supremum norm

$$\|f\|_\infty := \sup_{z \in G} |f(z)| \quad (89)$$

on G . This function F maps G conformally to a disk of a certain radius R , the conformal radius introduced at the beginning of Section 3.

In view of (88) the admissible functions are of form $f(z) = z - g(z)$ with functions g , analytic in G such that $g(0) = g'(0) = 0$. The minimum in (89) is attained when

$$\|z - g\|_\infty := \sup_{z \in G} |z - g(z)| \quad (90)$$

is as small as possible. In this formulation the function g is an *approximation of the identity* z (see, e.g., Opfer [200]).

With a polynomial ansatz for g , this leads to a problem of uniform approximation (Opfer [200]). Krabs and Opfer [147] describe an algorithm for the numerical solution of this kind of approximation problem. The experiments by Hartmann and Opfer [100] show that for some regions (such as a “dented square”) the polynomial ansatz does not yield useful approximations. This is due to the fact that polynomials are analytic at some boundary points where the mapping function has singularities. As a remedy, singular ansatz functions should be included which reflect the singular behavior of the mapping function at corners.

One can use instead of the modulus $|z|$ a more general norm $N(z)$ on \mathbb{C} , and define instead of (89) the norm

$$\|f\|_N := \sup_{z \in G} N(f(z)). \quad (91)$$

There is a unique function F_N which gives among all analytic univalent functions f on G with side condition (88) minimum norm $\|f\|_N$. This function F_N maps G conformally onto a “disk” $\{z: N(z) < R\}$ with a suitable $R > 0$ (Opfer [201]). The standard case is included in this general framework for $N(x+iy) = \sqrt{x^2 + y^2}$. By using instead of a norm a suitable positively homogeneous functional, one can also characterize conformal mappings from G onto any star-shaped region S by extremal properties. If the region S is a convex polygon, the extremal problem can be treated numerically by linear programming methods (Opfer [202]).

Samli [237] shows that for a star-shaped region G there are univalent polynomials P_n on G such that $|P_n|$ approximates on the boundary the constant $\equiv 1$ best in the uniform norm. He describes also how to construct such a P_n which then can be used as an approximation to the conformal mapping $F: G \rightarrow D$.

Problems of uniform approximation, however, are not very convenient from the computational point of view. Much easier to handle are approximation problems in Hilbert spaces. There are two major ways to make a Hilbert space of analytic functions in G .

The set $B(G)$ of all functions f analytic in G such that the integral (in the Lebesgue sense)

$$\|f\|_B^2 := \int_G |f(z)|^2 dx dy \quad (92)$$

is finite is called the *Bergman space* of G . It is a Hilbert space when provided with the scalar product

$$(f, g)_B := \int_G f(z) \overline{g(z)} dx dy. \quad (93)$$

This space was first studied by Bergman in 1922 (see [13]). Bergman gives in his book [14] a comprehensive presentation of this space of analytic functions and its relation to conformal mapping.

$B(G)$ is a closed linear subspace of the Lebesgue space $L^2(G)$ of all square integrable functions on G . Let f_1, f_2, \dots be a complete orthonormal system of functions in $B(G)$; then the projection of $L^2(G)$ onto $B(G)$ is determined by the bilinear series

$$k_B(z, w) := \sum_{l=1}^{\infty} f_l(z) \overline{f_l(w)} \quad (94)$$

for $z, w \in G$. This series converges for each fixed $w \in G$ as a function of z in $L^2(G)$, but it converges also pointwise and uniformly for z in every compact subset of G . Therefore, the sum on the right-hand side of (94) defines a function k_B of two variables, the *Bergman kernel function* of the region G . The integral operator \mathbf{k}_B with kernel k_B is called the *Bergman projection*. It projects $L^2(G)$ onto $B(G)$.

In view of the definition of the inner product (93), the integral operator \mathbf{k}_B applied to a function $f \in B(G)$ gives the representation of f in terms of the orthonormal system f_1, f_2, \dots . This proves the *reproducing property* of the kernel

$$f(w) = \int_G \overline{k_B(z, w)} f(z) dx dy = (f, k_B(\cdot, w))_B \quad (95)$$

for all functions $f \in B(G)$ and points $w \in G$.

The interest for the Bergman kernel for conformal mapping comes from the following fact. The conformal mapping $F_w(z)$ from G to the unit disk normalized by

$$F_w(w) = 0, \quad F'_w(w) > 0 \quad (96)$$

is related to the kernel k_B by the equation

$$k_B(z, w) = \frac{1}{\pi} F'_w(z) F'_w(w). \quad (97)$$

This equation can be used to represent F'_w in terms of the kernel k_B .

THEOREM 13. *The conformal mapping $F_w : G \rightarrow D$ normalized by the conditions (96) is related to the Bergman kernel by the equation*

$$F'_w(z) = \sqrt{\frac{\pi}{k_B(w, w)}} k_B(z, w) \quad (98)$$

for $z \in G$.

The mapping function F_w can be calculated from (98) by integration. Kerzman and Trummer [134], however, noted that the boundary values of F_w can be retrieved from (98) without integration by

$$F_w(\eta(t)) = -i \frac{\dot{\eta}(t) F'_w(\eta(t))}{|\dot{\eta}(t) F'_w(\eta(t))|}. \quad (99)$$

These results suggest the following procedure for approximating the mapping function F . Given a complete set of functions v_1, v_2, \dots in $B(G)$, the finite subset v_1, \dots, v_N is orthonormalized by means of the *Gram–Schmidt process* to give a set of orthonormal functions f_1, \dots, f_N . Henrici [107, p. 545] gives hints for the numerical treatment of the Gram–Schmidt orthonormalization. The double integrals are transformed to line integrals using the equation

$$(f, g')_B := \int_G f(z) \overline{g'(z)} dx dy = \frac{1}{2i} \int_{\Gamma} f(z) \overline{g(z)} dz \quad (100)$$

which can be derived from Green's formula. The inner products must be calculated as accurate as possible, since the Gram–Schmidt procedure is extremely sensitive to errors in the scalar products.

The series (94) is truncated to give the approximation

$$k_{B,N}(z, w) := \sum_{l=1}^N f_l(z) \overline{f_l(w)}. \quad (101)$$

This approximation procedure is called the *Bergman kernel method* (BKM) with basis f_1, \dots, f_N . The BKM has as a major shortcoming that the Gram–Schmidt process is usually numerically unstable. This means that only a limited number of functions can be orthonormalized. Therefore, it is of great practical importance to choose an appropriate set of basis functions v_1, \dots, v_N .

It is not always possible to use polynomial basis functions, since there are regions G for which the functions z^j , $j = 0, 1, 2, \dots$, are not complete in $B(G)$. The disk with a slit $G = D \setminus [1/2, 1]$ is an example. But for regions G whose boundary ∂G is contained in the boundary ∂E of a region E which is disjoint to G the polynomials are dense in $B(G)$ (see Bieberbach [20]). All Jordan regions have this property since ∂G is also the boundary of the complement of G in \mathbb{C} .

The convergence of the series (94) calculated from orthonormalized polynomials z^j is often very slow. This is due to the presence of singularities of $k_B(z, w)$ in the complement of G , close to or on the boundary ∂G . Therefore, it is advisable to augment the polynomial basis by suitable singular functions. In many cases sufficient information about the singular behavior of $k_B(z, w)$ is available.

Levin et al. [164] take into account two types of singularities:

1. *Poles*: The damaging effect of poles on the convergence of the series (94) is exemplified by the mapping $F_w(z) := (z - w)/(1 - \bar{w}z)$ of the unit disk onto itself with $F_w(w) = 0$. This mapping has a pole at $z = 1/\bar{w}$. The polynomial series for the Bergman kernel function

$$k_B(z, w) = \frac{1}{\pi} \sum_{l=1}^{\infty} l(\bar{w}z)^{l-1} \quad (102)$$

converges rapidly when $|w|$ is small. It converges very slowly, when $|w|$ is close to 1. In general, the damaging influence of poles on the numerics of the BKM can be removed by introducing appropriate rational functions into the basis set. When F has a pole at $z = p$ outside G , then the polynomial basis should be augmented by the function $(z/(z - p))'$ (see [164, p. 175] for more details).

2. *Branch points*: When the boundary of G has a corner at z_0 of interior angle $\alpha\pi$, formed by two analytic arcs, the mapping in the neighborhood of z_0 is represented by a series in fractional powers $(z - z_0)^{k/\alpha}$, $k = 0, 1, 2, \dots$. Therefore, if $1/\alpha$ is not an integer, F and k_B have a branch point singularity at z_0 which affects the rate of convergence of the polynomial series at least in the neighborhood of z_0 . The polynomial basis should be augmented by the function $(z - z_0)^{k/\alpha-1}$ [164, p. 175].

When the boundary curve Γ consists of analytic arcs then the position of the poles can be determined in favorable cases by a symmetry principle which is a generalization of Schwarz's reflection principle (Papamichael et al. [219]). The use of a basis augmented by singular functions can deteriorate the stability of the orthonormalization process but it can also speed up the convergence of the numerically calculated approximations to F (Papamichael and Warby [218]).

For ellipses the Chebyshev polynomials of the second kind form a set of orthogonal basis functions, and the kernel function can be calculated explicitly (see Nehari [189, p. 258]). Burbea [23] calculates the mapping from ellipses and squares to the disk using the orthonormalized polynomials z^j and compares the result with theoretical values.

In view of the numerical difficulties of the calculation of the Bergman kernel via an orthonormalization procedure, it is interesting to note that the boundary values of k_B satisfy an integral equation of the second kind with Neumann kernel (Razali et al. [231]). Assume that the boundary of G has a parametric representation by a twice differentiable function η and fix a point $w \in G$. Then the function $\phi(t) := \dot{\eta}(t)k_B(\eta(t), w)$ satisfies the equation [231, p. 343]

$$\phi(t) + \int_0^{2\pi} K_1(s, t)\phi(s) ds = -\frac{1}{\pi} \frac{\overline{\dot{\eta}(t)}}{(\eta(t) - \bar{w})^2} \quad (103)$$

with the Neumann kernel K_1 defined in (69). Equation (103) has a unique solution. It can be solved numerically by the Nyström method. Since the functions involved are all 2π -periodic, the integrals are best evaluated by the trapezoidal rule on an equidistant grid. For regions with m -fold symmetry, the integral equation can be restricted to $1/m$ of the boundary (Razali et al. [231]). When the equations arising from the Nyström discretization with N grid points are solved by the generalized minimum residual method, the computational cost can be reduced from $O(N^3)$ to $O(N^2)$ (Razali et al. [232]).

If $G = G_1 \cup \dots \cup G_m$ is the union of a finite number of regions G_j , then the Bergman projection (95) of the region G can be described in terms of the Bergman projections of the subregions G_j (Skwarczynski [243]). This representation uses the principle of alternating projections (von Neumann [190], Skwarczynski [244]).

For a region G bounded by a rectifiable Jordan curve Γ one can consider the set $S(G)$ of all functions f analytic in G , such that, for almost all (in the Lebesgue sense) points $\xi \in \Gamma$, the nontangential limit $f(\xi) = \lim_{z \rightarrow \xi} f(z)$ exists and the line integral

$$\|f\|_S^2 := \int_{\Gamma} |f(\xi)|^2 |d\xi| \quad (104)$$

($|d\xi|$ is the differential of arclength) is finite. With the inner product

$$(f, g)_S := \int_{\partial G} f(\xi) \overline{g(\xi)} |d\xi| \quad (105)$$

$S(G)$ becomes a Hilbert space, which is sometimes called *Szegö space* in honour of Szegö who first studied this space and its bearing on conformal mapping in 1921 (see [256]).

The Szegö space $S(G)$ is a closed linear subspace of the Lebesgue space $L^2(\partial G)$. With a complete orthonormal system of functions g_1, g_2, \dots in $S(G)$ one can define the bilinear series

$$k_S(z, w) := \sum_{l=1}^{\infty} g_l(z) \overline{g_l(w)} \quad (106)$$

for $z, w \in G$. This series converges for each fixed $w \in \partial G$ as a function of z in $L^2(\partial G)$, but it also converges pointwise and uniformly for z in every compact subset of G (see, e.g., Gaier [65, p. 134]). Therefore, the sum on the right-hand side of (106) defines a function k_S of two variables, the *Szegö kernel function* of the region G . The integral operator \mathbf{k}_S with this kernel defines the *Szegö projection*, that is the projection of $L^2(\partial G)$ onto $S(G)$. This implies the reproducing property

$$g(w) = \int_{\partial G} \overline{k_S(\xi, w)} g(\xi) |d\xi| = (g, k_S(\cdot, w))_S \quad (107)$$

of the Szegö kernel function for functions $g \in S(G)$ and points $w \in G$.

The Szegö kernel is connected with the conformal mapping function in a similar way as the Bergman kernel.

THEOREM 14. *The conformal mapping $F_w : G \rightarrow D$ normalized by the conditions (96) is related to the Szegö kernel by the equations*

$$F'_w(z) = \frac{2\pi}{k_S(w, w)} k_S^2(z, w) \quad (108)$$

for $z \in G$.

It follows from (98) and (108) that the Bergman and Szegö kernels are related by the equation

$$k_B(z, w) = 4\pi k_S^2(z, w). \quad (109)$$

The Szegö kernel has for a long time not been very popular for numerical conformal mapping, since it requires the tedious orthogonalization of polynomials on the boundary curve. This situation has changed, however, since it has been noticed that the Szegö kernel can be conveniently calculated from a Fredholm integral equation of the second kind.

Both the Cauchy and the Szegö kernels map functions in $L^2(\partial G)$ to boundary values of analytic functions in G . Both are projectors, the Szegö projector is orthogonal in $L^2(\partial G)$, the Cauchy projector is not. The Cauchy kernel can be written down very easily, the Szegö kernel can be written down only if a conformal mapping $F : G \rightarrow D$ is known. Kerzman and Stein [133] found that the Szegö projector can be obtained by “orthogonalizing” the Cauchy projector. This leads to an integral equation for k_S .

We present here the version of Trummer [266] which is convenient for numerical treatment. Let

$$H(s, t) := \frac{1}{2\pi i} \frac{\dot{\eta}(t)}{|\dot{\eta}(t)|} \frac{1}{\eta(t) - \eta(s)} \quad (110)$$

be the Cauchy kernel. Then the nonsymmetric part is defined by

$$A(s, t) := \overline{H(t, s)} - H(s, t) \quad (111)$$

for $s \neq t$, and by $A(s, s) = 0$ on the diagonal. When the boundary parameterization η is in C^2 then A is a continuous function. It is skew-symmetric: $A(s, t) = -\overline{A(t, s)}$. The Szegő kernel satisfies the Kerzman–Stein integral equation [133]

$$\begin{aligned} k_S(\eta(t), w) + \int_0^{2\pi} A(t, s) k_S(\eta(s), w) |\dot{\eta}(s)| ds \\ = -\frac{1}{2\pi i} \frac{\overline{\dot{\eta}(t)}}{|\dot{\eta}(t)|(\eta(t) - \bar{w})} \end{aligned} \quad (112)$$

for any fixed $w \in G$. This is a second kind Fredholm integral equation for $k_S(\eta(\cdot), w)$ with continuous kernel A . Equation (112) is similar to (103) for the Bergman kernel.

Equation (112) has been used by Kerzman and Trummer [134] for numerical purposes. Trummer [266] solves (110) by Nyström's method using equidistant grid points and the trapezoidal rule for integration. The ensuing linear system of equations is solved by a conjugate gradient method.

Each iterative step of the conjugate gradient (CG) method requires multiplication of a vector by a matrix. The operation count for this scales like $O(N^2)$ with the number N of grid points. O'Donnell and Rokhlin [194] give a variant of this method where by means of the Fast Multipole Method the operation count for this matrix multiplication is decreased to $O(N)$. But the constant of this $O(N)$ is quite large, so that methods based on FFT with their $O(N \log N)$ operation count are likely to be considerably faster. On the other hand, the performance of this method is not affected by crowding, making it a method of choice for elongated regions [194, p. 476]. Lee and Trummer [159] have improved the numerics of this method further by using a multi-grid approach. The multi-grid seems to outperform the CG for elongated regions where a large number of grid points is needed in view of crowding. But CG seems to be preferable when the boundary contains some sharp changes [159, p. 43]. Lee and Trummer [159] calculated successfully examples of regions with nonsmooth boundaries with corners and cusps. Thomas [260] provided the theoretical framework for this experimental finding by extending equation (112) to domains with piecewise C^∞ boundaries. The Szegő kernel for such domains is defined as the limit of the Szegő kernels of certain subdomains with smooth boundaries.

Murid et al. [186] give a unified derivation of the integral equations for the Bergman and the Szegő kernels.

Both the Bergman and the Szegö norms are very useful for characterizing the conformal mapping from G to a disk by extremum principles:

THEOREM 15. *Let F be the conformal mapping from G to a disk normalized by (88). Then*

- (a) *F' is the unique function which minimizes $\|f'\|_B$ among all functions $f \in B(G)$ satisfying $f(0) = 1$.*
- (b) *$\sqrt{F'}$ is the unique function which minimizes $\|f\|_S$ among all functions $f \in S(G)$ satisfying $f(0) = 1$.*

The dilatation of a function f is equal to $|f'|$. Therefore, the image of the region G under the mapping f has area $\|f'\|_B^2$. Statement (a) is called the *principle of minimum area*. For the same reason $\|\sqrt{f'}\|_S^2$ is the length of the boundary of the image region $f(G)$. Statement (b) is called the *principle of minimum length* (see Bieberbach [20]).

In numerical calculations one solves the minimization problems of the theorem not in the whole space $B(G)$ but in a finite-dimensional subspace generated by basis functions g_1, \dots, g_n , i.e., by a Ritz ansatz as is generally applied in the calculus of variations (see, e.g., Kantorowitsch and Krylow [132]). Methods based on this approach are called *Ritz methods*. Usually one takes the space Π_n of polynomials of degree $\leq n$. Once again, however, one has to keep in mind that for general regions it can happen that the polynomials are not dense in $B(G)$.

The Ritz method applied with functions g_1, \dots, g_n gives the approximation F'_n for F' as an expansion

$$F'_n(z) = \sum_{j=1}^n a_j g_j(z) \quad (113)$$

in terms of given basis functions. The coefficients a_j are determined by the minimization. Therefore, these methods are also called *expansion methods* (Papamichael [220]).

When the minimization problem is to be solved in the space Π_n of n th degree polynomials, systems of linear equations arise which are in general ill-conditioned (Švecová [252]). The minimizing polynomials in general do not give conformal mappings. Opfer [198] gives several illustrative examples.

There is an analogy to statement (a) of Theorem 15: There is a unique polynomial p_n which minimizes $\|p\|_B$ among all $p \in \Pi_n$ with $p(0) = 1$. The primitives π_n of these polynomials p_n normalized by $\pi_n(0) = 0$ are called *Bieberbach polynomials*. The importance for conformal mapping stems from the fact that, when F is the conformal mapping normalized by (88), the p_n also solve the problem of minimizing $\|F' - p\|_B$ among all $p \in \Pi_n$ (see Gaier [65, p. 122]).

The Bieberbach polynomials also give nearly best approximations in the uniform norm. When Γ is a Jordan curve with parametric representation $\eta \in C^\alpha$ with $\alpha \geq 3/4$ then

$$\|F - \pi_n\|_B = O(\log n) E_n(F, G), \quad (114)$$

where $E_n(F, G)$ denotes the minimal error of uniform approximation of F on G by polynomials of degree $\leq n$. For piecewise analytic curves, however, with exterior angles $\lambda_j \pi$ ($0 < \lambda_j < 2$) and without cusps, the estimate

$$\|F - \pi_n\|_B = O(\log n) n^{-\gamma} \quad (115)$$

holds with

$$\gamma := \min_j \frac{\lambda_j}{2 - \lambda_j}, \quad (116)$$

and this exponent is the best possible for general regions (Gaier [73]). For corners of a special type, however, one can get an improvement: For corners with interior angles of form π/N for some $N = 1, 2, \dots$ one can insert into the right-hand side of (116), $2\lambda_j/(2 - \lambda_j)$ (Gaier [76]).

Gaier [72] generalized a lemma of Andrievskii which is useful for transforming estimates for the norm $\|\cdot\|_B$ into those for the supremum norm $\|\cdot\|_\infty$ on G .

Assume that the conformal mapping $\Phi : D \rightarrow G$ is Hölder continuous. Then there is a constant $c(G)$ which depends on G only such that for every polynomial P of degree $n \geq 2$ with $P(0) = 0$ the estimate

$$\|P\|_\infty \leq c(G) \sqrt{\log n} \|P'\|_B \quad (117)$$

holds. The order $\sqrt{\log n}$ is best possible even in the case of the unit disk.

Maymeskul et al. [171] consider *augmented Bieberbach polynomials* which contain in addition to powers of z also suitable fractional powers and logarithmic functions such as occur in the asymptotic expansion of the mapping function near corners (see Section 2.3).

Papamichael and Kokkinos [208] compare the Ritz method and the Bergman kernel method. They find that both methods are extremely efficient provided the set of polynomial basis functions is suitably augmented by singular functions. Both methods produce results of comparable accuracy and need about the same computational effort. In the BKM the basis can be easily enlarged by new basis functions. But in the Ritz method after each change of the basis one has to start from the scratch again.

For each fixed $w \in G$, the approximate kernel $k_{B,N}(\cdot, w)$ converges to $k_B(\cdot, w)$ in the L^2 norm of G as $N \rightarrow \infty$. The speed of convergence depends on the smoothness of the boundary curve. Let H be a subregion of G . Then $k_{B,N}$ converges also in the L^2 norm of H . When $\bar{H} \subset G$ then the convergence in $L^2(H)$ can be much faster than in $L^2(G)$. When the boundary ∂H contains a subarc of ∂G , however, the rates of convergence in $L^2(H)$ are not substantially different from those in $L^2(G)$ (Papamichael and Saff [213]).

3.3. Osculation methods

The osculation method (Schmiegsverfahren) of Koebe [140] approximates F by a composition of elementary maps. It is universally applicable, since it requires no hypotheses at all concerning the boundary ∂G of the region G .

Briefly, the idea is the following: When $0 \in G$ and G is contained in the unit disk D , the quantity

$$\rho(G) = \min_{\zeta \in \partial G} |\zeta| \leq 1 \quad (118)$$

measures how far the region deviates from the disk which has $\rho(D) = 1$. Starting with $G_1 = G$, a sequence of regions G_n is constructed recursively by applying mappings h_n from a certain set of osculating functions (Schmieungsfunktionen) in such a way that $\rho(G_n)$ increases monotonically to 1. Ostrowski [205] and Henrici [106] have shown that the speed of convergence is $1 - \rho(G_n) = O(1/n)$.

Grassmann [86] has made some experiments which gave unexpectedly good results. We cite some of his findings: It is very important that the osculating functions are chosen carefully. The experience gained indicates that the method converges asymptotically very slowly, but it works surprisingly fast at the beginning. Therefore, it may well be competitive with other methods if the required accuracy is not higher than 1%.

Grassmann's experiments led him to the conclusion [86, p. 883] that "... the methods of successive approximation [= osculation methods] are competitive and deserve more attention than they obtain at present".

Gaier [65, p. 173] gives an overview of several classes of Schmieungsfunktionen used in the literature. Grassman [86] describes three classes of Schmieungsfunktionen particularly suitable for automatic calculations. Henrici [106] gives a general theory of osculation methods which covers several variants. He gives also some bounds for $\rho(G_n)$ which explain why the method converges faster initially.

Osculation methods are applicable without any requirements about shape or smoothness of the region. The more efficient rapidly convergent methods for numerical conformal mapping often require smoothness of the boundary and work best for nearly circular regions. Therefore, osculation methods are sometimes applied for preprocessing a region with the aim to make it nearly circular and to smooth the boundary. In such a way one can combine the advantages of the osculation method (fast initial convergence) with the advantages of other methods (fast convergence for nearly circular regions). Wahl [272] discusses the construction of suitable rational functions for preprocessing.

Rabinovich and Tyurin [229,230] use the original region G to construct slightly perturbed disks and then map these nearly circular regions to the unit disk using Lavrentev's variational principle (see (128) in Section 4.1).

Marshall maps first the region to a region bounded by the negative real axis plus a curve which connects 0 to infinity. Then he uses explicit mappings from the exterior of the negative real axis plus an attached segment of a circle to force one pair of grid points after the other to lie on the negative real axis. He offers a program with the illustrative title "zipper" on the Internet. (See Marshall and Rohde [170].)

3.4. Accuracy

When an approximation \tilde{F} for F is calculated, then it is easy to get a bound ε for the accuracy of the modulus of \tilde{F} . However, it is in general impossible to get from ε a bound

for the error in the argument of \tilde{F} . But under an additional assumption such an estimate can be obtained as the following theorem of Grinshpan and Saff [87, Corollary 2.4] shows.

THEOREM 16. *Let \tilde{F} be analytic and univalent in G with $\tilde{F}(0) = 0$, $\tilde{F}'(0) > 0$, and assume that the image $\tilde{F}(G)$ is starlike with respect to 0. If*

$$|\tilde{F}(z)| - 1 \leq \varepsilon \leq \frac{1}{2} \quad \text{for } z \in \Gamma, \quad (119)$$

then

$$|\arg \tilde{F}(z) - \arg F(z)| \leq 4\varepsilon^{1/2} \quad \text{for } z \in G. \quad (120)$$

4. Mapping from the disk to the region

Let G be a bounded simply connected region with $0 \in G$. There is a unique conformal mapping $\Phi : D \rightarrow G$ normalized at zero by the conditions (11). In what follows it will be more convenient to relax this condition slightly to

$$\Phi(0) = 0, \quad \operatorname{Im} \Phi'(0) = 0. \quad (121)$$

When the region G is bounded by a curve Γ then in view of Theorem 3 the conformal mapping $\Phi : D \rightarrow G$ can be extended continuously to the closure \bar{D} . When the curve Γ is parameterized by a 2π -periodic complex function $\eta(s)$ in such a way, that G is to the left of the curve when it is traversed with increasing parameter values s , then the boundary correspondence can be expressed by

$$\Phi(e^{it}) = \eta(S(t)) \quad (122)$$

with the (*inverse*) *boundary correspondence function* $S(t)$. The *reduced boundary correspondence function* $S(t) - t$ is 2π -periodic. This condition guarantees that the right-hand side of (122) goes once around G in the counterclockwise direction when t increases from 0 to 2π .

In view of equation (122) the boundary can be parameterized by the boundary values $\Phi(e^{it})$ of the conformal mapping function. Kantorowitsch and Krylow [132] call this the *normal representation*.

The *boundary correspondence equation* (122) and its variants are the basis of all methods which calculate the mapping from the disk to the region. It is interpreted as an equation which determines at the same time the conformal mapping Φ and the boundary correspondence function $S(t)$. The equation is nonlinear in S . Therefore, any solution method must be iterative.

4.1. Mapping to nearby regions

There are many results about how the conformal mapping Φ from the disk to a region G depends on the region. Generally speaking, one can say that the mapping function varies continuously with the region. Warschawski [275] reviews these results, which are useful to obtain error estimates for numerically calculated conformal mappings.

One can use the implicit mapping theorem to infer from the boundary correspondence equation (122) how the conformal mapping depends on the boundary curve of G . Particularly useful is information about how the mapping function reacts on small changes of the boundary.

The main problem for the implicit mapping theorem consists in the proof of the Fréchet differentiability of the right-hand side of (122). We quote a result of Wegmann [291] about differentiability in the Sobolev space W . When η is three times differentiable and the third derivative is Lipschitz continuous, then the mapping B defined by

$$B : W \ni S(t) - t \rightarrow \eta \circ S \in W \quad (123)$$

is Fréchet differentiable with derivative

$$DB(U)(t) = \dot{\eta}(S(t))U(t), \quad (124)$$

where on the right-hand side of (124) the function $U \in W$ is multiplied by $\dot{\eta}(S(t))$.

Assuming that the conditions for differentiability are satisfied we get from (122) the equation

$$D\Phi(e^{it}) = \dot{\eta}(S(t))DS(t) + D\eta(S(t)) \quad (125)$$

which connects the changes $D\Phi$ of the conformal mapping function and DS of the boundary correspondence function with the change $D\eta$ of the boundary curve. Therefore, equation (125) describes how Φ and S react to small changes of the region G .

Since DS is a real function the relation (125) can be transformed to an RH problem

$$\operatorname{Im} \frac{D\Phi(e^{it})}{\dot{\eta}(S(t))} = \operatorname{Im} \frac{D\eta(S(t))}{\dot{\eta}(S(t))} \quad (126)$$

which relates directly the change $D\Phi$ of the mapping function Φ to the change $D\eta$ of the curve. The analytic function $D\Phi$ must satisfy the normalization $D\Phi(0) = 0$ and $\operatorname{Im} D\Phi(0) = 0$. It follows from Corollary 1 that $D\Phi$ is uniquely determined by (126).

The right-hand side of (126) can be written in the form $(D\eta)_n / |\dot{\eta}|$ with the component $(D\eta)_n$ of the shift of the boundary curve with respect to the inner normal of Γ . The tangential component of the shift has (in first order) no influence on the mapping Φ . It affects only a change DS of the parameterization.

Most important is the special case, when G is close to the unit disk. When the boundary is parameterized by

$$\eta(s) = (1 + \tau\rho(s))e^{is} \quad (127)$$

with a real function ρ , the boundary values of the conformal mapping Φ are in first order of τ :

$$\Phi(e^{it}) = e^{it} \left(1 + \tau [\rho(t) + i\mathbf{K}\rho(t)] \right), \quad (128)$$

with the operator \mathbf{K} of conjugation defined in Section 2.5 (see Nehari [189, p. 265]). This formula is closely related to *Hadamard's variational formula* for the Green's function (see Nehari [189, p. 263]). The boundary correspondence function for the disturbed disk region (127) is in first order of τ :

$$S(t) = t + \tau \mathbf{K}\rho(t). \quad (129)$$

This is *Lavrentev's principle* [158].

When ρ is in the Hölder space $C^{n,\alpha}$ with $0 < \alpha < 1$ then there is an expansion

$$\log \frac{\Phi(z)}{z} = \sum_{v=1}^n \Phi_v(z) \tau^v + O(|\tau| |\tau \log \tau|^n) \quad (130)$$

with functions Φ_v analytic in D and continuous in \bar{D} independently of τ (see Yoshikawa [296]). The first function is determined by $\operatorname{Re} \Phi_1(e^{it}) = \rho(t)$.

Kantorovich and Krylow [132] consider the case when the boundary of G is given in implicit form by an equation

$$\Gamma = \{z = x + iy: H(x, y) = 0\} \quad (131)$$

with an analytic function H in two real variables. One can insert the ansatz

$$\Phi(e^{it}) = \sum_{k=1}^{\infty} A_k e^{ikt} \quad (132)$$

into the equation (131) for the boundary. The condition $\Phi(e^{it}) \in \Gamma$ is equivalent to the condition that the Fourier coefficients of the 2π -periodic function $H(\operatorname{Re} \Phi(e^{it}), \operatorname{Im} \Phi(e^{it}))$ all vanish. This gives an infinite system of equations for the coefficients A_k in (132). These equations become particularly simple in the case when the region is close to a disk [132, p. 381].

4.2. Projection

The boundary correspondence equation (122) says that the conformal mapping Φ is characterized by two properties:

1. Φ is an analytic function in the disk normalized by the constraints (121),
2. Φ maps the unit circle onto the boundary ∂G of the region G .

This interpretation offers the possibility of constructing the mapping Φ by an iterative procedure, which alternately calculates functions which have either the first property (normalized analytic functions) or the second property (the boundary values are in ∂G). The functions are constructed by a sort of projection onto suitable linear spaces or manifolds. This approach resembles closely the well-known procedure of determining the intersection of two subspaces of a Hilbert space by alternating projection. This method was first applied by von Neumann [190]. Therefore, it is appropriate to call methods based on this idea *alternating projection* (AP) methods.

For regions with smooth boundaries alternating projection can be applied in the following simple way:

The iteration starts with a function S_0 such that $S_0(t) - t$ is 2π -periodic. The simplest choice is $S_0(t) \equiv t$.

When S_k is determined for some $k \geq 0$ then the Fourier coefficients B_l of the boundary function

$$\eta(S_k(t)) = \sum_{l=-\infty}^{\infty} B_l e^{ilt} \quad (133)$$

are calculated. The function

$$f_k(t) = (\operatorname{Re} B_1) e^{it} + \sum_{l=2}^{\infty} B_l e^{ilt} \quad (134)$$

represents the boundary values of an analytic function

$$\Phi_k(z) = (\operatorname{Re} B_1) z + \sum_{l=2}^{\infty} B_l z^l \quad (135)$$

which obviously satisfies the conditions (121). This is the first projection step. The second step calculates a new boundary correspondence function by

$$S_{k+1}(t) := S_k(t) - \operatorname{Re} \frac{g_k(t)}{\dot{\eta}(S_k(t))} \quad (136)$$

with the nonanalytic part

$$g_k(t) = \sum_{l=-\infty}^0 B_l e^{ilt} + i(\operatorname{Im} B_1) e^{it} \quad (137)$$

of the boundary function (133). Equation (136) means that g_k is projected onto the tangent at the point $\eta(S_k(t))$ and the shift along the tangent is then replaced by a shift along the curve induced by a shift in the function S . This gives a new boundary correspondence $e^{it} \rightarrow \eta(S_{k+1}(t))$ which completes the second step of the alternating projection.

It has been proved by Wegmann [287] that this iteration converges when the boundary parameterization η is in the Hölder space $C^{3,\alpha}$ for some $\alpha \in (0, 1]$ whenever the initial approximation S_0 is sufficiently close to the correct function $S(t)$. Convergence is linear. It has been noted by Gaier [65, p. 110], that convergence of the AP method in this simple version is slow. This can easily be seen for nearly circular regions with boundary parameterization (127). Starting from $S_0(t) = t$ the next iterate gives in first order $S_1(t) = t + \frac{1}{2}\tau\mathbf{K}\rho$. Therefore, only half of the first order change $\tau\mathbf{K}\rho$ according to (129) is recovered in the first step. For nearly circular regions the rate of convergence is $1/2$. This is caused by the general fact that alternating projection methods in Hilbert spaces approach the solution always from one side.

Wegmann [287] observed that this drawback of slow convergence can be remedied by overrelaxation in the following way: The new function S_{k+1} is calculated by (136) with the function

$$g_k(t) = 2 \sum_{l=-\infty}^0 B_l e^{ilt} + i(\operatorname{Im} B_1) e^{it} \quad (138)$$

instead of (137). Note that overrelaxation with a factor 2 is applied to all terms $B_l e^{ilt}$ in (133) with $l \leq 0$ but not to the term $i(\operatorname{Im} B_1) e^{it}$. We call this overrelaxed method the *OAP method*. Analysis for nearly circular regions shows that in the first iteration the full first-order term is recovered by the OAP method. Convergence is linear. It has been shown by Wegmann [287, p. 304], that for regions with parameterization (127) the rate q of convergence of the OAP method can be estimated by

$$q \leq 2\tau \|\dot{\rho} - \mathbf{K}\rho\|_\infty + o(\tau). \quad (139)$$

Although the method converges linearly, convergence can be very fast for some regions.

The method can be applied numerically on a grid with $N = 2n$ equidistant grid points $t_j = (j - 1)2\pi/N$. Fourier analysis of the boundary function at the grid points

$$\eta(S_k(t_j)) = \sum_{l=-n}^{n-1} B_l e^{ilt_j} \quad (140)$$

gives the coefficients B_l . With these coefficients the polynomial

$$g_k(t) = \sum_{l=-n}^0 B_l e^{ilt} + i(\operatorname{Im} B_1) e^{it} \quad (141)$$

is formed which is inserted (with a factor 2 in front of the sum for the OAP method) into (136) to calculate the values of the new function S_{k+1} at the grid points.

This AP method needs only a subroutine which calculates the Fourier analysis (140) of the boundary mapping and the Fourier synthesis (141) of the nonanalytic part. This can be

very efficiently done by FFT. The AP method is certainly one of the simplest numerical methods for conformal mapping. It is easy to apply and very robust.

Convergence of the AP method means that the curves parameterized by the functions f_k defined in analogy to (134) by

$$f_k(t) = (\operatorname{Re} B_1)e^{it} + \sum_{l=2}^{n-1} B_l e^{ilt} \quad (142)$$

approach the curve Γ as $k \rightarrow \infty$.

We show this at an example.

EXAMPLE 1. An ellipse with axes a and b rotated by an angle α and shifted by z_0 is parameterized by

$$\eta(s) = z_0 + e^{i\alpha}(a \cos s + ib \sin s). \quad (143)$$

Figure 6 shows the mapping Φ from the disk to the ellipse of Example 1 for parameters $a = 1$, $b = 0.7$, $z_0 = -0.4 - 0.2i$, $\alpha = 0$. The calculation is done on a grid with $N = 256$ points with the OAP method starting with $S_0(t) = t$. The dotted lines are the curves parameterized by the functions f_k defined in (142) for $k = 0, 1, 2, \dots$. These curves approximate the ellipse better and better as k increases. Only the first two functions f_0 and f_1 differ significantly from the ellipse.

We use several indicators for convergence and accuracy. First, we take the maximum change in each step over all grid points t_j :

$$\delta_k := \max_j |S_{k+1}(t_j) - S_k(t_j)|. \quad (144)$$

As a measure of analyticity of the boundary values $\eta(S_k(t))$ one can use the L^2 norm of the nonanalytic part

$$\alpha_k := \|g_k\|_2 = \left(\sum_{l=-n}^0 |B_l|^2 + (\operatorname{Im} B_1)^2 \right)^{1/2}. \quad (145)$$

As a measure for the accuracy achieved one can take the distance of the boundary values of the polynomial f_k to the curve Γ . To this aim we evaluate f_k on a refined grid $t_j^* = (j-1)\pi/N$, $j = 1, \dots, 2N$. We define $S_k(t_j^*)$ for odd values of j by trigonometric interpolation of $S_k(t_j) - t_j$, and define

$$\varepsilon_k = \max_j |f_k(t_j^*) - \eta(S_k(t_j^*))|. \quad (146)$$

The right panel of Figure 6 shows the maximum change δ_k in S_k in each iterative step k , and the measures α_k and ε_k for analyticity and accuracy. All three of these quantities decrease geometrically like q^k with a convergence factor of $q \approx 0.85$. The convergence is

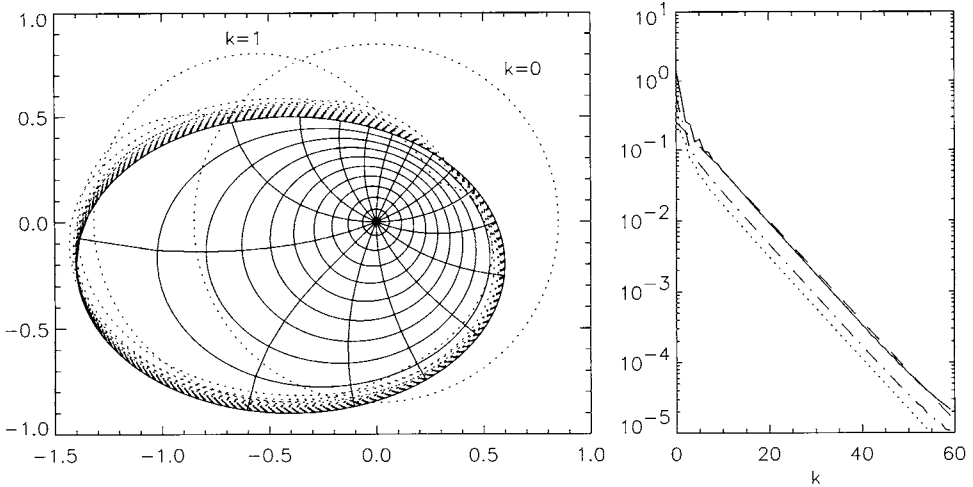


Fig. 6. Conformal mapping from the unit disk to an eccentric ellipse with parameterization (143). The solid lines show images of 10 concentric circles and 16 spokes. The dotted lines are the curves parameterized by the functions f_k defined in (142) during iteration with the OAP method. The right panel shows δ_k (solid), α_k (dotted), ε_k (dash-dotted) and Cq^k (dashed) for each iterative step k .

much faster in the first two iterations, where the f_k approach the ellipse. The AP method converges at a rate $q \approx 0.895$.

Convergence of the AP method is proved only for smooth curves. But the iteration, consisting of the steps (140), (141) and (136), can be performed also for piecewise smooth curves. Numerical experiments show that the AP method works also for such cases. We demonstrate this with two examples.

EXAMPLE 2. Square, shifted by z_0 , with boundary parameterization

$$\eta(s) = z_0 + \begin{cases} \frac{\pi}{4}(1 - i) + si & \text{for } 0 \leq s \leq \frac{\pi}{2}, \\ \frac{\pi}{4}(3 + i) - s & \text{for } \frac{\pi}{2} \leq s \leq \pi, \\ \frac{\pi}{4}(-1 + 5i) - si & \text{for } \pi \leq s \leq \frac{3\pi}{2}, \\ \frac{\pi}{4}(-7 - i) + s & \text{for } \frac{3\pi}{2} \leq s \leq 2\pi. \end{cases} \quad (147)$$

The mapping from the disk to the square of Example 2 with shift $z_0 = -0.2 + 0.2i$ is calculated with the AP method. The iteration is started with $S_0(t) = t$. The calculation is done with $N = 1024$ grid points. The curves parameterized by the f_k converge to the square. The rate of convergence is about $q = 0.92$. The speed of convergence depends to some extent on the number of grid points. Convergence is slower for a finer grid, when more and more of the corner regions becomes resolved. The maximum δ_k of the shift is a little jumpy (see Figure 7), since the projection to the curve changes when a grid point is pushed from one edge to the next across a corner. The measure α_k for analyticity decreases only up to a certain point, since on 1024 grid points the slowly decaying Taylor coefficients

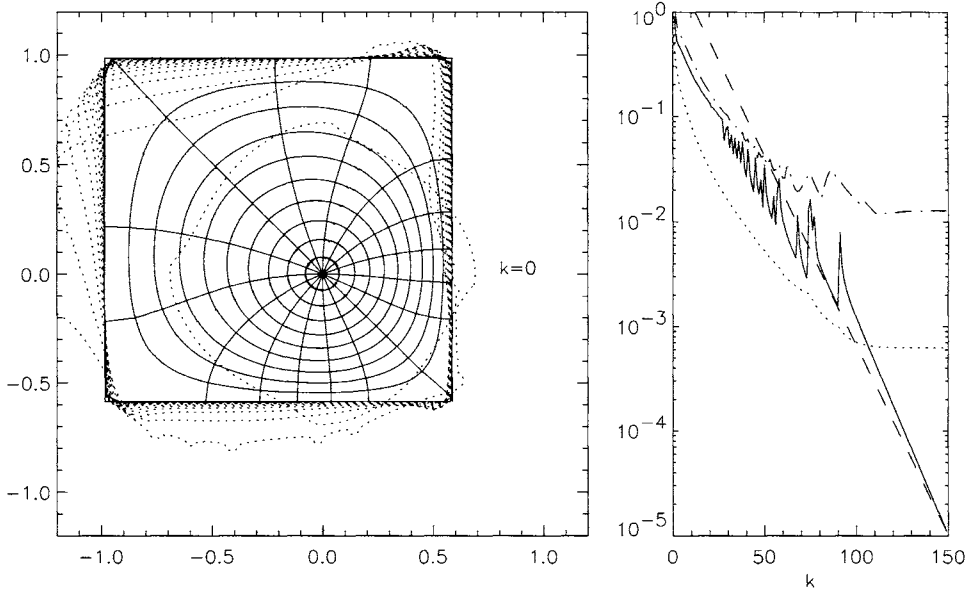


Fig. 7. The same as Figure 6 for the conformal mapping from the unit disk to the shifted square of Example 2 calculated with the AP method. The functions f_k defined in (142) are shown only for every fifth step.

of Φ cannot all be represented to machine precision. The accuracy achieved is about 0.01 as measured in ε . It cannot be further improved on this grid.

One can avoid the problems with the discontinuous $\dot{\eta}$ by replacing it by a smooth function ξ which retains to some extent the orientation of $\dot{\eta}$. Instead of the orthogonal projection onto the tangent an oblique projector is applied. The second step in this method (we call it *smoothed AP method*) is

$$S_{k+1}(t) := S_k(t) - \operatorname{Re} \frac{g_k(t)}{\xi(S_k(t))} \quad (148)$$

instead of (136).

EXAMPLE 3. Eccentric heart with boundary is parameterized by

$$\eta(s) = z_0 + \begin{cases} 1 + 2(-1 + i)s/\pi & \text{for } 0 \leq s \leq \frac{\pi}{2}, \\ 0.5(-1 + i) \\ + \exp(i(2s - 3\pi/4))/\sqrt{2} & \text{for } \frac{\pi}{2} \leq s \leq \pi, \\ -0.5(1 + i) \\ + \exp(i(2s - 5\pi/4))/\sqrt{2} & \text{for } \pi \leq s \leq \frac{3\pi}{2}, \\ -i + 2(1 + i)(s - 3\pi/2)/\pi & \text{for } \frac{3\pi}{2} \leq s \leq 2\pi. \end{cases} \quad (149)$$

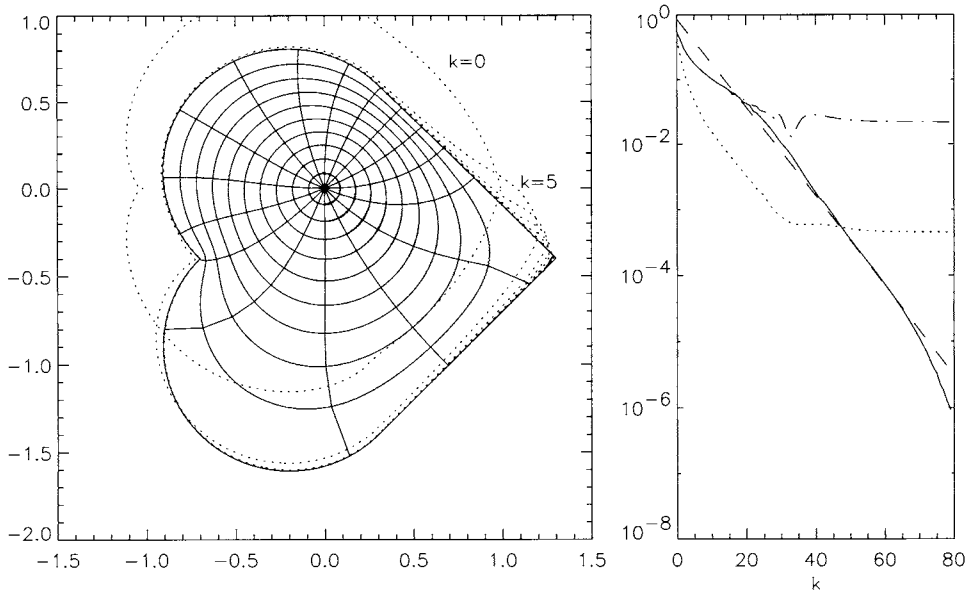


Fig. 8. The same as Figure 7 for the conformal mapping from the unit disk to the heart of Example 3 calculated by the smoothed AP method.

Figure 8 shows the result of a calculation with the smoothed AP method with $\xi(s) = ie^{is}$ for the eccentric heart of Example 3 with $z_0 = 0.3 - 0.4i$. The iteration was started with $S_0(t) = t$ and performed on a grid with $N = 1024$ points. The accuracy is about 0.02. The rate of convergence is $q = 0.855$. The rate of convergence for the (nonsmoothed) AP method was $q = 0.935$. This example demonstrates that the AP method works well even for regions with reentrant corners.

There are several variants of the projection method. All have in common the first projection step (135) which extracts the analytic part of $\eta \circ S_k$. But they differ in the way the nonanalytic part is used to change the boundary correspondence function.

The original version of Bergström [16] (see also Gaier [65, p. 109]) is applicable for star-shaped regions with parameterization $\eta(s) = \rho(s)e^{is}$. The second projection is along lines of equal argument, i.e.,

$$S_{k+1} := \arg f_k(t). \quad (150)$$

Bishopp [21] determines a least-square approximation to the solution of the boundary correspondence equation. In an alternating iterative procedure he determines first an approximation to $\eta(S_k(t))$. This is the f_k of (134). The vanishing of the first variation of S_k gives the condition

$$\operatorname{Re}(\overline{\dot{\eta}(S_k(t))}(f_k(t) - \eta(S_k(t)))) = 0. \quad (151)$$

Newton's method for this equation gives an update for S_k which differs only slightly from (136).

Klonowska and Prosnak [136] arrange the new parameter points $S_{k+1}(t_j)$ in such a way that the distance between adjacent points $\eta(S_{k+1}(t_j))$ and $\eta(S_{k+1}(t_{j+1}))$ on Γ and the distance between two adjacent points $f_k(t_j)$ and $f_k(t_{j+1})$ on the curve parameterized by $f_k(t)$ (both measured by arclength) are in the same ratio for all intervals. This method is also applicable for nonsmooth curves. A normalization $\Phi(1) = \eta(s_0)$ must be used instead of $\Phi'(0) > 0$.

Li and Syngellakis [165] determine $S_{k+1}(t_j) = s^*$ as the parameter value s^* of that point on Γ which is closest to the point $f_k(t_j)$, i.e., gives the minimum Euclidean distance $|f_k(t_j) - \eta(s)|$ among all s . This method is applicable also for nonsmooth curves.

Li and Syngellakis [165] conjecture that their method converges globally. This is empirically supported by several examples. These authors point out that the numerical effort in each iteration of their algorithm is less than in the Newton methods. This is true. They claim even that their “algorithm should be more efficient than Wegmann's method” [165, p. 637]. This is not true in general (see Figure 16).

For a star-shaped region with boundary parameterization

$$\eta(s) = \rho(s)e^{is} \quad (152)$$

one can write the boundary correspondence equation in the form

$$\Psi(e^{it}) = \log \rho(S(t)) + i(S(t) - t) \quad (153)$$

with the auxiliary analytic function

$$\Psi(z) := \log(\Phi(z)/z), \quad (154)$$

which satisfies

$$\operatorname{Im} \Psi(0) = 0 \quad (155)$$

since $\Psi(0)$ is the logarithm of the positive number $\Phi'(0)$. Upon eliminating Ψ from equation (153) with Theorem 8 using (155), the *integral equation of Theodorsen* [258]

$$S(t) = t + \mathbf{K}[\log \rho(S(t))] \quad (156)$$

is obtained. It involves the operator \mathbf{K} of conjugation. Equation (156) has a unique continuous solution S whenever the derivative ρ' is continuous. For unicity it is even sufficient that ρ' exists and is bounded (von Wolfersdorf [294]). Each solution S of (156) gives a function Φ which automatically satisfies the normalization $\Phi'(0) > 0$.

The usual way to solve the nonlinear integral equation (156) is by iteration (Theodorsen [258], Theodorsen and Garrick [259]). This approach has become even more attractive since now FFT can be applied to evaluate the conjugation operator numerically very efficiently (Henrici [103,104]).

Starting from a function S_0 such that $S_0(t) - t$ is 2π -periodic, the next iterates are calculated by *successive conjugation*

$$S_{k+1}(t) = t + \mathbf{K}[\log \rho(S_k(t))]. \quad (157)$$

There are several interpretations of this process. One can think of it as a projection method which in the first step calculates the boundary values of an analytic function

$$f_k(t) := \rho(S_k(t)) \exp(i(S_{k+1}(t))). \quad (158)$$

These values are in general not on the boundary curve. Therefore, a second projection must be applied which gives values $\rho(S_{k+1}(t)) \exp(i(S_{k+1}(t)))$ on the curve. The projection is here along lines of equal argument.

The iterates S_k defined by (157) converge uniformly whenever the function ρ is absolutely continuous and satisfies a so-called *epsilon condition*

$$\left| \frac{\dot{\rho}(s)}{\rho(s)} \right| \leq \varepsilon \quad \text{for almost all } s, \quad (159)$$

with a number $0 < \varepsilon < 1$. Convergence in L^2 is linear with a rate $\leq \varepsilon$. The rate q of uniform convergence is $\leq \sqrt{\varepsilon}$ (see Gaier [71,65]). This rate, however, can be improved if the boundary is sufficiently smooth (Gaier [65, p. 71]).

One can check the epsilon condition also in a general parameterization $\eta(t) = x(t) + iy(t)$ of the curve using

$$\frac{\dot{\rho}(s)}{\rho(s)} = \frac{xx' + yy'}{xy' - yx'}, \quad (160)$$

where on the right-hand side differentiation is with respect to the curve parameter t . For an ellipse with axes a, b with $b < a$ one obtains $\varepsilon = (a^2 - b^2)/2ab$ which is less than 1 for $b/a > \sqrt{2} - 1 = 0.414\dots$

The Theodorsen equation (156) is discretized in an obvious way. The functions S_k are evaluated at $N = 2n$ grid points t_j , and the conjugation operator \mathbf{K} is replaced by \mathbf{K}_N as defined in (32). A system of N nonlinear equations is generated

$$S(t_j) = t_j + \mathbf{K}_N[\log \rho(S(t))], \quad j = 1, \dots, N. \quad (161)$$

Note that \mathbf{K}_N requires only the values of $\log \rho(S(t))$ on the grid. These equations are very well investigated. We quote Gaier [71]: "... probably no nonlinear system of equations has received more attention than (T_d) [= the discrete Theodorsen equations (161)]".

When the boundary curve satisfies an epsilon condition (159) with $\varepsilon < 1$ then the discrete Theodorsen equation can be solved by the method of successive conjugation. The iterates converge linearly with a rate $\leq \varepsilon$ (Opitz [203]).

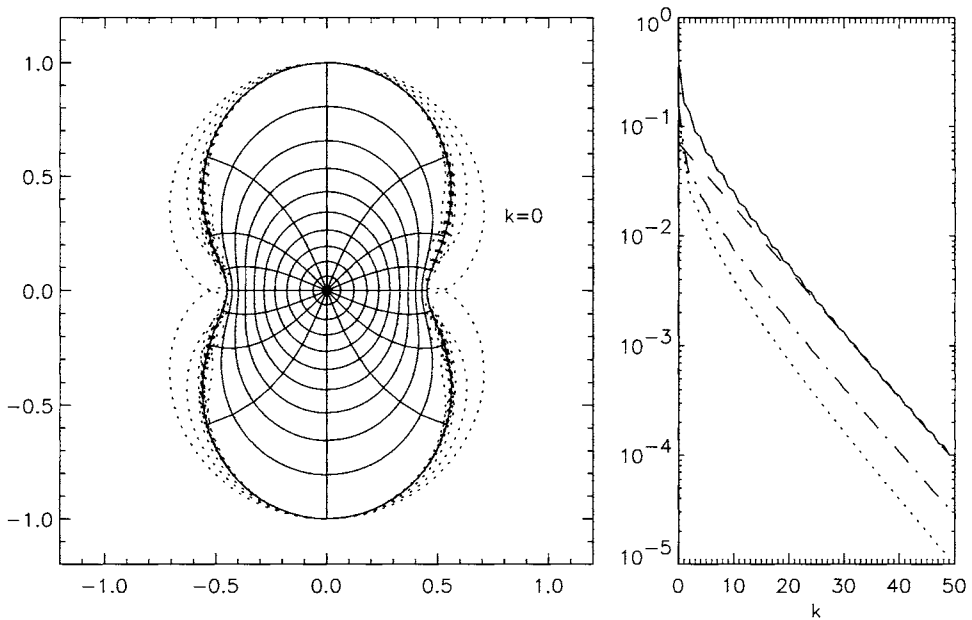


Fig. 9. Conformal mapping from the unit disk to an inverted ellipse with parameterization (162) by the Theodorsen method. The dotted lines are the curves parameterized by the functions f_k defined in (158). The right panel shows δ_k (solid), α_k (dotted), ε_k (dash-dotted) and Cq^k (dashed) for each iterative step k .

EXAMPLE 4. Inverted ellipse with parameterization (152) where ρ is the function

$$\rho(s) := \sqrt{1 - (1 - p^2) \cos^2 s}. \quad (162)$$

Figure 9 shows the result of a calculation with Theodorsen's method for the mapping of the disk to an inverted ellipse (Example 4) with parameter $p = 0.45$. This curve satisfies the epsilon condition for $\varepsilon = 0.886$. The calculation is performed with 256 grid points. The analytic functions f_k defined in (158) approach the boundary curve. The right panel of the figure shows the maximal change in each step and the measures of accuracy α_k and ε_k defined in (145) and (146). The iteration converges linearly with a rate $q = 0.883$. The images of the grid points crowd near the waist of the wasplike figure.

One can exploit the checkerboard structure of the Wittich matrix (see Gaier [65, p. 76] for definition and details) to separate the values with odd and even indices. This leads to two coupled systems of equations, which can be treated by an “Einzelstschrittverfahren”. This converges twice as fast as the “Gesamtschrittverfahren”, i.e., the method of successive conjugation (Niethammer [191], Hübner [119]).

For nearly circular regions with a boundary parameterization (125) the iteration starting from $S_0(t) = t$ gives already in the first step the approximation $S_1(t) = t + \tau \mathbf{K} \rho + o(\tau)$ which is accurate in first order of τ in view of Lavrentev's principle (128). Therefore, nothing can be gained by over- or underrelaxation – at least for nearly circular regions.

This is different for general regions. The iterative solution of the discrete Theodorsen equation can be interpreted as a Jacobi iterative method. It was found in several investigations (Niethammer [191], Gutknecht [92,94,95], Kaiser [131]) that the convergence can be accelerated by underrelaxation, i.e., instead of (157) the equation

$$S_{k+1}(t) = (1 - \omega)S_k(t) + \omega[t + \mathbf{K}(\log \rho(S_k))] \quad (163)$$

is used for iteration with an ω in the range $0 < \omega < 1$. For some cases, the choice of the relaxation parameter

$$\omega = \frac{2}{1 + \sqrt{1 + L^2}} \quad (164)$$

with $L := \|\dot{\rho}/\rho\|_\infty$ is optimal (Niethammer [191], Gutknecht [92,95]). Gutknecht [94] reports experiences (convergence and accuracy) from a number of test calculations with several variants of stationary iteration methods and optimal and nearly optimal relaxation parameters.

Gutknecht [94, p. 4] wrote in 1983: "It is still an open question which method is best in which situation. But numerical experiments presented here show that our methods [Theodorsen with underrelaxation] are definitely among the fastest".

The iteration with underrelaxation converges sometimes even when the boundary does not satisfy the epsilon condition (159) with $\varepsilon < 1$. On the other hand, Hübner [120] has shown that there are regions satisfying an epsilon condition with $\varepsilon > 1$ such the iteration (163) diverges for any choice of ω .

EXAMPLE 5. Regular pentagon with parameterization (152), where ρ is the function

$$\rho(s) := 1/\cos(s - (2j-1)\pi/5) \quad \text{for } 2j\pi/5 \leq s \leq 2(j+1)\pi/5, \quad (165)$$

for the five sides $j = 0, 1, \dots, 4$.

Theodorsen's method can easily be applied for regions with corners. This is demonstrated by Example 5. The result of a calculation with $N = 1024$ grid points is shown in Figure 10. The rate of convergence is $q = 0.5$. The pentagon satisfies the epsilon condition with $\varepsilon = 0.72$. In this example the rate of convergence is less than ε . The accuracy achieved is about 0.01.

The square satisfies (159) only with $\varepsilon = 1$. Theodorsen's method does not converge.

Theodorsen's method becomes inaccurate if the boundary is not smooth. Often the numerically calculated approximations to $S(t)$ are not monotone. Gutknecht [94] recommended to remove the corners by preliminary maps.

Nitsche [193] considers the solution of the Theodorsen equation (153) by a finite element method. The solution of Theodorsen's equation by a Newton method will be discussed in Section 4.3.

Theodorsen's method is very simple to program. It is remarkably stable. The iteration converges globally if only the epsilon condition is satisfied with $\varepsilon < 1$. This is a very

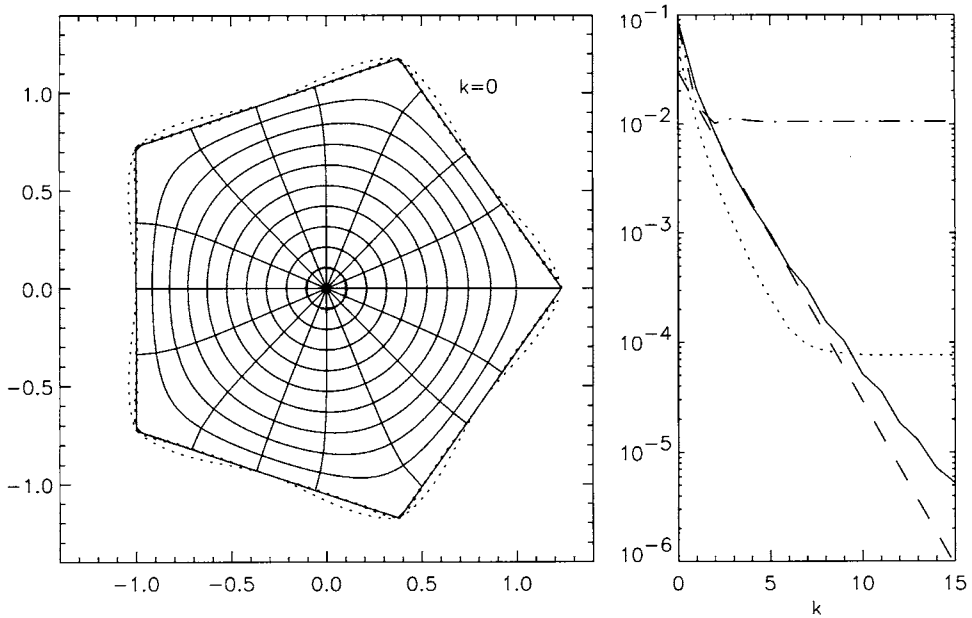


Fig. 10. Conformal mapping from the unit disk to the regular pentagon of Example 5 by the Theodorsen method.
For the interpretation see Figure 9.

remarkable property. Most of the other iterative methods converge only locally, i.e., only if a sufficiently good initial approximation is known in advance. On the other hand, the requirement that the boundary curve must be parameterized in polar coordinates (152) is a real obstacle in practical applications.

There are other projection methods. Melentev (see [132, p. 415]) and Kulisch [151] propose for star-shaped regions the following iterative method which is based on the observation that the function $\mathcal{E}(z) := \Phi(z)/z$ has boundary values

$$\mathcal{E}(e^{it}) = \rho(S(t)) \exp[i(S(t) - t)]. \quad (166)$$

Starting from $\mathcal{E}_0(z) = z$, a sequence of analytic functions \mathcal{E}_k and boundary correspondence functions S_k is constructed for $k \geq 1$ iteratively by

$$S_k(t) := t + \arctan \frac{\operatorname{Im} \mathcal{E}_{k-1}(e^{it})}{\operatorname{Re} \mathcal{E}_{k-1}(e^{it})}. \quad (167)$$

This is a projection of $\mathcal{E}(e^{it})$ onto the curve, since $\rho(S_k(t)) \exp[i(S_k(t) - t)]$ is on Γ . If S_k is inserted on the right-hand side of (166), it will not give the boundary values of an analytic function. The new \mathcal{E} is constructed in such a way that it has the same real part as the function obtained by inserting S_k in the right-hand side of (166):

$$\mathcal{E}_k(e^{it}) := (\mathbf{I} + i\mathbf{K})[\rho(S_k(t)) \cos(S_k(t) - t)]. \quad (168)$$

This method is suitable for a graphical solution procedure (see [132]). In the first step (168) the points are pushed parallel to the imaginary axis and in the second step (167) in the radial direction. For nearly circular regions the Melentev–Kulisch method coincides with the Theodorsen method up to terms of order $O(\tau^2)$. In particular, it recovers in the first step the full first-order correction $\tau \mathbf{K}\rho$ to the initial guess $S_0(t) = t$. Kulisch [151] presents a wiring diagram for an analog computer which performs this iteration.

A test calculation with the Melentev–Kulisch method for an inverted ellipse with parameter $p = 0.35$ (Example 4) converged linearly with a rate $q = 0.86$. There is an x - y -asymmetry in the method. It converges no longer when the boundary curve is rotated by 90° . It does not converge for the pentagon of Example 5.

Lotfullin [167] uses a projection method for the calculation of the inverse mapping $F : G \rightarrow D$. First the region is preprocessed by an osculation method to make it nearly circular. This gives an approximation $F_0(z)$ for F .

Starting with this analytic function the iteration proceeds as follows for $k \geq 1$. The function

$$g_k(s) := \exp[i \arg(F_{k-1}(\eta(s)))] \quad (169)$$

has values on the unit circle. Equation (169) means that the boundary values of F_{k-1} are projected onto the unit circle along rays through the origin. From the function g_k the analytic part, extracted by means of Plemelj's formula

$$F_k(\eta(t)) := \frac{1}{2} g_k(t) + \frac{1}{2\pi i} \int_{\Gamma} \frac{g_k(s)}{\eta(s) - \eta(t)} d\eta(s), \quad (170)$$

gives the next approximation F_k for F .

The numerical evaluation of the principal value integral in (170) is not so simple for a general region. Therefore, projection methods are mainly used to calculate the mapping Φ from the disk to the region, but rarely for the inverse function F .

4.3. Newton methods

One can solve the boundary correspondence equation (122) also by the Newton method. Linearization yields the equation

$$\Phi(e^{it}) + D\Phi(e^{it}) = \eta(S(t)) + \dot{\eta}(S(t))DS(t) \quad (171)$$

which connects the change $D\Phi$ of the analytic function Φ with the change $DS(t)$ of the boundary correspondence function $S(t)$. One can use this relation to solve (122) at least in first order. Since $DS(t)$ must be a real function it can be eliminated from (171) and a boundary problem

$$\operatorname{Im} \frac{\Psi(e^{it})}{\dot{\eta}(S(t))} = \operatorname{Im} \frac{\eta(S(t))}{\dot{\eta}(S(t))} \quad (172)$$

for the analytic function $\Psi := \Phi + D\Phi$ remains. It is a Riemann–Hilbert problem as discussed in Section 2.5. The necessary change of S to satisfy (122) in first order is given by

$$DS(t) = \operatorname{Re} \frac{\Psi(e^{it})}{\dot{\eta}(S(t))} - \operatorname{Re} \frac{\eta(S(t))}{\dot{\eta}(S(t))} \quad (173)$$

with a solution Ψ of (172). This is the basis of the following iterative method first proposed by Wegmann [282,283].

When the parameterization is differentiable with Lipschitz continuous derivative $\dot{\eta} \neq 0$, the derivative can be written in the form

$$\dot{\eta}(s) = r(s)e^{i\theta(s)} \quad (174)$$

with Lipschitz continuous functions θ and $r > 0$.

The iteration starts with a function $S_0(t)$ such that $S_0(t) - t$ is a 2π -periodic function in the Sobolev space W . (The natural choice is $S_0(t) = t$.)

When S_k is determined for some $k \geq 0$ then the following functions and numbers must be calculated (\mathbf{K} and \mathbf{J} are the conjugation and averaging operators defined in Section 2.5):

$$v(t) := \theta(S_k(t)) - t = \arg[e^{-it}\dot{\eta}(S_k(t))], \quad (175)$$

$$w := \mathbf{K}v, \quad \alpha := \mathbf{J}v, \quad (176)$$

$$g(t) := r(S_k(t)) \exp(w(t)) \operatorname{Im} \frac{\eta(S_k(t))}{\dot{\eta}(S_k(t))}, \quad (177)$$

$$h := \mathbf{K}g, \quad \gamma := \mathbf{J}g, \quad (178)$$

$$DS(t) = -\frac{\gamma \cot \alpha + h(t)}{r(S_k(t)) \exp(w(t))} - \operatorname{Re} \frac{\eta(S_k(t))}{\dot{\eta}(S_k(t))}, \quad (179)$$

$$S_{k+1}(t) := S_k(t) + DS(t). \quad (180)$$

The functions v, w, g, h, DS and the numbers α, γ depend on the iteration number k . We have omitted the index k for notational convenience.

When η is differentiable with Lipschitz continuous derivative $\dot{\eta}$, the method converges in W provided the iteration starts with a function S_0 which is sufficiently close to the correct boundary correspondence function \tilde{S} . When η is twice differentiable and $\ddot{\eta}$ satisfies a Hölder condition with exponent μ then the order of convergence is at least $1 + \mu$. In particular, for Lipschitz continuous $\dot{\eta}$ convergence is quadratic (Wegmann [282, Theorem 1]).

The method can be applied numerically in a straightforward way on a grid of $N = 2n$ equidistant points $t_j = (j - 1)2\pi/N$ in the interval $[0, 2\pi]$. In the formulas above everywhere the operator \mathbf{K} has to be replaced by its discrete approximation \mathbf{K}_N on this grid. In each iterative step two conjugations must be calculated, namely in (176) and (178). This requires four FFTs. Using a grid with N points, where N is a power of 2, the computational cost is of the order $O(N \log_2 N)$.

This method works very well and follows the quadratic convergence closely as long as the discretization error is small compared with the changes DS . It has been noted by several people (Song [245], Wegert [279] and several personal communications) that the method approaches the solution very fast in the first iterations but then has a tendency to turn away. It may even diverge finally. Convergence cannot be enforced by increasing the number of grid points, or by starting with a better S_0 , or by calculating with higher precision. This was nicely demonstrated by Song [245]. She calculated with quadruple precision, got very precise results – but the iteration diverged finally.

Wegmann [288] investigated this convergence–divergence phenomenon. He showed that the method, when discretized in this straightforward way, does not converge. The nuisance is generated by a $\cos nt$ term. Although this term is negligibly small for smooth curves and large N , it is inevitably generated by roundoff errors. Wegmann [288] showed that the discretized method converges at least for nearly circular regions, when the annoying $\cos nt$ term is removed. This can be done by using instead of (179) the modified formula

$$DS(t) = -\frac{\gamma \cot \alpha + h(t) + \beta \cos nt}{r(S_k(t)) \exp(w(t))} - \operatorname{Re} \frac{\eta(S_k(t))}{\dot{\eta}(S_k(t))}, \quad (181)$$

where β is the coefficient of the $\cos nt$ term in the trigonometric interpolation polynomial of order n for the function v on a grid with $N = 2n$ equidistant points.

Strictly speaking the discretized method converges only linearly. But this linear convergence pertains only to the final stage where small changes occur. In the first stage where the gross features of the parameter functions are modeled, convergence follows the quadratic behavior of the continuous method. Baty and Morris [8] report some practical experiences with this method.

This method has been carried over by Wegert [279] to the solution of nonlinear RH problems. Wegert noted that the convergence can be improved by smoothing the function DS . Song et al. [246, 247] apply a low-frequency filter. It has been shown by Wegmann [291] that the problem of divergence is connected with the fact that the approximations \mathbf{K}_N for the conjugation operator as Banach space operators converge strongly to \mathbf{K} as $N \rightarrow \infty$ but not uniformly. But when the operators are restricted to a compact subset, convergence is uniform. This can be enforced by the restriction to a suitable finite subspace. This is the main reason why convergence of the discrete method can be reestablished by the following smoothing procedure.

Let $M := 2m < N$ be a fixed natural number. The function DS is calculated by (179). The Fourier coefficients are determined

$$DS(t) := \sum_{l=0}^n a_l \cos lt + \sum_{l=1}^{n-1} b_l \sin lt \quad (182)$$

and then DS is replaced by the truncated trigonometric polynomial

$$DS^*(t) := \sum_{l=0}^m a_l \cos lt + \sum_{l=1}^m b_l \sin lt \quad (183)$$

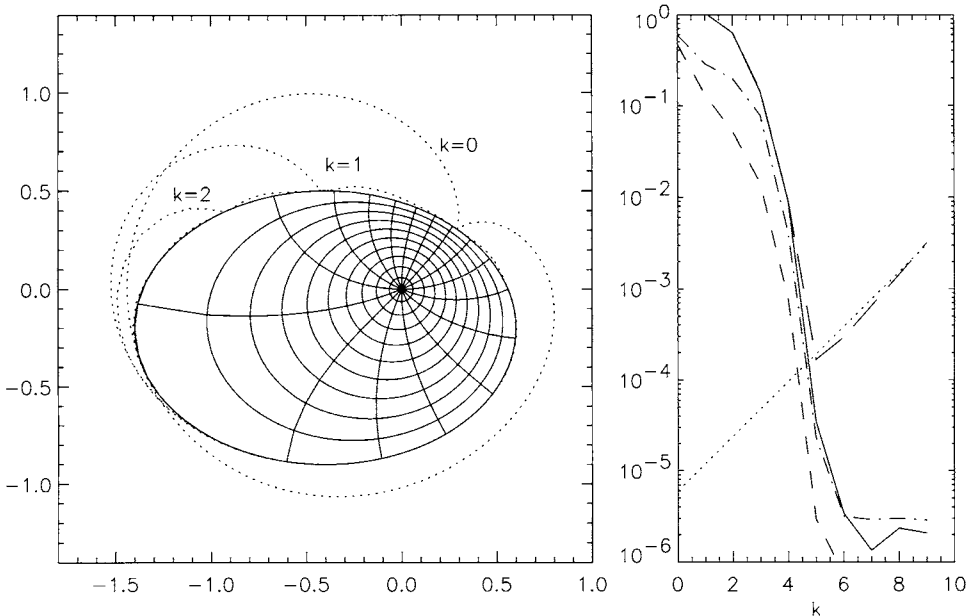


Fig. 11. Conformal mapping to the ellipse of Example 1 with the (damped) Wegmann method. The dotted lines show the boundary values of the analytic functions Φ_k of (184). The right panel shows the $\delta_k, \alpha_k, \varepsilon_k$ during the iteration. For the long-dashed and dotted lines see the text.

which then is used to calculate the new iterate $S_{k+1} = S_k + DS^*$.

The effect of this smoothing is demonstrated by a calculation for Example 1 (parameters: $a = 1, b = 0.7, z_0 = -0.4 - 0.2i, \alpha = 0$) with the Wegmann method with $N = 256$ grid points. A damping according to (183) is performed with $m = 108$. The result is shown in Figure 11. The curves

$$\Phi_k(e^{ir}) = \eta(S_k(t)) + \dot{\eta}(S_k(t))(S_{k+1}(t) - S_k(t)) \quad (184)$$

which by construction are the boundary values of analytic function Φ_k differ noticeably from Γ only for $k = 0, 1, 2$. This can be compared with Figure 6.

After eight steps the iteration becomes stationary in single precision. Convergence is quadratic initially. For comparison, the values of δ_k are inserted for the method without damping (long-dashed). These values increase after the 6th iteration in geometric progression. The long-dashed curve points back to a point around 5×10^{-6} (dotted line) on the ordinate, indicating that the noise is generated by rounding errors, which are amplified in each step.

One might be afraid that the damping according to (182) and (183) requires two other Fourier transforms and therefore causes much additional cost. But in many cases it is quite sufficient to damp a few of the highest terms, with the number $L = n - m$ of damped coefficients independent of the number N of grid points. This requires only computing time of the order $O(N)$. We demonstrate this at the same example as before. Figure 12

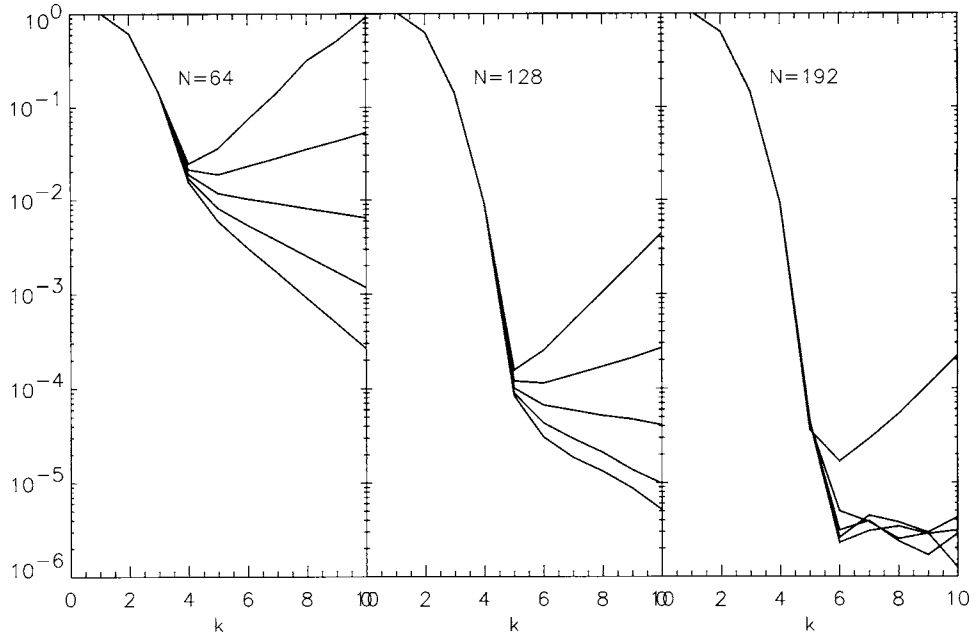


Fig. 12. The shift δ_k during the calculation with Wegmann's method for the same ellipse as in Figure 11 for three values of N and $L = 0, 1, 2, 3, 4$ damped Fourier coefficients.

shows the convergence, measured by the shift δ_k in each step, for different numbers of grid points and $L = 0, 1, 2, 3, 4$ damped Fourier terms. Apparently for each N the damping of 2 terms suffices to make the iteration convergent. The rate of the final convergence (or divergence) depends mainly on L . Convergence is faster, when more Fourier terms are damped.

Henrici [107, p. 422] wrote in 1986: "In view of its quadratic convergence [...] and its $O(n \log n)$ operations count per iteration step, Wegmann's method may well be the best mapping method in existence, but sufficient experimental documentation is as yet lacking".

Vertgeim [270] considered in 1958 boundary curves with the representation

$$\eta(s) = \exp(f_1(s) + i f_2(s)) \quad (185)$$

with real functions f_1, f_2 such that $f_1(s)$ and $f_2(s) - s$ are 2π -periodic. It is assumed that f_1, f_2 have Lipschitz continuous second derivatives and the first derivative $\dot{f}_2 - i\dot{f}_1$ does not vanish. The 2π -periodic functions θ and $r > 0$ are defined by

$$\dot{f}_2(s) - i\dot{f}_1(s) = r(s) \exp(i\theta(s)). \quad (186)$$

A boundary correspondence equation analogous to (122) can be written in the form

$$\Psi(e^{it}) = f_1(S(t)) + i[f_2(S(t)) - t] \quad (187)$$

with the analytic function $\Psi(z)$ defined in (154). This is equivalent to the functional equation for S ,

$$P[S] := f_2(S(t)) - t - \mathbf{K}f_1(S(t)) = 0. \quad (188)$$

The Newton method for this equation starts with an initial guess S_0 and calculates the change $DS = S_{k+1} - S_k$ in the k th iteration from the linearized equation (188)

$$\dot{f}_2(S_k(t))DS - \mathbf{K}[\dot{f}_1(S_k(t))DS] = -P[S_k]. \quad (189)$$

After multiplication of (189) by \dot{f}_1 the equation attains the form of an RH problem

$$\operatorname{Re}[(\dot{f}_2 + i\dot{f}_1)\mathcal{E}(e^{it})] = -\dot{f}_1 P \quad (190)$$

for the analytic function \mathcal{E} in D with boundary values

$$\mathcal{E}(e^{it}) = (\mathbf{I} + i\mathbf{K})(\dot{f}_1 DS). \quad (191)$$

The function DS is obtained from \mathcal{E} using $\dot{f}_1 DS = \operatorname{Re} \mathcal{E}(e^{it})$.

The RH problem (190) for \mathcal{E} can be solved by the standard method using the operators \mathbf{K}, \mathbf{J} of conjugation and averaging. When the functions and numbers

$$v(t) := \theta(S_k(t)), \quad w := \mathbf{K}v, \quad \alpha := \mathbf{J}v, \quad (192)$$

$$h := -\frac{e^w \dot{f}_1 P}{r} \quad (193)$$

are calculated, the change $DS = S_{k+1} - S_k$ is obtained by

$$DS = -\frac{\dot{f}_2 P}{r^2} + \frac{1}{re^w}(\mathbf{K} - \tan \alpha \mathbf{J})h. \quad (194)$$

The $(\tan \alpha)$ -term in (194) comes from the condition $\operatorname{Im} \mathcal{E}(0) = 0$ which follows from the representation (191).

Vertgeim [270] did not take full advantage of his approach. He applied a quasi-Newton method, insofar as he inserted everywhere in the formulas (192), (193) and (194) the initial guess S_0 . He proved that the iterates converge in a Hölder-norm, provided the initial guess S_0 is sufficiently close to the correct parameter mapping S and $\cos \alpha \neq 0$. The same proof, however, can be applied to show the convergence of the full Newton method, where in the formulas (192)–(194) everywhere the last iterate S_k is inserted. Then convergence is quadratic.

The Vertgeim method needs in each iterative step three conjugations: one for the calculation of the right-hand side $P[S_k]$ of (189), one in (192) for the calculation of w and one for conjugation of h in (194). This must be compared with the Wegmann method which requires only two conjugations in each step.

One can parameterize any curve in the form (185). Even for star-shaped regions the representation (185) is flexible, since f_2 can be any monotone function. The usual representation (152) for star-shaped regions is obtained with

$$f_1(s) = \log(\rho(s)), \quad f_2(s) = s. \quad (195)$$

Then (188) gives Theodorsen's equation (156). When Vertgeim's method is specialized to this case, it gives an efficient solution procedure for Theodorsen's equation by a Newton method. This approach was (re)discovered and exploited by Hübner [123] in 1986, who proved that the iteration converges whenever the second derivative of ρ is Lipschitz continuous.

When discretized in the straightforward manner on a grid with N equidistant points, replacing \mathbf{K} by \mathbf{K}_N , the Hübner–Vertgeim method converges for regions close to the unit disk (Wegmann [288]). Although in the initial phase the discretized method follows the quadratic convergence of the continuous version, convergence of the discretized method is finally only linear [288]. Similarly as for the Wegmann method, the turnover from quadratic to linear convergence depends on the number N of grid points, but the rate of the final linear convergence is independent of N . The Hübner–Vertgeim method converges not only in cases where the epsilon condition (159) is satisfied with $\varepsilon < 1$. It converges, e.g., for the inverted ellipse (162) with parameter $p = 0.23$, where (159) is satisfied only with $\varepsilon = 2$.

The iterative methods discussed in this section converge locally and quadratically in suitable function spaces. The corresponding discretized methods converge in the initial phase quadratically, but as soon as the changes are of the order of the discretization error, convergence becomes only linear (Wegmann [288]). The rate q of the final linear convergence is independent of the number of grid points, but the turnover from quadratic to linear convergence is rather sensitive to the number of grid points. This is shown in Figure 13 where the maximum changes in each step of the iteration are shown for a calculation of the mapping from the unit disk to a shifted ellipse (Example 1 with $a = 1, b = 0.7, z_0 = -0.3, \alpha = 0$) with the Wegmann method, using $N = 32, 64, 96, 128, 160$ grid points, respectively. The linear convergence occurs for all N with a rate $q = 0.38$. Also the rate $q = 1.77$ of divergence is the same for all N .

Chakravarty and Anderson [27] try to satisfy the condition

$$\operatorname{Re} \eta(S(t)) + \mathbf{K}[\operatorname{Im} \eta(S(t))] - \gamma = 0 \quad (196)$$

which must be satisfied by the boundary correspondence function S with $\gamma = \operatorname{Re} \Phi(0)$. They start with a guess S_0 and use a conjugate gradient method and a Newton method to change iteratively the function $S_k(t)$ and the real number γ_k in such a way that the left-hand side in (196) is minimized.

Sallinen [236] uses a continuation method to determine the conformal mappings to a family of regions $G(t)$ depending on a parameter $t \in [0, 1]$. Starting from the known mapping from the disk to $G(0)$, the mappings for the other t are calculated by increasing t in small steps and changing the mapping with Newton's method. The Newton step leads to an RH problem which can be solved explicitly.

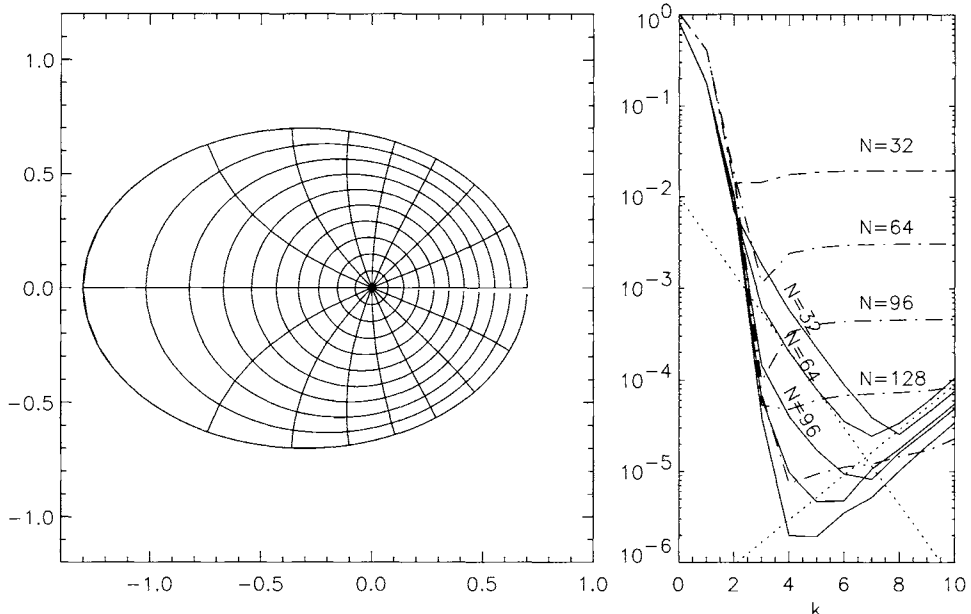


Fig. 13. Mapping to a shifted ellipse with the (undamped) Wegmann method. The right panel shows δ_k and ε_k during the iteration for calculations with $N = 32, 64, 96, 128$ and 160 grid points. The dotted lines are proportional to 0.38^k and 1.77^k .

4.4. Interpolation

The Newton methods discussed in Section 4.3 converge locally and quadratically in suitable function spaces. The corresponding discretized methods converge in the initial phase quadratically, but eventually only linearly. The discretized Newton methods are not Newton methods in the strict sense.

The methods of Section 4.3 first linearize the boundary correspondence equation (122) and then discretize. One can reverse the order. One can first discretize (122), and then solve the ensuing system of nonlinear equations by a Newton method. This then really gives a locally and quadratically convergent iteration. There are two major problems connected with this approach.

The first problem is a theoretical one: Does there exist a solution of the discretized boundary correspondence equation? Recall, that the proof of the convergence of the Newton method requires apart from mild differentiability conditions, the existence of a solution! While the existence of a solution of (122) follows from Riemann's mapping theorem, the solvability of the discretized equation is a nontrivial problem, as we will see below.

The second problem is a numerical one: How to perform the Newton method for the discretized equation numerically in an efficient way? This problem will also be discussed below.

We discuss first the question, of whether solutions to the discrete equations exist. We follow the reasoning of Wegmann [286]. Let $t_j = (j - 1)2\pi/N$ be N equidistant grid points in the interval $[0, 2\pi]$ with an even number $N = 2n$. A *discrete boundary correspondence equation* can be written in the following way:

$$P_n(e^{it_j}) = \eta(s_j), \quad j = 1, \dots, N, \quad (197)$$

which must be satisfied by a polynomial P_n ,

$$P_n(z) = \sum_{l=1}^{n+1} p_l z^l, \quad (198)$$

of degree $n + 1$ with complex coefficients $p_l, l = 2, \dots, n$, but real lowest- and highest-order coefficients, i.e.,

$$\operatorname{Im} p_1 = 0, \quad \operatorname{Im} p_{n+1} = 0. \quad (199)$$

The polynomial P_n is an approximation for the mapping function $\Phi : D \rightarrow G$. The real numbers s_j are approximations for the values $S(t_j)$ of the boundary correspondence function S . The condition that P_n must be a polynomial of form (198) can be written as a condition on the Fourier coefficients of the right-hand side of (197), namely

$$\sum_{j=1}^N e^{ilt_j} \eta(s_j) = 0 \quad (200)$$

for $l = 0, 1, \dots, n - 2$, and

$$\operatorname{Im} \sum_{j=1}^N e^{ilt_j} \eta(s_j) = 0 \quad (201)$$

for $l = -1$ and $l = n - 1$. Thus, the polynomial P_n is eliminated from (197), and a system of N real nonlinear equations for the N real unknowns s_j remains. The solvability of this system of equations has been discussed by Wegmann [286].

One can interpret (197) as an interpolation problem of the following kind: Determine a polynomial P_n of degree $n + 1$ of the form (198) satisfying the constraints (199) such that the values of the polynomial at the grid points e^{it_j} lie on the boundary curve Γ of the region G . In this sense the polynomial P_n interpolates the curve Γ . The values at the grid points are not given explicitly, but only in the implicit form, that they are required to lie on Γ . In interpolation problems usually the number of grid points equals the degree of the polynomial. Here only half of the information about the function values is prescribed, and the number of grid points is about twice the degree.

Wegmann [286] proved the following result:

THEOREM 17. *When η is twice differentiable with Lipschitz continuous second derivative then there exists for all sufficiently large $N = 2n$ a polynomial (198) normalized by (199) such that the interpolation condition $P_n(e^{it_j}) \in \Gamma$ is satisfied for all $j = 1, \dots, N$. In a neighborhood of the conformal mapping Φ there is exactly one such P_n . The sequence of these P_n converges to Φ in the sense that the boundary values $P_n(e^{it})$ converge to $\Phi(e^{it})$ in the Sobolev norm $\|\cdot\|_W$.*

In addition, Wegmann [286] has proved for curves η with a Lipschitz continuous third derivative that for sufficiently large N the derivatives P'_n of the polynomials do not vanish in D , and the P_n are conformal mappings of D to some regions G_n which are close to G .

The second of the conditions (199) is somewhat artificial. It has no counterpart in the continuous conformal mapping theory. It has been pointed out by Wegert [280] that this condition can be replaced by the more general one,

$$\operatorname{Re}(e^{i\alpha} p_{n+1}) = 0 \quad (202)$$

for any prescribed angle α .

Fornberg [62] made an ansatz by a polynomial P_n of degree n ,

$$P_n(z) = \sum_{l=1}^n p_l z^l, \quad (203)$$

with complex coefficients p_1, \dots, p_n . The interpolation problem (197) with this type of polynomials seems to be well posed at first glance, since the number N of unknowns s_j equals the number N of equations (200) which must be satisfied for $l = 0, 1, \dots, n - 1$. The polynomials (203), however, do not satisfy the second normalization condition that $P'_n(0)$ is real. Therefore, one must not expect uniqueness. In fact, it has been proved by Wegmann [286] that for sufficiently large N there exist at least N solutions of (197) with polynomials of type (203). More precisely: For every $k = 1, \dots, N$, there exists such a solution $P_{n,k}$ with the property

$$(k-1)\frac{2\pi}{N} < \arg P'_{n,k}(0) \leq k\frac{2\pi}{N}. \quad (204)$$

Hence, one can find a solution of (197) with an n th degree polynomial (203) which satisfies the second normalization condition, $\arg P'_n(0) = 0$, with an error of at most $2\pi/N$.

When using polynomials (203) one should, instead of the condition $\operatorname{Im} P'_n(0) = 0$, better use the normalization

$$P_n(1) = \eta(s_1) \quad (205)$$

with a prescribed value of s_1 . If the interpolation condition (197) for $j = 1$ is omitted, a system of $N - 1$ equations for the remaining unknowns s_2, \dots, s_N is obtained, which is solvable for sufficiently large N (see Fornberg [62], Wegmann [286]).

This theoretical discussion is in a sense academic, since for sufficiently large N the highest-order coefficient p_{n+1} is below roundoff error anyway. Then, numerically, one cannot distinguish between the conditions $p_{n+1} = 0$ or $\text{Im } p_{n+1} = 0$ and will find a solution numerically, despite the fact that an exact solution of the underlying system of equations does not exist. Theory guarantees that this numerical solution is close to the conformal mapping.

Fornberg [62] proposed in 1980 an efficient method for solving the problem (197). We follow here Wegmann [284] who adapted Fornberg's method to the calculation of polynomials of form (198).

The Newton method for equations (197) starts from the linearized equations

$$\eta(s_j) + \dot{\eta}(s_j)Ds_j = P_n(e^{it_j}) \quad (206)$$

which must be satisfied with a polynomial P_n of form (198) and real numbers Ds_j .

The conditions (206) are satisfied by a polynomial P_n if and only if the Fourier coefficients c_l of the left-hand side vanish for $l = n + 2, \dots, N$ and are real for $l = 1$ and $l = n + 1$. This is equivalent to the property that the Fourier polynomial formed with these coefficients,

$$f_0(t) = i(\text{Im } c_1)e^{it} + i(\text{Im } c_{n+1})e^{i(n+1)t} + \sum_{l=n+2}^N c_l e^{ilt}, \quad (207)$$

vanishes identically. In what follows, the necessary condition, $f_0(t_j)/\dot{\eta}(s_j) = 0$ for all j , is used to build up a system (208) of linear equations.

Let \mathbf{x} and \mathbf{u} be the vectors with components $x_j := \dot{\eta}(s_j)/|\dot{\eta}(s_j)|$ and $u_j := Ds_j|\dot{\eta}(s_j)|$, respectively. Then equations (206) can be written as a linear system of equations

$$\mathbf{A}\mathbf{u} = -\mathbf{r} \quad (208)$$

with a real $N \times N$ matrix \mathbf{A} and a real vector \mathbf{r} .

It is not necessary to calculate the matrix \mathbf{A} . One needs only a recipe of how to calculate the product $\mathbf{A}\mathbf{u}$ for a given real vector \mathbf{u} . The product $\mathbf{A}\mathbf{u}$ is calculated by the following steps.

First calculate the Fourier coefficients

$$a_l := \frac{1}{N} \sum_{j=1}^N x_j u_j e^{-ilt_j}, \quad l = 1, \dots, N, \quad (209)$$

and the values of the Fourier polynomial

$$e_j = i(\text{Im } a_1)e^{it_j} + i(\text{Im } a_{n+1})e^{i(n+1)t_j} + \sum_{l=n+2}^N a_l e^{ilt_j}, \quad j = 1, \dots, N. \quad (210)$$

Then the components of \mathbf{Au} are equal to

$$(\mathbf{Au})_j = \text{Re}(\bar{x}_j e_j), \quad j = 1, \dots, N. \quad (211)$$

The right-hand side of (208) is calculated in a similar way. The function η is Fourier analyzed

$$b_l := \frac{1}{N} \sum_{j=1}^N \eta(s_j) e^{-ilt_j}, \quad l = 1, \dots, N, \quad (212)$$

and the values

$$h_j = i(\text{Im } b_1)e^{it_j} + i(\text{Im } b_{n+1})e^{i(n+1)t_j} + \sum_{l=n+2}^N b_l e^{ilt_j}, \quad j = 1, \dots, N, \quad (213)$$

are calculated. The components r_j of \mathbf{r} are then equal to $r_j := \text{Re}(\bar{x}_j h_j)$.

It has been shown by Wegmann [286] that the matrix \mathbf{A} so defined is symmetric, positive semidefinite and has norm ≤ 1 in the Euclidean \mathbb{R}^N . If equation (206) has a unique solution (which is the generic case) then \mathbf{A} is even positive definite.

Since the matrix \mathbf{A} has these favorable properties, the system (208) can be solved by the conjugate gradient method (CGM). The calculation of the right-hand side \mathbf{r} requires two Fourier transforms. In each iteration of the CGM \mathbf{Au} has to be evaluated for a vector \mathbf{u} . This again requires two Fourier transforms. This can be done efficiently with FFT. The computational cost is of the order $O(N \log N)$ with a coefficient $K_{\text{CGM}} + 2$ which depends on the number K_{CGM} of iterations needed in the CGM. It has been shown by Wegmann [286] that the matrix \mathbf{A} is up to a matrix of rank less than or equal to 2 a discretized version of the operator $\frac{1}{2}(\mathbf{I} + \mathbf{R}_\beta)$ with the operator \mathbf{R}_β introduced in (54) formed with the tangent angle β defined by $\exp(i\beta(s)) := \dot{\eta}(s)/|\dot{\eta}(s)|$. It follows from Theorem 11 that for sufficiently smooth boundary functions η only a few eigenvalues of \mathbf{R}_β differ significantly from zero. Therefore, the eigenvalues of \mathbf{A} cluster around 1/2. This has the consequence that the CGM converges fast. The number K_{CGM} of iterations needed to achieve a desired accuracy depends only on the eigenvalue distribution of \mathbf{A} . It is largely independent of N . Therefore, the computational cost of this method is $O(N \log N)$.

One can exploit the checkerboard structure of the matrix \mathbf{A} to reduce the system (208) to two-coupled systems of equations of order n . From these an n -order equation is obtained for the components of \mathbf{u} with even index j with a matrix which is a discretization of the operator $\mathbf{I} - \mathbf{R}_\beta^2$. This matrix is positive definite. For sufficiently smooth curves

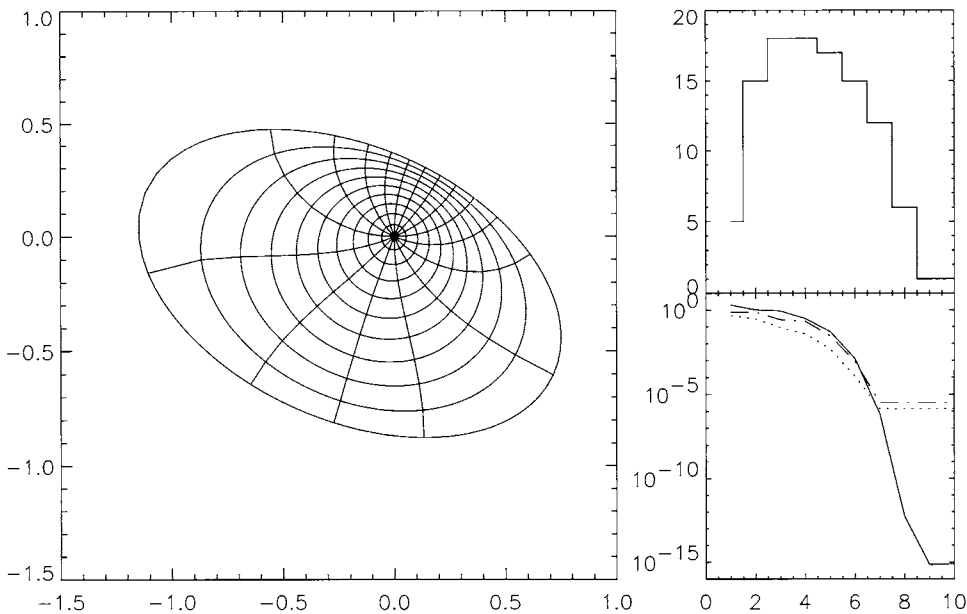


Fig. 14. The mapping from the disk to a shifted and rotated ellipse calculated by the interpolation method with 256 grid points. The lower right panel shows the maximum change δ_k in each step (solid) and the measures α_k and ε_k of accuracy, the upper right panel shows the number of iterations needed in the CGM.

the eigenvalues cluster at 1. This property has been detected in numerical experiments by Fornberg [62]. It is very favorable for the use of CGM (for details see Fornberg [62], Wegmann [286]). For an analysis of Fornberg's method, and its variant for the mapping of exterior regions see DeLillo and Pfaltzgraff [44].

Hübner [122] observed, that the Newton method for the discrete Theodorsen equation can be performed very efficiently since the ensuing linear equations can be transformed to a system with a Toeplitz matrix. For such systems fast solution methods are available which require work of the order $O(N \log^2 N)$. Unfortunately, these fast Toeplitz solvers can become unstable in some cases. Wegmann [286] carried this idea over to the solution of the linear system (206) which can also be transformed into a Toeplitz system.

Figure 14 shows the result of a calculation for an ellipse (Example 1 with $a = 1$, $b = 0.6$, $z_0 = -0.2 - 0.2i$, $\alpha = -0.4$) with the interpolation method with 256 grid points. The lower right panel shows that the method converges quadratically. The upper right panel shows that in the initial stages at most 18 iterations are needed in the CGM. This is reduced to 1 when the outer iteration has converged.

Figure 15 shows the result of a calculation for an ellipse (Example 1 with $a = 1$, $b = 1.4$, $z_0 = 0.3 - 0.4i$, $\alpha = 0.5$) with the Fornberg method with 256 grid points. The lower right panel demonstrates that the method converges quadratically. The upper right panel shows that in the initial stages at most 10 iterations are needed in the CGM. This is reduced to 1 when the outer iteration has converged.

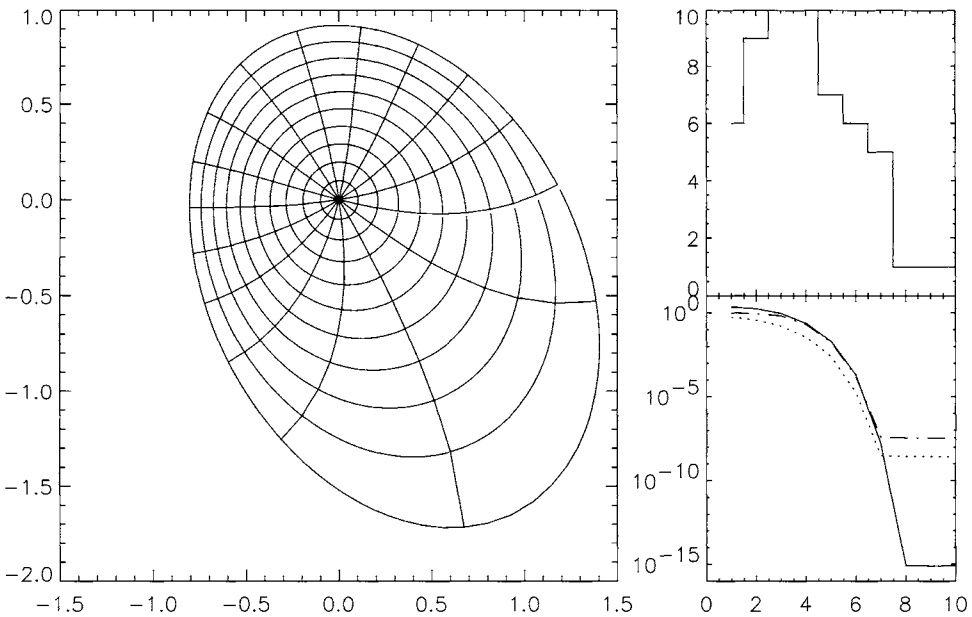


Fig. 15. The mapping from the disk to a shifted and rotated ellipse calculated by the Fornberg method with 256 grid points. The lower right panel shows the maximum change δ_k in each step (solid) and the measures α_k and ϵ_k of accuracy, the upper right panel shows the number of iterations needed in the CGM.

The discretized version of the method of alternating projections described in Section 4.2 converges to an interpolating polynomial (if it converges at all).

Porter [225] constructs the interpolating polynomial of degree n by alternately interpolating an n th degree polynomial at the points z_j with even/odd index j . The values w_j which the polynomial has to take are calculated from the values of the last polynomial at the points z_j with even/odd index j projected back to the curve. The resulting projection method converges linearly. This method is not new. It is already described in the book of Fil'čakov [57, p. 404]. A similar iterative method was used by Ugodčikov [267], who started from initial data obtained by an electrical model.

Opitz [203] interpreted the discrete Theodorsen equation (161) as an interpolation problem. The equation asks for a polynomial P_n of degree less than or equal to n with real lowest- and highest-order coefficients p_0 and p_n , which satisfies

$$z_j \exp(P_n(z_j)) \in \Gamma \quad (214)$$

for all $z_j := e^{ij2\pi/N}$, $j = 1, \dots, N = 2n$. The condition (214) resembles closely the condition (197) with the only difference that there is an exponential in (214).

In view of this close similarity, it is surprising that the discrete Theodorsen equation has a solution for all N provided only that ρ is a continuous function (Gutknecht [90]). If the boundary curve satisfies an epsilon condition (159) with $\varepsilon < 1$ then the solution of the discrete Theodorsen equation is unique. Hübner [120] has shown that for any $\varepsilon \geq 1$

and for any $n \geq 2$ there is a region G whose boundary curve satisfies (159) with this value of ε so that the Theodorsen equation discretized with $2n$ points has infinitely many solutions. Gutknecht [94] notes that there is strong experimental evidence, that even for quite simple boundaries the discrete Theodorsen equation may have more than one solution. He proposes to use a continuation method to reach the only “reasonable solution”.

Hübner [121] showed that for analytic boundary curves there is for all sufficiently large N a solution of the discrete Theodorsen equation which is close to the boundary correspondence function. This solution can be computed by the Newton method described in Section 4.3.

4.5. Accuracy

The result of a numerical calculation is an approximation $\widehat{\Phi}$ to the mapping function $\Phi : D \rightarrow G$ which in most cases is a polynomial. When the calculation is done on a grid with $N = 2n$ points, then the approximating polynomial is of degree n or $n + 1$. This is most obvious in the projection and interpolation methods. It is well known from approximation theory that the degree of approximation by polynomials to Φ depends on the smoothness of Φ . We have seen in Section 2.2 that the smoothness of Φ is about the same as the smoothness of the boundary curve Γ of the region.

Methods based on function conjugation can be only as accurate as the approximation \mathbf{K}_N of the conjugation operator on the grid. The error of \mathbf{K}_N is discussed in Section 2.5.

When $\eta(s)$ is analytic in a strip $A_\tau := \{s + i\sigma : |\sigma| < \tau\}$ then Φ can be extended to an analytic function in the disk $\{z : |z| < R\}$ with $R := e^\tau$. Uniform approximation on the unit disk D by polynomials of degree less than or equal to n is possible with an error of order $O(R^{-n})$. This is the error for mappings of D to regions G with analytic boundaries. For Theodorsen’s method this is shown in Gaier’s book [65, p. 95]. Wegmann [282] obtained an error estimate with the same order for his method in a Sobolev norm under the additional hypothesis that $\dot{\eta} \neq 0$ in A_τ . DeLillo [37] reports a series of test calculations which confirm these estimates.

When η is in a Hölder space $C^{l,\alpha}$ for $l \geq 2$ and $0 < \alpha < 1$, the Sobolev norm of the error of Wegmann’s method is of order $O(N^{2-l-\alpha})$. The numerical results reported by Wegmann [282] indicate that the supremum norm of the error behaves like $O(N^{-(l+\alpha)})$.

To get a feeling for the efficiency of several of the methods discussed in this section we have calculated the mapping from the disk to an inverted ellipse (Example 4) with parameter $p = 0.45$ by the AP, the OAP, the Theodorsen and the Wegmann methods. After each iteration we calculated the achieved accuracy (measured by ε) and the number N_F of FFTs. Since the computational cost is mainly determined by the Fourier transforms, we measure it by the quantity $P := N_F N \log_2 N$ where N is the number of grid points. The result is shown in Figure 16. For low accuracy the OAP method is the most efficient. Its rate of convergence for this example is $q = 0.45$. The AP and the Theodorsen methods converge with rates $q = 0.77$ and $q = 0.81$, respectively. Newton methods have a slow start but they accelerate. They are therefore best suited for high accuracy calculations. This is most clearly seen in the right panel of Figure 16.

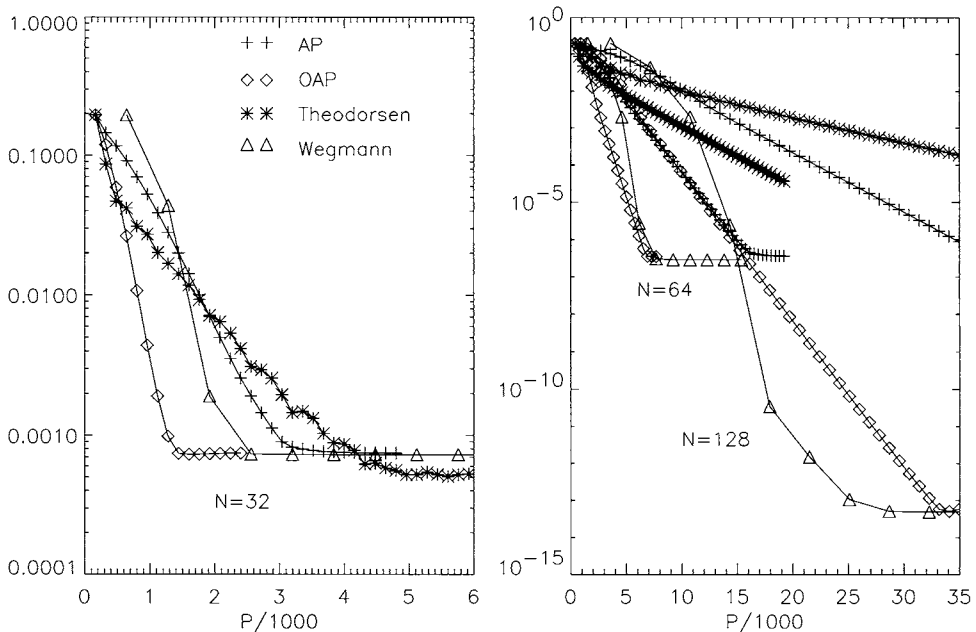


Fig. 16. The accuracy ε as a function of the computational cost P for the calculation of the mapping to an inverted ellipse with the AP (+ sign), OAP (diamond), Theodorsen (asterisk) and Wegmann (triangle) method with $N = 32$ (left panel) and $N = 64$ and $N = 128$ (right panel).

5. Mapping from an ellipse to the region

The fast Newton methods of Section 4.3 for calculating the conformal mapping from the unit disk to a region rely mainly on the following two properties:

- (a) The conjugate harmonic function can be calculated very efficiently using FFT.
- (b) Functions f analytic in the disk can be developed in Taylor series converging in the disk.

The fast methods for the disk can be carried over to other canonical regions where these properties hold in a suitable modified form.

For general regions the Taylor series has to be replaced by the Faber series in order to get a development in a series of polynomials convergent in the whole region (see Henrici [107, p. 507 ff]).

The Faber polynomials of ellipses are multiples of the Chebyshev polynomials. For $q > 1$ let E_q be the ellipse whose boundary is parameterized by

$$\xi(t) := \frac{1}{2}(qe^{it} + q^{-1}e^{-it}). \quad (215)$$

The *Chebyshev polynomial* T_n of degree n has the boundary values

$$T_n(\xi(t)) = \frac{1}{2}(q^n e^{int} + q^{-n} e^{-int}). \quad (216)$$

This has been exploited by DeLillo and Elcrat [39] to carry over Fornberg's method (see Section 4.4) from the disk to an ellipse as canonical region. DeLillo, Elcrat and Pfaltzgraff [41] carried this idea further and applied it to cross-shaped regions.

The conjugate harmonic function on an ellipse can be calculated very easily. When a real function on the boundary of E_q as a function of the parameter t in the representation (215) is developed in a Fourier series

$$f(\xi(t)) = a_0 + \sum_{l=1}^{\infty} (a_l \cos lt + b_l \sin lt), \quad (217)$$

the conjugate harmonic function $g := \mathbf{K}_E f$ has Fourier series

$$g(\xi(t)) = \sum_{l=1}^{\infty} \left(-D_l b_l \cos lt + \frac{a_l}{D_l} \sin lt \right) \quad (218)$$

with the factors

$$D_l := \frac{1 + q^{-2l}}{1 - q^{-2l}} \quad (219)$$

(Wegmann [291]). The l th Fourier coefficients of the conjugate function depend only on the l th coefficients of the original function. The factors D_l are close to 1 for large l . For high-order coefficients conjugation on the ellipse is almost the same as conjugation on the disk (compare (218) with (27)).

The formula (218) resembles the formula (299) for conjugation on an annulus (see Section 11.1). In fact, there is a close relationship between these two types of regions, since the Joukowski map $\Psi(z) := \frac{1}{2}(z + z^{-1})$ maps the annulus $\{z : 1/q < |z| < q\}$ onto a Riemann surface, which covers the ellipse E_q twice. In particular, Ψ maps the unit circle to the interval $[-1, 1]$.

The operator \mathbf{K}_E plays the same role for the ellipse E_q as the operator \mathbf{K} for the disk. In particular, Theorem 8 holds with D and \mathbf{K} replaced by E_q and \mathbf{K}_E , respectively. This has the consequence that methods which are based on function conjugation can easily be carried over to ellipses. For the Wegmann method this has been done in [291]. The behavior of this modified method is quite similar to that for the disk. It is more prone to divergence. Convergence can be enforced by damping of the higher Fourier terms as described in (183).

Ellipses as canonical regions have the advantage that crowding can be avoided to some extent. For this purpose the q should be chosen so that the ellipse E_q has nearly the same aspect ratio as the target region (see DeLillo and Elcrat [39]).

EXAMPLE 6. Sportground of length 2π is bounded by two semicircles of radii R_S and two straight line segments of length $(1 - R_S)\pi$.

Figure 17 shows the mapping of an ellipse with $q = 1.25$ (aspect ratio 0.22) to the sportground of Example 6 with $R_S = 0.25$ which has aspect ratio 0.175. The example is

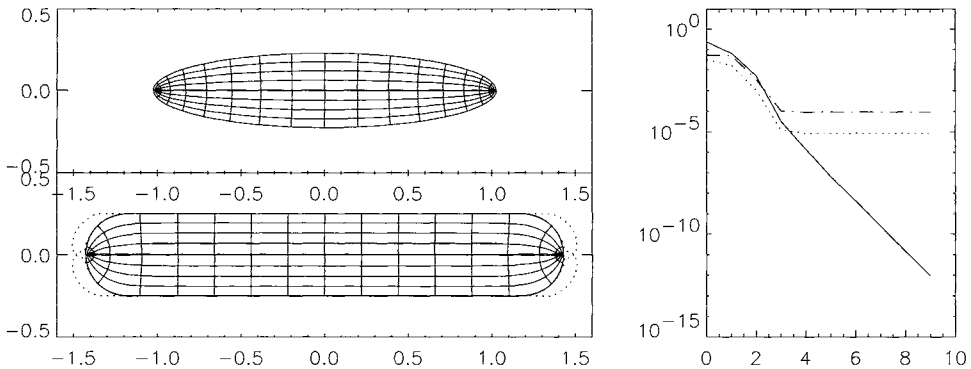


Fig. 17. The mapping of the ellipse with $q = 1.25$ (upper panel) to the sportground of Example 6 (lower panel). The right panel shows the maximum change δ_k (solid) in each iteration and the error measures α_k and ϵ_k .

calculated on a grid with $N = 512$ points by the method described in [291] with damping as described in (183). Convergence is quadratic in the beginning but then turns to linear. There is little distortion and no crowding.

6. Waves

An important application for conformal mapping is the study of waves (see, e.g., Lamb [153, p. 363]). There are a few explicitly known mapping functions. In general the wave form must be calculated from the equilibrium conditions of gravity and capillary forces. This requires special techniques.

We consider here only the case where the wave form is known, and the velocity field (u, v) must be determined. The region G is bounded from below by the wave with wavelength λ . We assume that $\lambda = 2\pi$. The region G is mapped by $z \rightarrow w = \exp(iz)$ to a simply-connected bounded region G' . Since the flow field is 2π -periodic, it can be expressed as a function of the variable $w \in G'$. Therefore, it is only necessary to find a conformal mapping Φ from the unit disk to the region G' satisfying $\Phi(0) = 0$. This function Φ can be calculated with the methods described before. When the wave is described by $s + i\hat{y}(s)$ with a 2π -periodic function $\hat{y}(s)$, the auxiliary region G' is star-shaped with boundary parameterization $\eta(s) = \exp(-\hat{y}(s))e^{is}$.

EXAMPLE 7. Cosine wave is bounded by $\hat{y}(s) = D \cos s$.

Figure 18 shows the flow in a cosine wave (Example 7 with $D = 0.7$) over two wavelengths. The lines are contours of the streamfunction (= the streamlines) and of the velocity potential. The figure shows also the auxiliary region G' and the conformal mapping from the disk to G' . This mapping is calculated with the Wegmann method on a grid with $N = 256$ points.

Menikoff and Zemach [176] consider the mapping Φ from the upper half-plane $U := \{w: \operatorname{Im} w > 0\}$ to the region $G := \{z = x + iy: y > \hat{y}(x)\}$ above a line described by an even

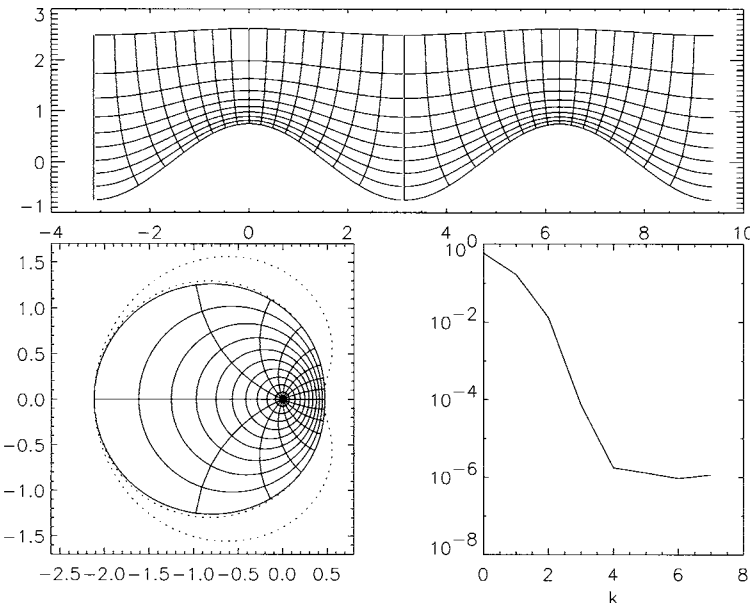


Fig. 18. Upper panel: streamlines and velocity potential for the flow in the cosine wave of Example 7 for $D = 0.7$. Lower left: the conformal mapping from the disk to the auxiliary region G' . Lower right: the δ_k during the iteration.

2π -periodic function $\hat{y}(x)$. Such regions occur in a natural way in the study of water waves and other free surface flows (see Menikoff and Zemach [176] and Meiron et al. [175]). The mapping is standardized by the condition that the interval $[-\pi, \pi]$ corresponds to the boundary part $x + i\hat{y}(x)$, $-\pi \leq x \leq \pi$, of G and $i\infty$ is mapped to $i\infty$. The mapping can be described by a boundary correspondence function $u(x)$ defined by the property $\Phi(u(x)) = x + i\hat{y}(x)$. A nonlinear singular integral equation (which is related to Theodorsen's) for the function $u(x)$ is derived, discretized and solved by a Newton method. The singular integral equation is transformed by integration by parts to an equation with a logarithmic kernel. This form of the equation gives the best results. Gauss quadrature is applied. There occurs severe crowding near boundary points where the function $\hat{y}(x)$ attains a minimum. Zemach [297] gives an approximate formula which allows calculation of $u(x)$ near points of severe crowding, which are characterized by the condition $du/dx \ll 1$. He calculates cosine waves (Example 7) with $D = 100$, a “very hard case”, where crowding is of the order $du/dx \approx 10^{-124}$.

7. Mapping from a quadrilateral to a rectangle

A Jordan region Q where on the boundary Γ four distinct points A, B, C, D are prescribed in counterclockwise order, is called a *quadrilateral*. There is a uniquely defined number q such that there is a conformal mapping F of Q to the rectangle $R_q := \{z = x + iy: 0 < x < 1, 0 < y < q\}$ in such a way that the points A, B, C, D are mapped to the corners

$0, 1, 1 + qi, qi$, in this order. The height q of the rectangle is unknown. It must be determined together with F . The quantity $m(Q) := q$, called the *conformal module* of the quadrilateral, is of interest in problems of electric conductivity. When Q is a sheet of metal of specific resistivity 1 and the segments AB and CD are kept at the potentials 0 and 1, respectively, while the remaining segments are insulated, then the sheet Q between the electrodes AB and CD has resistance $m(Q)$ (see, e.g., Henrici [107, p. 431]). Papamichael [207] gave a review of possible applications of the conformal mapping $F : Q \rightarrow R_q$, and of available numerical methods to compute approximations to F and $m(Q)$. Gaier [75] gave a survey of old and new methods to determine the module by direct methods (without computation of the conformal map). Gaier [66] calculated approximations for $m(Q)$ by finite element methods.

Since the mapping from a rectangle to the disk can be expressed explicitly in terms of elliptic integrals of the first kind, the problem of approximating F is solved (at least in theory) when a mapping $\tilde{F} : Q \rightarrow D$ to the disk is known.

A method for the mapping of a rectangle R_q onto a region of the form $G = \{z = x + iy : 0 < x < 1, 0 < y < f(x)\}$ is described by Challis and Burley [26]. The method works for functions f which can be developed into cosine series (the so-called even periodic geometry). The boundary values of the mapping are constructed by a projection method. Underrelaxation with a factor of 0.5 is recommended. Gaier and Papamichael [79] point out that this method is closely related to Garrick's method for mapping an annulus to a doubly-connected region (see Section 11.2).

For some quadrilaterals of a special form one can transform the problem to a mapping of a doubly connected domain onto an annulus (see Papamichael [207, p. 69]). Papamichael et al. [211] compare calculations via an annulus with calculations via the disk. It turns out that the former are preferable in the case of "long" quadrilaterals where crowding prevents a sufficiently exact location of the images of the specified points A, B, C, D .

We have already mentioned in Section 2.4 that crowding may cause problems. Let ϕ_1 be the smallest arc between the images of A, B, C, D on the unit circle. Then it follows from (19) that $\phi_1 \sim 8 \exp(-\pi m(Q)/2)$ for large $m(Q)$ (see, e.g., Papamichael and Stylianopoulos [216, p. 34]). Therefore, for quadrilaterals with large module, the images of the points A, B, C, D can hardly be distinguished on the circle unless the calculation is done with very high precision. For this reason it is sometimes advisable to calculate the mapping F to the rectangle directly.

For the numerical calculation of F one can use the fact that $\operatorname{Re} F$ and $\operatorname{Im} F$ are harmonic functions in Q , which are coupled via the boundary conditions. This is used by Vabishchevich and Pulatov [268] to construct an iterative scheme which requires in each step the solution of a Dirichlet problem for the Laplace equation on Q . A similar approach is used by Seidl and Klose [241] to construct iteratively the inverse mapping $\Phi : R_q \rightarrow Q$. This method takes advantage of the fact that for a rectangle fast Laplace solvers are available.

As shown before, crowding occurs for quadrilaterals with large module $m(Q)$. A way out comes from the observation that the mapping of elongated regions is often "localized" in the sense that a change of the region at one end has very little effect on the mapping function at the other end. This can be exploited by *domain decomposition methods* which approximate the mapping of a rectangle to an elongated region by the mapping of rectan-

gles to suitable subregions. For some geometries explicit exponentially small error bounds are given by Papamichael and Stylianopoulos [214], Laugesen [156] and Falcão et al. [56].

When a “long” quadrilateral Q is decomposed by suitable crosscuts into two or more component quadrilaterals Q_j , the module $m(Q)$ can be well approximated by the sum $\sum m(Q_j)$ (Gaier [77,78], Papamichael and Stylianopoulos [215,216] and Falcão et al. [55]).

8. Mapping of exterior regions

One of the main problems of aerodynamics is the calculation of the flow around an airfoil. This requires in a natural way the conformal mapping from the exterior of the unit circle to the exterior of a curve. Therefore, it is not surprising that many methods have been developed for the calculation of the mapping to such exterior regions.

Let G now be the region exterior to a Jordan curve Γ . Then there exists a unique conformal mapping function Φ from the exterior D^- of the unit circle to G subject to the normalization

$$\Phi(z) = \gamma z + a_0 + O\left(\frac{1}{z}\right) \quad (220)$$

with a constant $\gamma > 0$, called the *capacity* of the boundary curve Γ or the *transfinite diameter* of the region G .

We distinguish sometimes exterior mappings and interior mappings by subscripts “e” and “i”. By applying the mapping R , defined by $R(z) := 1/z$, to both regions G and D^- , the function Φ_e is given by $\Phi_e = R \circ \Phi_i \circ R$, where Φ_i maps D conformally to the bounded region $R(G)$ and satisfies the usual conditions $\Phi_i(0) = 0$ and $\Phi'_i(0) > 0$. Therefore, the mapping of exterior regions can be calculated with the methods for interior regions.

For many of the methods presented so far, there are variants which can be used to calculate the mapping of exterior regions directly. And there are a few methods developed especially for exterior regions.

8.1. Mapping from the exterior region to the exterior of the disk

The mapping $F : G \rightarrow D^-$ is normalized by the condition at infinity

$$F(z) = \frac{1}{\gamma} z + b_0 + O\left(\frac{1}{z}\right) \quad (221)$$

with the capacity $\gamma > 0$. When Γ is a Jordan curve parameterized by a 2π -periodic complex function η , F can be extended to a continuous function on \overline{G} and the boundary values can be described by the (*exterior*) *boundary correspondence function* $T(s)$ which satisfies

$$F(\eta(s)) = \exp(iT(s)). \quad (222)$$

The counterpart to Gershgorin's equation (76) is the integral equation of Kantorovich–Krylow [132, p. 464]; see also Gaier [65, p. 13], Henrici [107, p. 397],

$$(\mathbf{I} + \mathbf{K}_1)T = \beta(s) := 2 \arg(\eta(s) - \eta(0)). \quad (223)$$

The ansatz (80) as a single layer potential is modified for the exterior problem by (Symm [254], Henrici [107, p. 379])

$$u(z) = -\log \gamma + \frac{1}{2\pi} \int_0^{2\pi} \log \left| 1 - \frac{\eta(s)}{z} \right| \sigma(s) ds. \quad (224)$$

The density σ satisfies Symm's exterior equation

$$\frac{1}{2\pi} \int_0^{2\pi} \log \left| 1 - \frac{\eta(s)}{\eta(t)} \right| \sigma(s) ds = \log \gamma - \log |\eta(t)|. \quad (225)$$

The density σ is normalized by

$$\frac{1}{2\pi} \int_0^{2\pi} \sigma(s) ds = 1. \quad (226)$$

In view of this, condition (225) can be reduced to the simpler form

$$\frac{1}{2\pi} \int_0^{2\pi} \log |\eta(t) - \eta(s)| \sigma(s) ds = \log \gamma. \quad (227)$$

If the capacity $\gamma \neq 1$, the pair of equations (227) and (226) has the unique solution $\sigma(s) = T'_e(s)$, the derivative of the exterior boundary correspondence function T_e . Equation (227) contains besides the unknown function σ also the unknown parameter γ . This makes the use of Symm's method for exterior regions more complicated than for interior regions. From (227) it becomes clear why the case $\gamma = 1$ is exceptional. The operator with logarithmic kernel then has an eigenvalue 0 with eigenfunction $T'_e(s)$. This affects the uniqueness of the interior equation (81) (see Theorem 12).

Murid et al. [185] carry the approach of Kerzman and Stein [133] over to exterior regions. DeLillo and Elcrat [40] propose an “inverse Timann method” which can be considered as a generalization of the Schwarz–Christoffel method and is also applicable for curved boundaries with corners. Papamichael and Kokkinos [209] study the Ritz method and the Bergman kernel method for the calculation of the conformal mapping F of a region G exterior to a Jordan curve satisfying the constraint $F(\infty) = 0$.

With any n points $z_1, \dots, z_n \in \Gamma$ one can form the *Vandermonde determinant*

$$V(z_1, \dots, z_n) := \prod_{1 \leq j < k \leq n} (z_j - z_k). \quad (228)$$

Points $z_j^{(n)}$, $j = 1, \dots, n$, for which $|V(z_1, \dots, z_n)|$ attains its maximum value V_n are called *Fekete points*. The power $V_n^{2/n(n-1)}$ converges to the transfinite diameter γ from above for $n \rightarrow \infty$. For the polynomials

$$P_n(z) := \prod_{j=1}^n (z - z_j^{(n)}), \quad (229)$$

the n th root $F_n := P_n^{1/n}$ converges to $\gamma F(z)$ for $n \rightarrow \infty$ when the branch of the root is taken so that $F_n(z) = z + \dots$ near ∞ (see Gaier [65, p. 177]). Convergence cannot be uniform in G since all P_n have zeros on Γ . Kleiner [135] gave a pointwise estimate $|\log F_n(z) - \log F(z)| = O(\log n / \sqrt{n})$ for each $z \in G$ (see also Pommerenke [221]). When Fekete points are represented as $z_j^{(n)} = \Phi(\exp(i\theta_{jn}))$ with the conformal mapping $\Phi : D^- \rightarrow G$, then the θ_{jn} are approximately equidistributed in the interval $[0, 2\pi]$ (see Pommerenke [222, 223] for more precise estimates). In [222] there are numerically calculated Fekete points for ellipses and for the square up to $n = 320$.

Fekete points are difficult to determine numerically. Leja [161] defined another system of points which can be recursively calculated.

Menke [177, 178] introduces *stationary point systems* which are determined by certain extremum properties. These points approximate directly the *Fejér points*, i.e., the images $z_j := \Phi(\exp(i(j-1)2\pi/n))$ of equidistant points on the circle. When the mapping $\Phi : D^- \rightarrow G$ is known, the Fejér points can easily be calculated.

Reichel [233] has shown that Fejér points can also be used to calculate the mapping of the interior. Let F_i be the mapping of the interior of Γ to the unit disk with $F_i(0) = 0$, and let P_n be the polynomial of degree $n-1$ which interpolates $F_i(z)/z$ at the n Fejér points z_j then $z P_n(z)$ is an approximation to $F_i(z)$.

Kühnau [150] describes a sort of osculation method which constructs an approximation for the mapping of the exterior of a curved slit S to the exterior of a disk. (Notice that pages 632 and 634 in [150] have to be interchanged.) The slit is subdivided into K adjacent pieces S_i . In the first step the first piece S_1 , which is assumed to be an endpiece, is approximated by a straight line and the exterior of this straight line is mapped by a function f_1 to the exterior of a disk. The image $f_1(S_1 \cup S_2)$ is approximately a circle with an attached circular arc. The exterior is mapped with f_2 to the exterior of a disk, and so on. All mappings are normalized by $f_i(z) = z + O(1/z)$ at infinity. Then the radii of the disks increase and the slit S is finally mapped approximately to a circle. The images $f_i(S)$ of the slits change like a growing tadpole. By an additional step the method can be applied also for the mapping of the exterior or the interior of a Jordan curve. The “zipper method” of Marshall (see Section 3.3) is based on similar ideas.

Homentcovschi [111] calculates an asymptotic expansion for the conformal mapping $F(z, \tau)$ of the exterior of a slender region bounded by the curves $\tau y_{\pm}(x)$ with $|x| \leq 1$ to the plane with a slit $[x_1, x_2]$ on the real axis.

8.2. Mapping from the exterior of the disk to the exterior region

The mapping $\Phi : D^- \rightarrow G$ has the form (220). It is quite sufficient to know the boundary values of Φ , since Φ can be reconstructed by Cauchy's formula

$$\Phi(z) = \gamma z + a_0 - \frac{1}{2\pi} \int_0^{2\pi} \frac{\Phi(e^{it})e^{it}}{e^{it} - z} dt, \quad (230)$$

with the coefficients

$$\gamma = \frac{1}{2\pi} \int_0^{2\pi} \Phi(e^{it})e^{-it} dt, \quad a_0 = \frac{1}{2\pi} \int_0^{2\pi} \Phi(e^{it}) dt. \quad (231)$$

The boundary values can be expressed by an (exterior inverse) boundary correspondence function $S(t)$ which is determined by the same equation (122) as for the interior mapping with the only difference that now Φ is required to be analytic in D^- and subject to the normalization (220) at infinity.

When the boundary is close to a circle, i.e., it has a parameterization (127), then the boundary values of Φ are in first order of τ given by

$$\Phi(e^{it}) = e^{it}(1 + \tau[\rho(t) - iK\rho(t)]). \quad (232)$$

The function S is in first order of τ :

$$S(t) = t - \tau K\rho(t). \quad (233)$$

The method of alternating projection (AP) described in Section 4.2 can easily be adapted for the exterior problem. The formulas must be modified in the following way: The iteration starts with a function S_0 such that $S_0(t) - t$ is 2π -periodic. The obvious choice is $S_0(t) \equiv t$.

When S_k is determined for some $k \geq 0$ then the boundary function is Fourier analyzed

$$\eta(S_k(t)) = \sum_{l=-\infty}^{\infty} B_l e^{ilt}. \quad (234)$$

The function

$$f_k(t) = (\operatorname{Re} B_1)e^{it} + \sum_{l=-\infty}^0 B_l e^{ilt} \quad (235)$$

represents the boundary values of an analytic function

$$\Phi_k(z) = (\operatorname{Re} B_1)z + \sum_{l=-\infty}^0 B_l z^l \quad (236)$$

which obviously is of form (220) with the only exception that the coefficient of z is real but not necessarily positive. This is the first projection step. The second step calculates a new parameter mapping by

$$S_{k+1}(t) := S_k(t) - \operatorname{Re} \frac{g_k(t)}{\dot{\eta}(S_k(t))}, \quad (237)$$

with the nonanalytic part of $\eta \circ S_k$

$$g_k(t) = \sum_{l=2}^{\infty} B_l e^{ilt} + i(\operatorname{Im} B_1) e^{it}. \quad (238)$$

This definition is applicable for differentiable curves. The nonanalytic part of $\eta \circ S_k$ is projected onto the tangent at the point $\eta(S_k(t))$ and the shift along the tangent is then replaced by a shift along the curve induced by a shift in the parameter function S . This gives a new boundary correspondence $t \rightarrow \eta(S_{k+1}(t))$. This construction of a boundary mapping is the second step of the alternating projection.

Figure 19 shows the mapping of the exterior of the disk to the exterior of an inverted ellipse (Example 4) with parameter $p = 0.4$ calculated by the AP method with $N = 256$ grid points. We use the measure ε_k of accuracy defined in (146). The measure of analyticity is changed to

$$\alpha_k := \|g_k\|_2 = \left(\sum_{l=2}^n |B_l|^2 + (\operatorname{Im} B_1)^2 \right)^{1/2}. \quad (239)$$

Fil'čakova [58] describes a method of trigonometric interpolation which determines iteratively a mapping function of form (236).

Now let G be a star-shaped region with a boundary curve parameterized by (152). It follows from (220) that the function Ψ defined as in (154) is analytic in D^- and assumes at infinity the real value $\Psi(\infty) = \log \gamma$. The boundary values of Ψ are as in (153). Real and imaginary parts are connected by the operator \mathbf{K} of conjugation which leads to Theodorsen's integral equation for exterior domains

$$S(t) = t - \mathbf{K}[\log \rho(S(t))] \quad (240)$$

which differs from (156) only in the minus sign in front of \mathbf{K} . The numerical treatment of (240) is quite analogous to the interior case, described in Section 4.2. In particular, the method of successive conjugation can be applied. It converges when the epsilon condition (159) is satisfied with $\varepsilon < 1$.

The application of Theodorsen's method is limited by the condition that the contour Γ must be close to the circle (the epsilon condition!). Moretti [184] proposed a way to overcome this difficulty by a sort of embedding which is based on the simple observation that, for a suitable α in the range $0 < \alpha < 1$, the contour Γ_1 parameterized by

$$\eta_1(s) := \alpha e^{is} + (1 - \alpha)\eta(s) \quad (241)$$

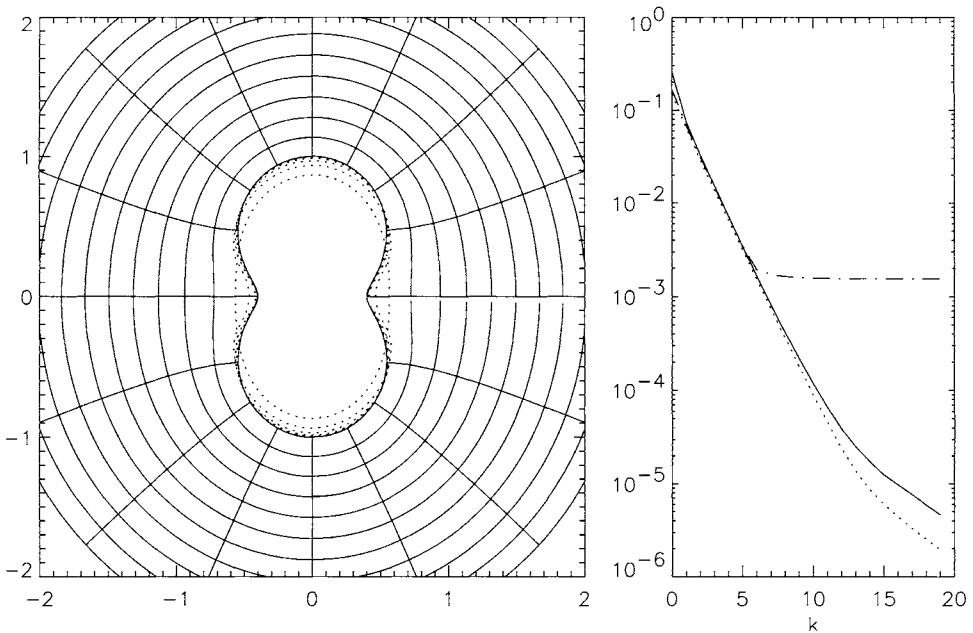


Fig. 19. Mapping from the exterior of the unit disk to the outside of an inverted ellipse with parameter $p = 0.4$ calculated with the AP method. The solid lines show images of 11 concentric circles with radii $1, 1.2, \dots, 3$. All other quantities as in Figure 6.

satisfies the epsilon condition.

Differentiation of (122) with respect to t yields the equation

$$ie^{it}\Phi'(e^{it}) = \dot{\eta}(S(t))S'(t) \quad (242)$$

which connects the boundary values of the analytic function Φ' with the derivatives of η and S . The function $\log \Phi'$ is analytic in D^- with boundary values

$$\log \Phi'(e^{it}) = \log r(S(t)) + \log S'(t) + i\left[\theta(S(t)) - t - \frac{\pi}{2}\right] \quad (243)$$

with the functions r and θ as defined in (174). The derivative Φ' as well as its logarithm have no $(1/z)$ -term in their Laurent expansion. Therefore, the integral

$$\int_0^{2\pi} \log \Phi'(e^{it}) e^{it} dt = 0 \quad (244)$$

vanishes. It has been noticed by Timman [263] that equation (243) can be used to devise a projection method (see also James [130], Henrici [107] and Gutknecht [95]).

Start from a function S_0 so that $S_0(t) - t$ is 2π -periodic.

If S_k is determined for some $k \geq 0$, calculate v as in (175). In order to take the condition (244) into account, the function w is not calculated by $w = \mathbf{K}v$ as in (176) but by $w = \mathbf{K}^{(1)}v$ with the conjugation operator modified so that it omits the first-order terms. It is defined in terms of the Fourier series (26) by

$$\begin{aligned}\mathbf{K}^{(1)}\phi(s) &= \sum_{l=2}^{\infty} (-iA_l e^{ils} + iA_{-l} e^{-ils}) \\ &= \sum_{l=2}^{\infty} (-b_l \cos ls + a_l \sin ls).\end{aligned}\quad (245)$$

The boundary correspondence function is determined from

$$S_{k+1}(t) := \frac{2\pi}{\int_0^{2\pi} \exp(w(\tau))/r(S_k(\tau)) d\tau} \int_0^t \frac{\exp(w(\tau))}{r(S_k(\tau))} d\tau \quad (246)$$

which is derived from the condition that in view of (243) the function $\exp(w)/r$ should be the derivative of the boundary correspondence function S . Henrici [107, p. 411] recommends the evaluation of the integrals in (246) by means of Fourier series.

If θ is twice continuously differentiable and the curvature θ'' is nearly constant and does not change rapidly (i.e., $|\theta''|$ is small), then the iterates S_k converge uniformly to the exact boundary correspondence function S as $k \rightarrow \infty$ (Nasyrov and Fokin [188]). Convergence in L^∞ was proved for nearly circular curves by Kaiser [131] under more restrictive smoothness requirements.

A simple convergence proof can be based on the theorem of Ostrowski (see Ortega and Rheinboldt [204, p. 300]). To this aim one has to show that the iteration operator $S_{k+1} = \mathbf{M}S_k$ defined in (246) is Fréchet differentiable and the derivative \mathbf{M}' has spectral radius < 1 . For the circle $\eta(s) = e^{is}$ one calculates

$$\mathbf{M}'(1) = \mathbf{M}'(\cos s) = \mathbf{M}'(\sin s) = 0, \quad (247)$$

$$\mathbf{M}'(\cos ls) = -\frac{1}{l} \cos ls, \quad \mathbf{M}'(\sin ls) = -\frac{1}{l} \sin ls \quad \text{for } l \geq 2.$$

If the method would be applied with the full conjugation operator \mathbf{K} instead of $\mathbf{K}^{(1)}$, one would get $\mathbf{M}'(\cos s) = -\cos s$ and $\mathbf{M}'(\sin s) = -\sin s$ instead of the first of the equations (247). The spectral radius of \mathbf{M}' would be 1 and the method would not even converge for the unit circle.

It follows from (247) that for nearly circular regions the iteration converges linearly with a rate $q \approx 1/2$ and that it oscillates around the limit function. This behavior suggests a relaxation method with the aim to damp the oscillations and to speed up convergence. Instead of the iteration defined by (246) one iterates functions \tilde{S}_k defined by

$$\tilde{S}_{k+1} := \alpha S_{k+1} + (1 - \alpha) \tilde{S}_k \quad (248)$$

with S_{k+1} defined by (246) and a relaxation parameter α . In view of the convergence rate $1/2$ for the disk, a value of $\alpha = 2/3$ seems to be a good choice. When the conformal mapping to the exterior of the peanut (Example 10) is calculated by Timman's method without relaxation, a convergence rate $q = 0.86$ is observed. Relaxation (248) with $\alpha = 2/3$ decreases the rate to $q = 0.40$.

EXAMPLE 8. Tear is parameterized by

$$\eta(s) = \cos s + 0.2 \cos(2s) + i[0.5 \sin s - 0.2 \sin(2s)]. \quad (249)$$

Figure 20 shows the result of a calculation for the mapping from D^- to the exterior of the tear (Example 8) with Timman's method on a grid with $N = 256$ points. The convergence rate with relaxation ($\alpha = 2/3$) is $q = 0.25$. Without relaxation the rate would be $q = 0.65$.

It must be noted that the only normalization achieved by Timman's method is $S(0) = 0$. The mapping function can have the general form near infinity $\Phi(z) = az + a_0 + O(1/z)$ with complex numbers a and a_0 .

The real part of (242) is up to a constant the conjugate of the imaginary part. When one uses the representation (28) of the operator of conjugation, a relation

$$\log[r(S(t))S'(t)] = \frac{1}{\pi} \int_0^{2\pi} \log \left| \sin \frac{s-t}{2} \right| d\theta(S(t)) + c \quad (250)$$

follows which expresses the ratio $d\sigma/dt = r(S(t))S'(t)$ of arclength $d\sigma$ on the curve to the arclength dt on the unit circle under conformal mapping by the changes $d\theta(S(t))$ in the tangent angle. This formula is applicable also for regions with corners, where the function $\theta(s)$ has jumps. When G is a polygon, (250) expresses $\log \Phi'(e^{it})$ in terms of the angles of the polygon. Thus the Schwarz–Christoffel formula can be easily derived. Equation (250) in its general form is the basis of the generalized Schwarz–Christoffel methods of Floryan and Zemach [59–61], the inverse Timman method of DeLillo and Elcrat [40] and the method of Nieto et al. [192]. With suitable modifications it can also be used for the mapping of interior regions.

One can combine Timman's and Theodorsen's methods in a way which was first studied by Friberg [64]. One can use a parameterization

$$\eta(s) = \rho(s)e^{i\beta(s)} \quad (251)$$

of the boundary curve. It follows from (242) and (122) that

$$\begin{aligned} & \log[i e^{it} \Phi'(e^{it}) / \Phi(e^{it})] \\ &= \log[r(S(t))S'(t) / \rho(S(t))] + i[\theta(S(t)) - \beta(S(t))] \end{aligned} \quad (252)$$

holds with r and θ as defined in (174). Therefore, S' can be reconstructed from the function $\theta - \beta$ (this is the angle of the tangent with the radius vector) by means of conjugation.

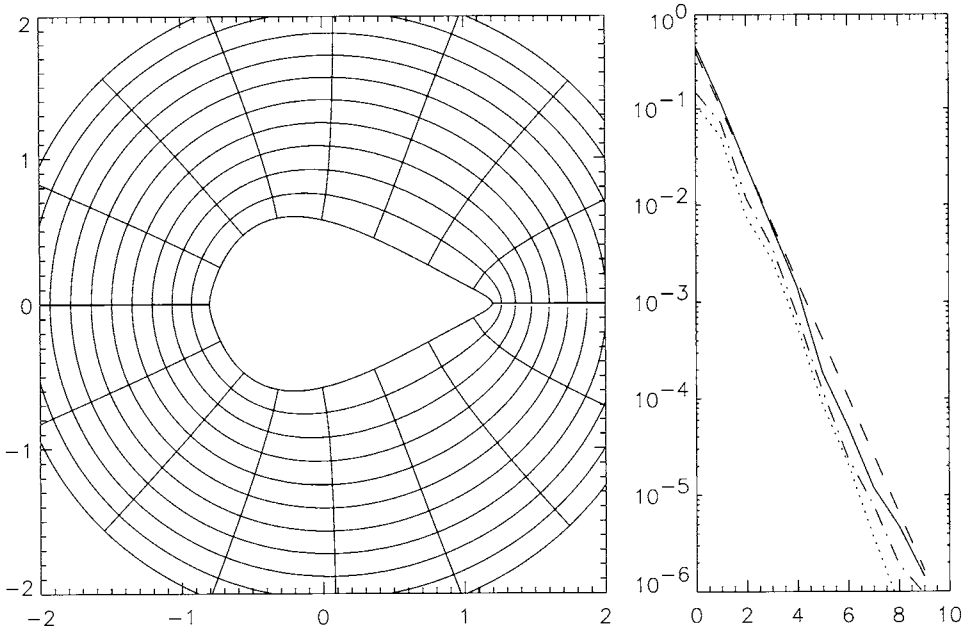


Fig. 20. Mapping from the exterior of the unit disk to the outside of the tear (Example 8) by Timman's method with relaxation parameter $\alpha = 2/3$.

This can be the basis of an iterative method. Start from a function S_0 such that $S_0(t) - t$ is 2π -periodic. For $k \geq 0$ put

$$v(t) := \theta(S_k(t)) - \beta(S_k(t)) \quad \text{and} \quad w = \mathbf{K}v. \quad (253)$$

The next approximation for the boundary correspondence function is then determined from

$$S_{k+1}(t) := c \int_0^t \frac{\rho(S_k(\tau)) \exp(w(\tau))}{r(S_k(\tau))} d\tau \quad (254)$$

with the norming factor

$$c := \frac{2\pi}{\int_0^{2\pi} \rho(S_k(\tau)) \exp(w(\tau))/r(S_k(\tau)) d\tau}. \quad (255)$$

Since $iz\Phi'(z)/\Phi(z)$ tends to i as $z \rightarrow \infty$, the constant c is equal to 1 for the exact mapping. But during the iteration values of c different from 1 can occur. This must be corrected in order to guarantee that $S_k(t) - t$ is a 2π -periodic function.

The iteration operator is described by equations (253)–(255). Its derivative, evaluated for the circle, is the null-operator. Therefore, the Friberg method converges for regions whose boundary is close to the circle in the same sense as discussed before for the Timman method. Convergence can be arbitrarily fast for curves very close to the circle. The method

does not converge for the peanut of Example 10 when started with $S_0(t) = t$. The iterates oscillate around the true function $S(t)$. Also, in this case relaxation helps. When the method is modified by relaxation with parameter $\alpha = 2/3$ then it converges at a rate $q = 0.59$ for the peanut example.

EXAMPLE 9. Curve is parameterized by (251) with

$$\rho(s) = 2 + 0.3 \cos s + 0.8 \cos(2s), \quad \beta(s) = s - 0.1 \cos s + 0.2 \sin s. \quad (256)$$

The conformal mapping from the disk to the exterior of the curve of Example 9 is calculated by Friberg's method on a grid of 256 points with a relaxation factor of $\alpha = 0.666$. The result is shown in Figure 21. Convergence is linear with a rate of $q = 0.92$. Without relaxation the rate would be $q = 0.94$.

Gutknecht [95] gives a very general framework which covers several of these projection methods. From Φ an auxiliary function H is derived. The condition that H must be analytic gives a nonlinear integral equation or integrodifferential equation for the boundary correspondence function which involves the conjugation operator \mathbf{K} . It is known a priori that the two functions $\Phi(z)/z$ and $\Phi'(z)$ do not vanish. Therefore, their logarithm is analytic in D^- . Linear combinations of these logarithms give suitable auxiliary functions from which "successive conjugation" methods are derived. The methods of Theodorsen, Timman and Friberg provide illustrative examples.

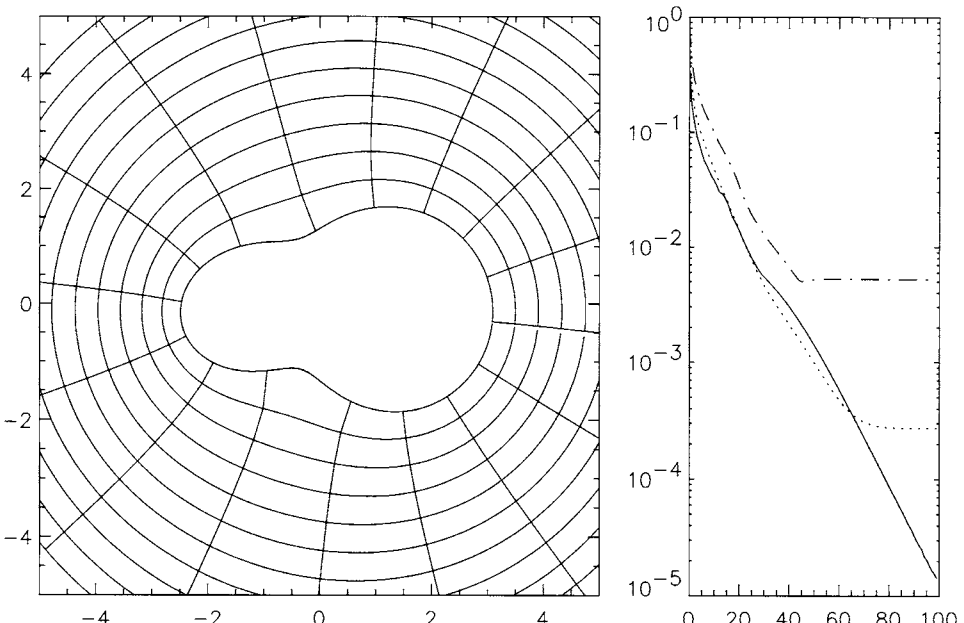


Fig. 21. The mapping from the exterior of a disk to the exterior of the curve of Example 9 calculated with Friberg's method.

Halsey [97] found in numerical experiments that Timman's method converges better than Theodorsen's. He attributes this to the possibility that the numerically calculated approximations to S can become nonmonotone in Theodorsen's method but not in Timman's. It must be noted, however, that all examples, where Halsey finds failure of Theodorsen's method, do not satisfy the epsilon condition with $\varepsilon < 1$. Therefore, a theoretician's explanation of divergence would be that the examples are outside Theodorsen's reach anyway.

Theodorsen's method converges for regions with nearly circular boundary linearly with a rate approximately $\|\rho'\|_\infty$, when the boundary curve is parameterized by (126). Therefore, convergence can be very fast or very slow, depending on ρ . Timman's method, on the other hand converges with a rate around $1/2$. Therefore, each of these methods has its range, where it converges better than the other.

The Newton methods described in Section 4.3 can be readily adapted to the exterior mapping problem. For the Wegmann method described by equations (175) to (179) only the signs in front of the functions w and h have to be changed.

Start with a function $S_0(t)$ such that $S_0(t) - t$ is a 2π -periodic function in W . (The natural choice is $S_0(t) = t$.)

When S_k is determined for some $k \geq 0$ then calculate the functions and numbers

$$v(t) := \theta(S_k(t)) - t = \arg[e^{-it} \dot{\eta}(S_k(t))], \quad (257)$$

$$w := \mathbf{K}v, \quad \alpha := \mathbf{J}v, \quad (258)$$

$$g := \frac{r(S_k(t))}{\exp(w(t))} \operatorname{Im} \frac{\eta(S_k(t))}{\dot{\eta}(S_k(t))}, \quad (259)$$

$$h := \mathbf{K}g, \quad \gamma := \mathbf{J}g, \quad (260)$$

$$DS(t) = \frac{\exp(w(t))(h(t) - \gamma \cot \alpha)}{r(S_k(t))} - \operatorname{Re} \frac{\eta(S_k(t))}{\dot{\eta}(S_k(t))}, \quad (261)$$

$$S_{k+1}(t) := S_k(t) + DS(t). \quad (262)$$

EXAMPLE 10. A peanut with boundary parameterization

$$\eta(s) = [1 + 0.5 \cos(2s) + 0.1 \cos(4s)]e^{is}. \quad (263)$$

Figure 22 shows the mapping from D^- to the exterior of a peanut described in Example 10 calculated with the Wegmann method on a grid with 256 points starting from $S_0(t) = t$.

DeLillo and Elcrat [38] performed a series of test calculations for mappings from the exterior of the unit disk to the exterior of ellipses, sportgrounds, inverted ellipses, cosine airfoils, perturbed circles and general spline curves. They compare the methods of Timman, Friberg, Wegmann and Theodorsen with regard to accuracy, computing time and convergence behavior. They come to the conclusion that "Wegmann is the most efficient and most robust. Friberg is superior to Timman for nearly circular domains [...] for extreme regions Timman is preferable if arclength is used as the parameter". They find also that the methods of Timman, Friberg and Wegmann after initial convergence may diverge finally. This is attributed to the term $r(S)$. An indication for this is the observation that this did not occur for Timman's method when parameterization by arclength is used [38, p. 415].

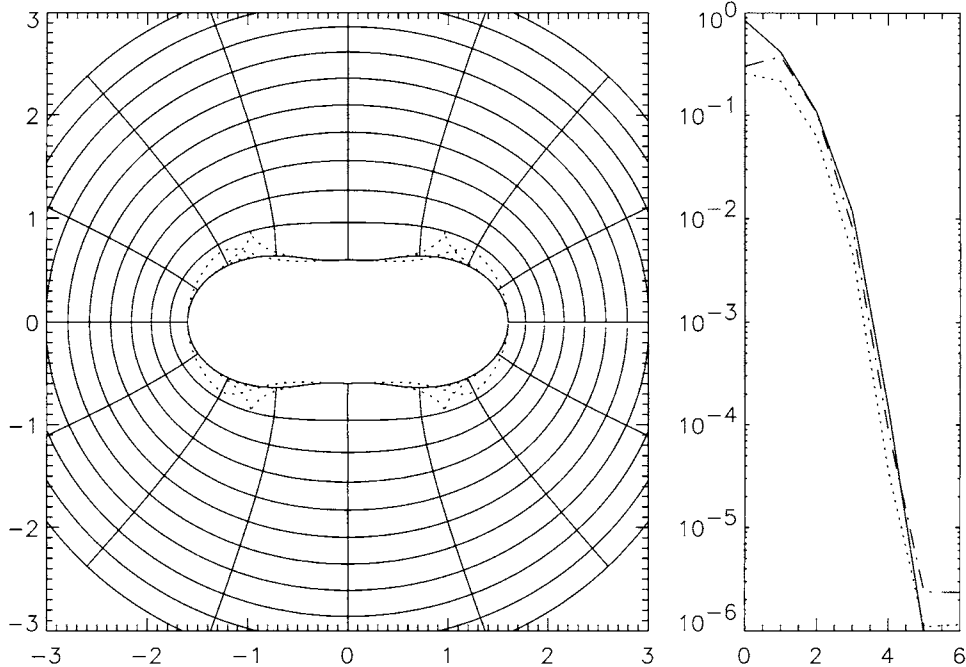


Fig. 22. The mapping from the exterior of a disk to the exterior of the peanut of Example 10 calculated with Wegmann's method.

9. Mapping to Riemann surfaces

The derivative Φ' of a conformal mapping Φ of the disk to a simply connected region does not vanish in D . The differentiated boundary correspondence equation (242) shows that the winding number of $\Phi'(e^{it})$ is connected to the winding number of $\dot{\eta}$ by

$$\text{wind}(\Phi'(e^{it})) = \text{wind}(\dot{\eta}) - 1. \quad (264)$$

Only in the case $\text{wind}(\dot{\eta}) = 1$, the winding number of $\Phi'(e^{it})$ is zero, which ensures by the argument principle that Φ' does not vanish in D . The same holds for exterior mappings: if $\text{wind}(\dot{\eta}) = 1$ then Φ' does not vanish in the exterior D^- of the disk.

When the curve Γ has self intersections, it can still be the boundary of a simply connected region G on a suitable Riemann surface. If $\text{wind}(\dot{\eta}) = 1$, the branch points of the Riemann surface must be outside G . In this case the methods for mapping D (or D^-) to the region, as described in Sections 4 and 8.2, can be applied without modification.

EXAMPLE 11. Figure 8 is parameterized by

$$\eta(s) = \cos s + i[0.5 \sin s + 0.8 \sin(3s)]. \quad (265)$$

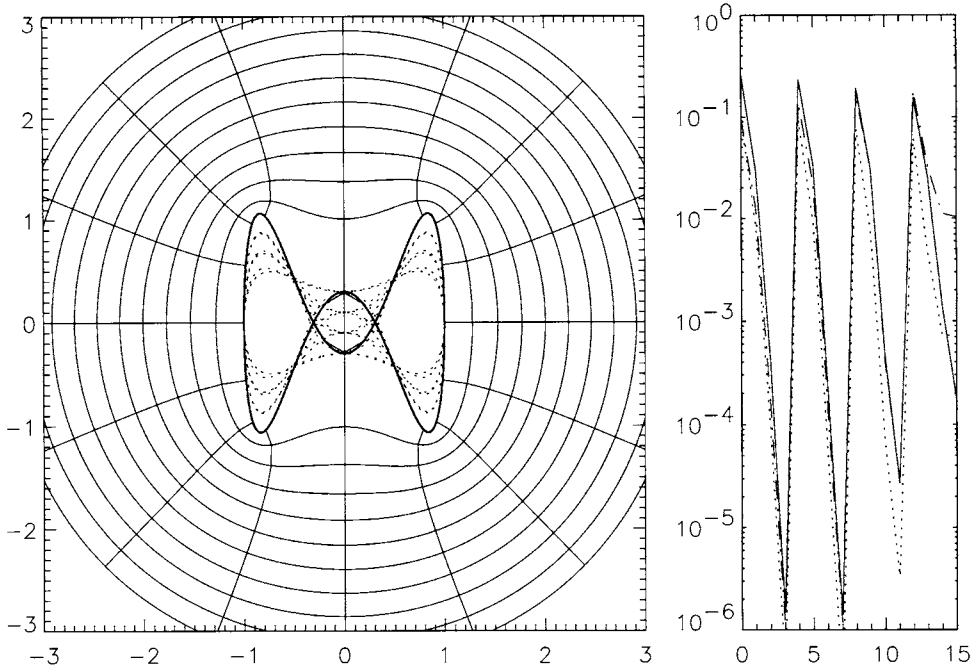


Fig. 23. The mapping from the exterior of a disk to the Riemann surface with boundary curve (265).

The region G outside of the curve of Example 11 covers a neighborhood of the origin twice. Figure 23 shows the conformal mapping from D^- to this region calculated by the Wegmann method on a grid with $N = 2048$ points. The computation is done in combination with a continuation method. The factor d in front of the $\sin(3s)$ term is gradually enlarged in four steps from 0.2, 0.4, 0.6, to 0.8. For each value of d four iterations are performed. Then the value of d is enlarged and the method is started with the result of the last iteration as S_0 . This explains the sawtooth behavior of the changes δ on the right panel of Figure 23. The achievable accuracy deteriorates as the region becomes more and more difficult. Crowding occurs at the flanks of the Figure 8. The wasp tail is only poorly resolved.

Figure 24 shows the image of 16 concentric circles of radii 1 (0.01) 1.15. For greater clarity only the image of the sector re^{it} for $|t + \pi/2| \geq \pi/128$ is shown.

The situation changes when $\text{wind}(\dot{\eta}) = 1 + l$, with $l > 0$ for the interior and $l < 0$ for the exterior mapping problem. It follows from the argument principle that, for each mapping Φ , the derivative Φ' must have l zeros in D or $-l$ zeros in D^- . These zeros correspond to branch points of the Riemann surface where G resides. These branch points lie in the target region G .

If the curve Γ is parameterized by a 2π -periodic function η such that $m := \text{wind}(\dot{\eta}) = 1 + l > 0$, one can still try to satisfy the boundary correspondence equation (122) with a function Φ analytic in D . The derivative Φ' of this function has zeros at l (not necessarily distinct) points $\zeta_1, \dots, \zeta_l \in D$. The curve Γ is then the boundary of a region G which

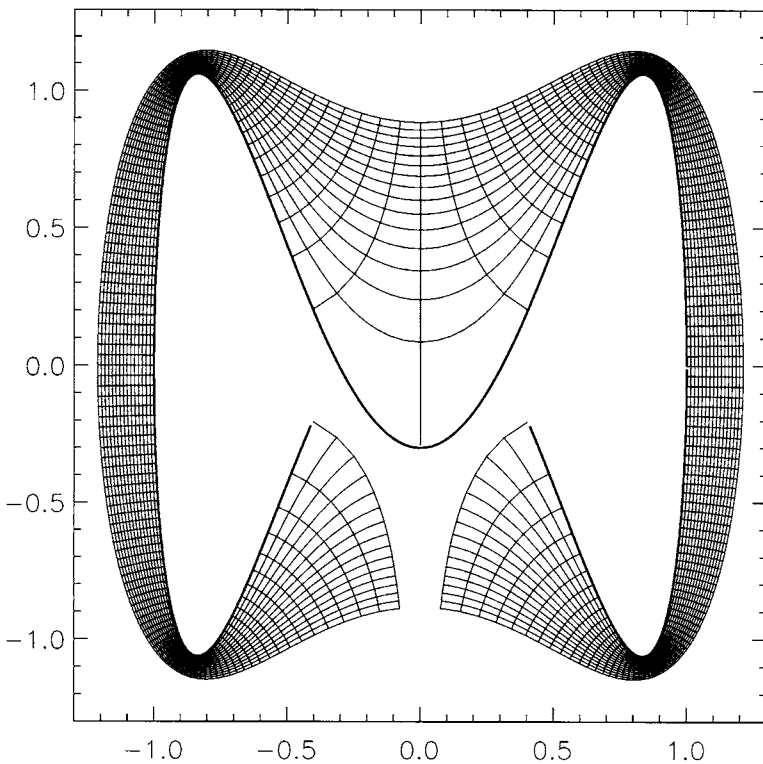


Fig. 24. Detail of Figure 23.

is part of the Riemann surface of the function Φ . The mapping $z \rightarrow \Phi(z)$ from D to G is conformal everywhere with the exception of the zeros ζ_j which are mapped to branch points of G .

The mapping is unique when the values

$$\Phi(z_j) = w_j \quad (266)$$

at m different points $z_j \in D$, $j = 1, \dots, m$, and at a boundary point $z_0 \in \partial D$ are prescribed. The values w_j are in G for $j = 1, \dots, m$ and in Γ for $j = 0$. There are other possibilities. One can prescribe instead the position of the preimages of the branch points, i.e., the zeros ζ_1, \dots, ζ_l of Φ' in D .

Wegmann [283] showed that his method (see equations (175) to (180)) can be adapted in the following way.

Let $m := \text{wind } \dot{\eta}$ be a positive number.

Start with $S_0(t)$ such that $S_0(t) - t$ is a 2π -periodic function in W . When S_k is determined for some $k \geq 0$, the change DS is calculated from the condition (171), which is equivalent to the RH problem (172). The RH problem is solved with Theorem 9. One has

to calculate the functions

$$v(t) := \theta(S_k(t)) - mt = \arg[e^{-imt} \dot{\eta}(S_k(t))], \quad (267)$$

$$w := \mathbf{K}v, \quad (268)$$

$$g := r(S_k(t)) \exp(w(t)) \operatorname{Im} \frac{\eta(S_k(t))}{\dot{\eta}(S_k(t))}, \quad (269)$$

$$h := \mathbf{K}g. \quad (270)$$

There are analytic functions Y and Ξ in D with boundary values

$$Y(e^{it}) = -w + iv, \quad \Xi(e^{it}) = -h + ig. \quad (271)$$

According to Theorem 9, the general solution of the RH problem (172) is

$$\Psi(z) = z^m \exp(Y(z)) (\Xi(z) + P_m(z)) \quad (272)$$

with a Laurent polynomial P_m of form

$$P_m(z) = \sum_{j=-m}^m p_j z^j \quad (273)$$

with complex coefficients p_j satisfying

$$p_{-j} = \overline{p_j} \quad \text{for } j = 0, \dots, m. \quad (274)$$

When the calculation is done on a grid of $N = 2n$ points, then the functions Y and Ξ are obtained as polynomials of degree n . The coefficients of these polynomials are obtained as a by-product of the process of conjugation. Therefore, the values of Y and Ξ at the points z_j , $j = 0, \dots, m$, can be easily calculated. Using the condition that Ψ must satisfy the interpolation conditions (266), the values of P_m at these points are evaluated as

$$P_m(z_j) = \frac{w_j}{z_j^m \exp(Y(z_j))} - \Xi(z_j). \quad (275)$$

The condition (274) is equivalent to

$$P_m(1/\overline{z_j}) = \overline{P_m(z_j)}. \quad (276)$$

Equations (275) and (276) yield interpolation conditions at the $2m + 1$ points $z_0, z_1, \dots, z_m, 1/\overline{z_1}, \dots, 1/\overline{z_m}$ for the polynomial $z^m P_m(z)$ of degree $\leq 2m$. Therefore, P_m is uniquely defined by (275) and (276). Inserting (272) into (171) gives the change

$$DS(t) = \frac{-h(t) + P_m(e^{it})}{r(S_k(t)) \exp(w(t))} - \operatorname{Re} \frac{\eta(S_k(t))}{\dot{\eta}(S_k(t))}. \quad (277)$$

Note that in view of (274) the function $P_m(e^{it})$ is real.

EXAMPLE 12. Trefoil with boundary parameterization

$$\eta(s) = \cos(2s) + 0.2 \sin s + i[\sin(2s) + 0.4 \cos s]. \quad (278)$$

Figure 25 shows the result of a calculation with this method for the mapping Φ of the unit disk to the trefoil of Example 12 satisfying the interpolation conditions (266) with

$$\begin{aligned} z_0 &= 1, & z_1 &= 0.8i, & z_2 &= -0.8i, \\ w_0 &= 1 + 0.4i, & w_1 &= w_2 &= -0.64. \end{aligned} \quad (279)$$

The calculation is done with 256 grid points.

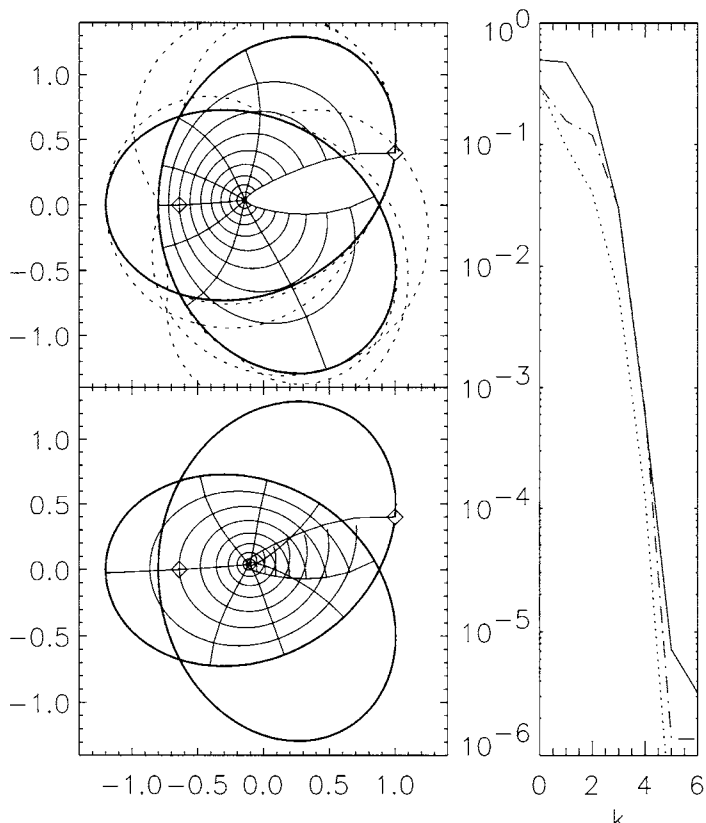


Fig. 25. Mapping from the unit disk to the trefoil of Example 12. The upper (lower) panel shows the image of the upper (lower) semidisc. The interpolation points (279) are indicated by diamonds. The graph on the right shows $\delta, \alpha, \varepsilon$ during the iteration.

10. Mapping of a doubly-connected region to an annulus

For $0 < q < 1$ let A_q be the *circular annulus* $A_q := \{z : q < |z| < 1\}$. It is well known that any doubly-connected region G such that each boundary component consists of more than one point is conformally equivalent to an annulus A_q . The number q is uniquely determined by G . The inverse $M := 1/q$ is called the *module* of G .

When a boundary component of G consists of a single point z_0 , then each conformal mapping of G has a removable singularity at z_0 and can therefore be extended to a conformal mapping of the simply connected region $G \cup \{z_0\}$.

Let G be a doubly-connected region bounded by Jordan curves Γ_1 from outside and Γ_2 inside (see Figure 26). The curves Γ_j are parameterized by 2π -periodic complex functions $\eta_j(s)$. Both curves are orientated in the counterclockwise direction. Let $F : G \rightarrow A_q$ be the conformal mapping which maps Γ_1 to the unit circle and Γ_2 to the circle with radius q . The mapping F is unique up to a rotation $e^{i\alpha}$ with an arbitrary real number α .

10.1. Potential theoretic methods

Symm [255] adapted his method for the mapping of doubly-connected regions in the following way. Assume that 0 is inside the inner boundary Γ_2 . Then the function $H(z) := \log(F(z)/z)$ defined as in (64) is analytic in G . Its real part $u := \operatorname{Re} H$ is a harmonic function in G with boundary values

$$u(\eta_1(s)) = -\log|\eta_1(s)|, \quad u(\eta_2(s)) = \log q - \log|\eta_2(s)| \quad (280)$$

on $\Gamma := \partial G = \Gamma_1 \cup \Gamma_2$. These conditions ensure that $|F| = 1$ on Γ_1 and $|F| = q$ on Γ_2 . The harmonic function u is represented as a single-layer potential with densities σ_1 and σ_2 on the boundary components as in (80):

$$u(z) = -\frac{1}{2\pi} \sum_{j=1}^2 \int_0^{2\pi} \log|z - \eta_j(s)| \sigma_j(s) ds. \quad (281)$$

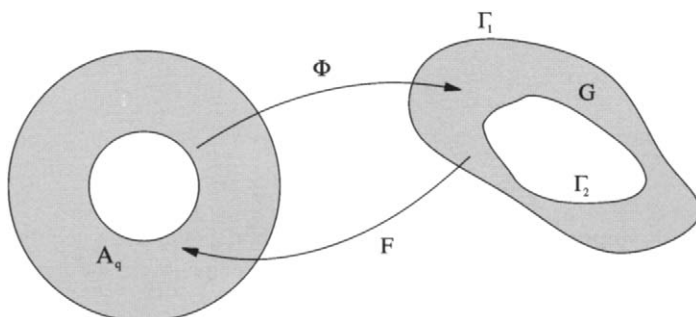


Fig. 26. The conformal mapping F from a doubly-connected region G to an annulus A_q and its inverse Φ .

This gives a pair of integral equations of the first kind:

$$\frac{1}{2\pi} \sum_{j=1}^2 \int_0^{2\pi} \log |\eta_1(t) - \eta_j(s)| \sigma_j(s) ds = \log |\eta_1(t)| \quad (282)$$

and

$$\frac{1}{2\pi} \sum_{j=1}^2 \int_0^{2\pi} \log |\eta_2(t) - \eta_j(s)| \sigma_j(s) ds + \log q = \log |\eta_2(t)|, \quad (283)$$

for the densities σ_j which still contain the yet unknown parameter q .

The single-layer potential u is single valued. The conjugate function v , however, which is needed in the representation $H = u + iv$ will in general not be single valued. Let C be a simple closed curve in G which surrounds Γ_2 once in the counterclockwise direction and let τ be arclength on C . Different branches of the (possibly) multivalued function v differ by integer multiples of

$$A := \int_C \frac{\partial v}{\partial \tau} d\tau = \int_C \frac{\partial u}{\partial n} d\tau. \quad (284)$$

The Cauchy–Riemann equations have been used to transform the first integral in (284) to an integral involving the derivative of u with respect to the outer normal n . The function v is single-valued if and only if $A = 0$. The last integral in (284) is proportional to the “charges” inside C . In view of the representation (281) the condition $A = 0$ is equivalent to the condition

$$\int_0^{2\pi} \sigma_2(s) ds = 0. \quad (285)$$

Equations (282), (283) and (285) are coupled integral equations for σ_1, σ_2 and q , which have a unique solution. The conformal mapping is $F(z) = z \exp(H(z))$ with

$$H(z) = -\frac{1}{2\pi} \sum_{j=1}^2 \int_0^{2\pi} \log(z - \eta_j(s)) \sigma_j(s) ds + i\alpha. \quad (286)$$

Inoue [125, 126] proposed a charge simulation method. He investigated theoretically the distribution of charge points and charges and discussed convergence of the approximations to the mapping function.

One can also transfer the integral equations with Neumann kernel to doubly-connected regions (see, e.g., Gaier [65, p. 190]).

10.2. Extremum principles

Let G be a finite doubly connected Jordan region. We assume that 0 is in the hole inside the inner curve Γ_2 . The norm $\|\cdot\|_B$ and the scalar product $(\cdot, \cdot)_B$ for functions f, g on G are defined by the integrals over G as in the simply connected case (see (92) and (93)). The Bergman space $B(G)$ consists of all analytic functions in G for which $\|f\|_B$ is finite and which possess a single-valued indefinite integral in G .

Let F be the conformal mapping of G to an annulus A_q . The derivative

$$H'(z) := \frac{F'(z)}{F(z)} - \frac{1}{z} \quad (287)$$

of the auxiliary function $H(z) = \log(F(z)/z)$ is in $B(G)$. The following theorem characterizes H' by an extremal property (see Gaier [65, p. 249] and Papamichael and Kokkinos [210]).

THEOREM 18. *The unique function $f_0 \in B(G)$, which has minimal norm $\|f\|_B$ among all functions $f \in B(G)$ with the side condition*

$$(f, H')_B = 1, \quad (288)$$

is related to H' by the equation

$$H'(z) = \frac{f_0(z)}{\|f_0\|_B^2}. \quad (289)$$

This characterization seems to be useless at first glance, since the constraint (288) involves the unknown function H' . However, the integral in (288) can be evaluated using Green's formula (100) and the boundary values of H simply by

$$(f, H')_B = i \int_{\partial G} f(z) \log |z| dz. \quad (290)$$

Papamichael and Kokkinos [210] treat the minimization problem of Theorem 18 numerically by a Ritz procedure.

When, on the other hand, an orthonormal set f_j of basis functions in $B(G)$ is given, one can represent H' directly by the formula

$$H'(z) = \sum_{j=1}^n \beta_j f_j(z) \quad \text{with } \beta_j := \overline{(f_j, H')} \quad (291)$$

The coefficients β_j can be calculated via (290) without knowing H' . This method is called *orthonormalization method* (ONM) (see [210]).

The conformal module M of G can be calculated from H' by

$$2\pi \log M = \int_G \frac{dx dy}{|z|^2} - \|H'\|_B^2 = -i \int_{\partial G} \frac{\log |z|}{z} dz - \|H'\|_B^2 \quad (292)$$

(see Papamichael et al. [212], Gaier [65, p. 250]).

The natural set of basis functions consists of the monomials z^j , $j \neq -1$. It is important to augment this set of basis functions by singular functions which are more suitable to describe the conformal mapping near corners of G . In [210] some results and examples are reported. The method works very well when the region has certain symmetries. The performance for nonsymmetric regions is disappointing. This may be due to the presence of pole type singularities in the complement of G , which cannot be dealt with. Papamichael and Warby [217] investigate pole type singularities of H' for some special geometries. It turns out that the poles occur in pairs at points ζ_1, ζ_2 , where ζ_1 and ζ_2 are symmetric with respect to both curves Γ_1 and Γ_2 .

When the monomials are taken as basis functions the approximation of H' is by rational functions of the form

$$R_{m,n}(z) := \sum_{j=-m, j \neq -1}^n a_j z^j \quad (293)$$

with the term $j = -1$ omitted. When the boundary curves Γ_1, Γ_2 are analytic, the mapping function F and the function H' can be extended analytically into a region containing \bar{G} . Papamichael et al. [212] investigate the question of how the portion of positive and negative powers in (293) should be chosen in an optimal way depending on the location of the singularities of the analytic extension of H' nearest to Γ_1 and Γ_2 . They show furthermore, that the approximations $R_{m,n}^*$ and the corresponding approximations to F obtained by the ONM converge uniformly on \bar{G} as $m, n \rightarrow \infty$ with an error proportional to r^{m+n} , for some $r \in (0, 1)$. There are also convergence results for piecewise analytic boundaries similar to the results for Bieberbach polynomials for simply connected regions given in (115). The ONM approximation to the conformal module M is more accurate than the corresponding approximation to the conformal mapping F (Papamichael et al. [212, p. 494]).

Burbea [24] determines the module of a doubly-connected region using a relation of M with the Bergman kernel function.

11. Mapping from an annulus to a doubly-connected region

The conformal mapping $\Phi : A_q \rightarrow G$, the inverse of the mapping F , is uniquely determined up to a rotation of A_q . To fix this ambiguity one can impose the condition

$$\Phi(1) = \eta_1(0). \quad (294)$$

Instead of (294) one can also impose the condition that the coefficient of z in the Laurent expansion of Φ is real, i.e.,

$$\operatorname{Im} \int_0^{2\pi} e^{-it} \Phi(e^{it}) dt = 0. \quad (295)$$

The function Φ is completely determined by its boundary values. These are described by boundary correspondence functions S_1, S_2 , which satisfy the boundary correspondence equations

$$\Phi(e^{it}) = \eta_1(S_1(t)), \quad \Phi(qe^{it}) = \eta_2(S_2(t)). \quad (296)$$

These two equations, together with the norming (294), determine the functions S_1, S_2 and the parameter q . The condition (294) is equivalent to

$$S_1(0) = 0. \quad (297)$$

11.1. Boundary value problems

Conjugation on the annulus A_q is effected by a (real) linear operator $\mathbf{K}_q(\phi_1, \phi_2)$ which is most easily defined in terms of the complex or real Fourier series

$$\phi_j(t) = \sum_{l=-\infty}^{\infty} A_{l,j} e^{ilt} = a_{0,j} + \sum_{l=1}^{\infty} (a_{l,j} \cos lt + b_{l,j} \sin lt) \quad (298)$$

of the functions ϕ_j , $j = 1, 2$. Then

$$\mathbf{K}_q(\phi_1, \phi_2)(t) = \sum_{l=-\infty}^{\infty} B_l e^{ilt} = \sum_{l=1}^{\infty} (\alpha_l \cos lt + \beta_l \sin lt) \quad (299)$$

with the coefficients

$$B_0 = 0, \quad B_l := \frac{2iA_{l,2} - (q^{-l} + q^l)iA_{l,1}}{q^{-l} - q^l} \quad \text{for } l \neq 0 \quad (300)$$

and

$$\alpha_l := \frac{2b_{l,2} - (q^{-l} + q^l)b_{l,1}}{q^{-l} - q^l}, \quad \beta_l := -\frac{2a_{l,2} - (q^{-l} + q^l)a_{l,1}}{q^{-l} - q^l} \quad (301)$$

for $l = 1, 2, \dots$. Since $q < 1$, it follows from (300) that for $l \rightarrow \infty$ the coefficients satisfy

$$B_l \approx -iA_{l,1}, \quad B_{-l} \approx iA_{-l,1}. \quad (302)$$

Comparison with (27) shows that the conjugation $\mathbf{K}_q(\phi_1, \phi_2)$ acts on the high-order Fourier-terms like ordinary conjugation $\mathbf{K}\phi_1$ on the unit disk.

The following theorem, analogous to Theorem 8, shows how to construct analytic functions in an annulus with prescribed real part on the two boundary circles.

THEOREM 19. *Let ϕ_1, ϕ_2 be real functions in W . There exists an analytic function Φ in A_q with boundary values*

$$\operatorname{Re} \Phi(e^{it}) = \phi_1(t), \quad \operatorname{Re} \Phi(qe^{it}) = \phi_2(t), \quad (303)$$

if and only if the right-hand sides satisfy

$$\int_0^{2\pi} \phi_1 dt = \int_0^{2\pi} \phi_2 dt. \quad (304)$$

The general solution of (303) can be constructed in terms of the conjugation operator

$$\begin{aligned} \Phi(e^{it}) &= \phi_1(t) + i\mathbf{K}_q(\phi_1, \phi_2)(t) + i\gamma, \\ \Phi(qe^{it}) &= \phi_2(t) - i\mathbf{K}_q(\phi_2, \phi_1)(t) + i\gamma \end{aligned} \quad (305)$$

with an arbitrary real constant γ .

Condition (304) is in contrast to the situation for the disk where a solution of the boundary problem (24) exists for every right-hand side (Theorem 8).

Let λ be a real number. One can consider instead of (303) the more general RH problem

$$\operatorname{Re} \Phi(e^{it}) = \phi_1(t), \quad \operatorname{Re}(e^{i\lambda} \Phi(qe^{it})) = \phi_2(t). \quad (306)$$

When λ is a multiple of π then this problem reduces to (303). In this case it is solvable only if (304) is satisfied. But when λ is not a multiple of π , the problem (306) has a unique solution for every right-hand side. The solution can be expressed by an operator $\mathbf{K}_{q,\lambda}(\phi_1, \phi_2)$ which is quite analogous to \mathbf{K}_q (see Wegmann [285] for details). This means that the RH problem (306) becomes degenerate when $\lambda = 0 \bmod \pi$.

The general RH problem on the annulus

$$\operatorname{Re}(\overline{A_1(t)} \Phi(e^{it})) = \psi_1(t), \quad \operatorname{Re}(\overline{A_2(t)} \Phi(qe^{it})) = \psi_2(t), \quad (307)$$

is formulated with two complex Hölder continuous functions A_1, A_2 . This RH problem can be solved explicitly in terms of the operator $\mathbf{K}_{q,\lambda}$ (Banzuri [7], Wegmann [285]). For regions with connectivity greater than or equal to 2, there are cases where the solvability properties of the RH problem are not only determined by the *index* of the problem. These are the *special classes* discussed by Vekua [269, p. 257]. Unfortunately, just these degenerate problems are needed in the conformal mapping methods discussed below. On the other hand, these degeneracies offer opportunities to determine the accessory parameters such as the modulus of a doubly-connected region.

11.2. Projection

Fornberg [63] proposed a projection method. We adapt it slightly so that the similarity with the method for the simply connected regions (see (133)–(136)) becomes clear.

The iteration starts with functions $S_{0,1}$ and $S_{0,2}$ such that $S_{0,j}(t) - t$ are 2π -periodic for $j = 1, 2$. When the functions $S_{k,j}$ are determined for some $k \geq 0$, then Fourier analysis of the boundary functions

$$\eta_j(S_{k,j}(t)) = \sum_{l=-\infty}^{\infty} B_l^{(j)} e^{ilt} \quad (308)$$

gives the coefficients $B_l^{(j)}$.

When the mapping function Φ has Laurent expansion

$$\Phi(z) = \sum_{l=-\infty}^{\infty} B_l z^l \quad (309)$$

then the solution

$$B_l = B_l^{(1)} = q^{-l} B_l^{(2)} \quad (310)$$

holds for all l . The strategy is to change $S_{k,1}$ in such a way that the relation (310) is approximately satisfied for $l \leq 0$, and to change $S_{k,2}$ so that (310) is improved for $l \geq 1$. The normalization (295) is implemented into the change of $S_{k,1}$. This leads to a prescription as follows. We assume that the functions η_j are differentiable with derivative $\dot{\eta}_j \neq 0$.

First form, with the coefficients $B_l^{(j)}$ from (308), the functions

$$g_1(t) = \sum_{l=-\infty}^0 (B_l^{(1)} - q_k^{-l} B_l^{(2)}) e^{ilt} + i \operatorname{Im} B_1^{(1)} e^{it}, \quad (311)$$

$$g_2(t) = i \operatorname{Im} B_1^{(2)} e^{it} + \sum_{l=2}^{\infty} (B_l^{(2)} - q_k^l B_l^{(1)}) e^{ilt}. \quad (312)$$

Then new approximations for the boundary correspondence functions are calculated by

$$S_{k+1,j}(t) := S_{k,j}(t) - \operatorname{Re} \frac{g_j(t)}{\dot{\eta}_j(S_{k,j}(t))}. \quad (313)$$

A new estimate for q is calculated by

$$q_{k+1} = \frac{|B_1^{(2)}| + |B_{-1}^{(1)}|}{|B_1^{(1)}| + |B_{-1}^{(2)}|}. \quad (314)$$

The boundary values of the conformal mapping can be approximated in the k th iteration by the functions f_1 and f_2 on the outer and inner contour as follows:

$$f_1(t) = \sum_{l=-\infty}^{-1} q_k^{-l} B_l^{(2)} e^{ilt} + B_0^{(1)} + \operatorname{Re} B_1^{(1)} e^{it} + \sum_{l=2}^{\infty} B_l^{(1)} e^{ilt}, \quad (315)$$

$$f_2(t) = \sum_{l=-\infty}^0 B_l^{(2)} e^{ilt} + \operatorname{Re} B_1^{(2)} e^{it} + \sum_{l=2}^{\infty} q_k^l B_l^{(1)} e^{ilt}. \quad (316)$$

Fornberg [63] gives more details about the most convenient organization of the computation. He gives also a graphical illustration of how the change in the S_j is determined from the error functions g_j . Fornberg changes S_1 and S_2 at the same time, as in formulas (313). But one can use instead a “Einzelschritt-iteration”. Then one determines the new $S_{k+1,1}$ first and then uses $S_{k+1,1}$ to calculate new $B_l^{(1)}$ via (308), before g_2 in (312) and $S_{k+1,2}$ in (313) are evaluated.

EXAMPLE 13. Region is bounded by two ellipses (see Figure 27)

$$\begin{aligned} \eta_1(s) &= \cos s + 0.2 \sin s + 0.7i \sin s, \\ \eta_2(s) &= -0.1 + 0.3 \cos s + i(-0.05 + 0.4 \sin s). \end{aligned} \quad (317)$$

The calculation for Example 13 is started with $S_{0,j}(t) = t$ and $q_0 = 0.5$. The calculated inverse module is $q = 0.46300$. The iteration converges linearly with a rate of 0.90. On each boundary component 128 grid points have been used. The approximation for q converges much faster than the iteration for the S_j . In general, the calculated q is more accurate than the boundary correspondence functions.

Garrick [81] carried over the method of Theodorsen to doubly-connected regions. Let G be bounded by two star-shaped curves

$$\eta_1(s) = \rho_1(s)e^{is}, \quad \eta_2(s) = \rho_2(s)e^{is} \quad (318)$$

with $0 < \rho_2(s) < \rho_1(s)$. The boundary correspondence equation for the auxiliary function $\Psi(z) := \log(\Phi(z)/z)$ can be written in the form

$$\Psi(e^{it}) = \log \rho_1(S_1(t)) + i(S_1(t) - t), \quad (319)$$

$$\Psi(qe^{it}) = \log \rho_2(S_2(t)) - \log q + i(S_2(t) - t). \quad (320)$$

Since Ψ is analytic in the annulus A_q (with unknown q), the real and imaginary parts of Ψ on the boundary circles are connected by the operator of conjugation. This leads to the pair of integral equations of Theodorsen–Garrick

$$S_1(t) = t + \mathbf{K}_q(\psi_1, \psi_2), \quad S_2(t) = t - \mathbf{K}_q(\psi_2, \psi_1), \quad (321)$$

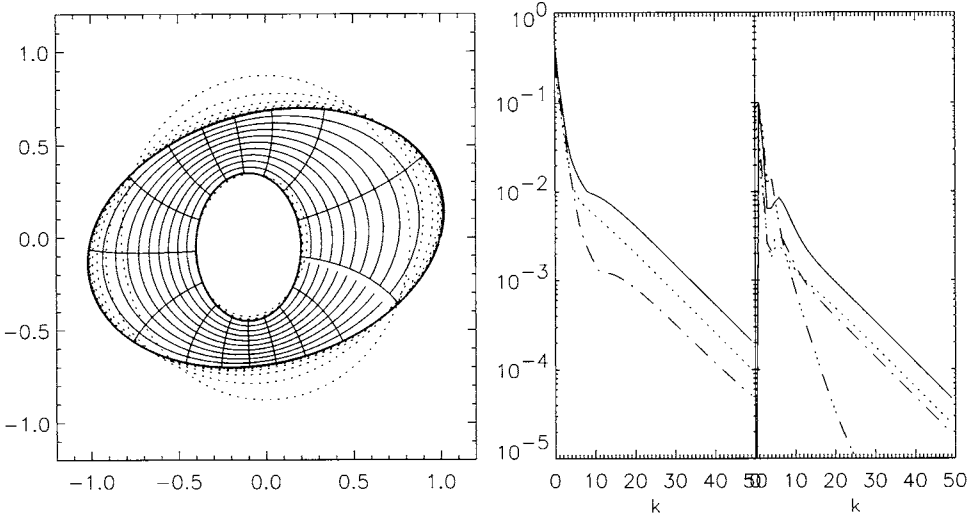


Fig. 27. Mapping from an annulus to the region of Example 13 calculated with the projection method. The left panel shows the images of 11 concentric circles and 16 spokes in A_q . The approximations f_1, f_2 according to (315) and (316) are dotted. The right panel shows the maximal changes δ_k of S_j in each iterative step and the L_2 norm of g_j (dotted) and the error ε_k (dash-dotted) on the outer (left) and inner contour (right). The long dash-dotted curve in the right panel shows the change in q in each step.

with

$$\psi_1(t) = \log \rho_1(S_1(t)), \quad \psi_2(t) = \log \rho_2(S_2(t)). \quad (322)$$

Equations (321) imply that

$$\int_0^{2\pi} (S_1(t) - t) dt = \int_0^{2\pi} (S_2(t) - t) dt = 0. \quad (323)$$

Hence the normalization (295) is satisfied. From $\int \operatorname{Re} \Psi(e^{it}) dt = \int \operatorname{Re} \Psi(qe^{it}) dt$ and equations (319) and (320) the representation

$$\log q = \frac{1}{2\pi} \int_0^{2\pi} (\log \rho_2(S_2(t)) - \log \rho_1(S_1(t))) dt \quad (324)$$

for q follows. This equation means that the module $1/q$ is the ratio of the geometric means of $\rho_1(S_1)$ and $\rho_2(S_2)$.

The system (321) of nonlinear equations can be solved by iteration (see Gaier [65, p. 202]). Start with a guess $q_0 \in (0, 1)$ for q and with functions $S_{0,j}(t)$ such that $S_{0,j}(t) - t$ are 2π -periodic and in W . When functions $S_{k,j}$ and a number $q_k \in (0, 1)$ are determined for some $k \geq 0$, then insert these into the right-hand side of (321) to calculate the new iterates $S_{k+1,j}$ and then use these to calculate a new value q_{k+1} by means of (324). The

iteration converges under conditions which roughly mean that G is already close to an annulus (see Gaier [65, p. 200] and Ostrowski [206] for more detail).

The discretized form of the equations (321) has been studied by Hammerschick [98]. He showed that under certain conditions on the curve there is a unique solution and the iterative method of solution converges.

EXAMPLE 14. A region bounded by two star-shaped curves is parameterized as in (318) with

$$\rho_1(s) = 1 + 0.5 \sin s, \quad \rho_2(s) = 0.5 + 0.2 \cos(2s). \quad (325)$$

Example 14 calculated on a grid with 256 points with the method of Theodorsen–Garrick is shown in Figure 28. The iteration converged with a rate of 0.82. The calculated inverse module is $q = 0.640174$.

Garrick expressed conjugation by integral operators (see Gaier [65, p. 194]). Calculations became much more efficient when the representation in terms of Fourier series (299) was used in combination with FFT (Ives [129]). The method of Garrick is described in detail by Gaier and Papamichael [79].

11.3. The Newton method

The Newton method for the equations (296) starts from the linearized equations

$$\Psi(e^{it}) = \eta_1(S_1(t)) + \dot{\eta}_1(S_1(t))DS_1(t), \quad (326)$$

$$\Psi(qe^{it}) + e^{it}\Phi'(qe^{it})Dq = \eta_2(S_2(t)) + \dot{\eta}_2(S_2(t))DS_2(t). \quad (327)$$

Since the functions DS_j are real, these equations can be transformed to an RH problem for the analytic function $\Psi := \Phi + D\Phi$ in A_q . The complication arises that this RH problem changes its character according to whether the number λ defined in (332) below is zero or not. One can incorporate the side condition (294) only when the RH problem becomes degenerate, i.e., in the case $\lambda = 0$. Therefore, in order to avoid this difficulty, the equation (327) is replaced by

$$\Psi(qe^{it}) + e^{it}\Phi'(qe^{it})Dq = \eta_2(S_2(t)) + e^{-i\lambda}\dot{\eta}_2(S_2(t))DS_2(t). \quad (328)$$

This leads to the following procedure. We follow here the approach of Lucchini and Manzo [168] which is simpler than that of Wegmann [285]. The method is analogous to the method for simply-connected regions as described in Section 4.3.

Assume that the functions $\eta_j(s)$ are differentiable with Lipschitz continuous derivatives $\dot{\eta}_j \neq 0$. These can be represented by

$$\dot{\eta}_j(s) = r_j(s)e^{i\theta_j(s)} \quad (329)$$

with Lipschitz continuous functions θ_j and $r_j > 0$.

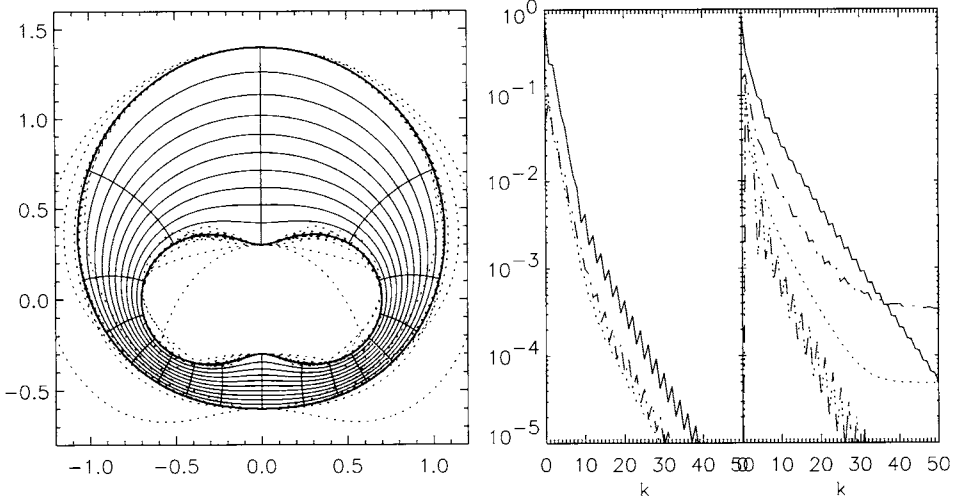


Fig. 28. Mapping from an annulus to the region of Example 14 calculated with the Theodorsen–Garrick iterative method. Meaning of the lines as in Figure 27.

Start with a guess $q_0 \in (0, 1)$ for q and with functions $S_{0,j}(t)$ such that $S_{0,j}(t) - t$ are 2π -periodic functions in W .

When functions $S_{k,j}$ and a number $q_k \in (0, 1)$ are determined for some $k \geq 0$, then calculate functions and numbers as follows. We put $p := q_k$ for brevity. The functions θ_j , r_j , and η_j are all evaluated at $S_{k,j}$.

The iteration from k to $k + 1$ is in several steps. First put

$$v_j(t) := \theta_j - t, \quad j = 1, 2, \quad (330)$$

$$w_1 := \mathbf{K}_p(v_1, v_2), \quad w_2 := -\mathbf{K}_p(v_2, v_1), \quad (331)$$

$$\lambda := \mathbf{J}(v_2) - \mathbf{J}(v_1). \quad (332)$$

Then calculate the functions

$$f_1 := \frac{r_1 e^{w_1} \eta_1}{\dot{\eta}_1}, \quad f_2 := \frac{r_2 e^{w_2} e^{i\lambda} \eta_2}{p \dot{\eta}_2}, \quad (333)$$

and put

$$g_j := \operatorname{Im} f_j, \quad j = 1, 2, \quad (334)$$

$$h_1 := \mathbf{K}_p(g_1, g_2), \quad h_2 := -\mathbf{K}_p(g_2, g_1), \quad (335)$$

$$\alpha := -h_1(0) - \operatorname{Re} f_1(0) + r_1(S_{k,1}(0)) \exp(-w_1(0)) S_{k,1}(0). \quad (336)$$

This gives finally the changes

$$DS_1(t) = -\frac{\exp(w_1(t))}{r_1} (h_1(t) + \operatorname{Re} f_1(t) + \alpha) \quad (337)$$

and

$$DS_2(t) = -\frac{p \exp(w_2(t))}{r_2} (h_2(t) + \operatorname{Re} f_2(t) + \alpha), \quad (338)$$

and the new functions

$$S_{k+1,j}(t) := S_{k,j}(t) + DS_j(t), \quad j = 1, 2. \quad (339)$$

The constant term α in (338) calculated by (336) enforces $S_{k+1,1}(0) = 0$. The next iteration satisfies the normalization (294).

The change of q is calculated from the term $e^{it}\Phi'(qe^{it})Dq$ in equation (328) which has not yet been taken care of. Differentiation of the boundary correspondence equations (296) yields for the conformal mapping

$$ie^{it}\Phi'(e^{it}) = \dot{\eta}_1(S_1(t))S'_1(t), \quad iqie^{it}\Phi'(qe^{it}) = \dot{\eta}_2(S_2(t))S'_2(t). \quad (340)$$

Comparison with (330) shows that

$$\arg(i\Phi'(e^{it})) = v_1(t), \quad \arg(i\Phi'(qe^{it})) = v_2(t), \quad (341)$$

and with (331),

$$\begin{aligned} i\Phi'(e^{it}) &= C \exp(-w_1(t) + iv_1(t)), \\ i\Phi'(qe^{it}) &= C \exp(-w_2(t) + iv_2(t)) \end{aligned} \quad (342)$$

with a constant $C > 0$. The function $\Phi(e^{it})$ parameterizes the outer curve Γ_1 . Therefore, $L_1 := \int |\Phi'(e^{it})| dt$ is the length of Γ_1 . Integrating the modulus in (342) on both sides yields

$$C = \frac{L_1}{\int e^{-w_1} dt}. \quad (343)$$

The term $e^{it}\Phi'(qe^{it})Dq$ in (327) gives the following contribution to g_2 in (334):

$$-\operatorname{Im} \frac{\Phi'(qe^{it})Dq}{q \exp(-w_2 + iv_2)} = \frac{CDq}{q}. \quad (344)$$

The solvability condition (304) for the conjugation problem

$$\operatorname{Im} \mathcal{E}(e^{it}) = g_1(t), \quad \operatorname{Im} \mathcal{E}(qe^{it}) = g_2(t) + \frac{CDq}{q} \quad (345)$$

yields for the constant term the condition $CDq/q = \mathbf{J}(g_1) - \mathbf{J}(g_2)$. This gives the following prescription for the update of q

$$q_{k+1} := q_k \left(1 + (\mathbf{J}(g_1) - \mathbf{J}(g_2)) \frac{\int \exp(-w_1(t)) dt}{L_1} \right). \quad (346)$$

EXAMPLE 15. Region is bounded by two ellipses

$$\begin{aligned} \eta_1(s) &= \cos s + 0.7i \sin s, \\ \eta_2(s) &= -0.2 + 0.3 \cos s + i(-0.1 + 0.5 \sin s). \end{aligned} \quad (347)$$

Figure 29 shows the result of the calculation of the mapping from an annulus to the region of Example 15 by the Newton method as described before. The calculation is done on a grid of 256 points. The iteration converges quadratically and reaches in the fifth step a stationary state. The calculated inverse module is $q = 0.593051$.

DeLillo and Pfaltzgraff [44] describe a quadratically convergent Fornberg-type method. They discretize the linearized boundary correspondence equations (326) and (327) and solve the system of equations by a conjugate gradient method. This approach is very efficient for the same reasons as described in Section 4.4 for the Fornberg method.

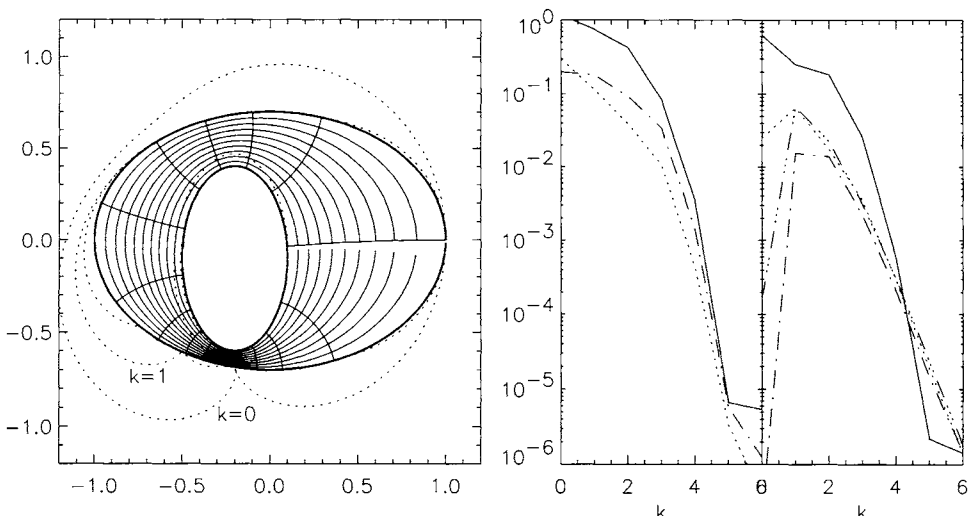


Fig. 29. Mapping from an annulus to the region of Example 15 calculated with the Newton iterative method.
Meaning of the lines as in Figure 27.

11.4. Other methods

When the region G is already close to an annulus one can calculate first-order approximations similar to those explained in Section 4.1. When the boundary curves are parameterized by

$$\eta_1(s) = (1 + \tau\rho_1(s))e^{is}, \quad \eta_2(s) = p(1 + \tau\rho_2(s))e^{is}, \quad (348)$$

then the boundary correspondence functions are approximated by

$$S_1(t) \approx t + \tau\mathbf{K}_p(\rho_1, \rho_2), \quad S_2(t) \approx t - \tau\mathbf{K}_p(\rho_2, \rho_1). \quad (349)$$

An estimate for the inverse module is given by

$$q \approx p(1 + \tau\mathbf{J}(\rho_2 - \rho_1)). \quad (350)$$

Rabinovich et al. [228,230] use this principle in a simplified form (based on the simple operator \mathbf{K} of conjugation only) to make the region G iteratively more and more annular.

Menke [179,180] considers regions G bounded by the unit circle from outside and by a Jordan curve Γ_2 from inside such that 0 is not in the closure \bar{G} . He defines for each natural number n “extremal point systems” z_j on Γ_2 and obtains from these point systems estimates for the inverse module q . An approximation to the conformal mapping $\Phi : A_q \rightarrow G$ is obtained by the Laurent polynomial which takes on equidistributed points on the circles $|z| = q$ and $|z| = 1/q$, the values z_j and their mirror images $1/\bar{z}_j$, respectively.

Hoidn [109] considered an osculation method for the construction of the mapping of G to an annulus. His experiences from a number of experiments are similar to those reported in Section 3.3 for the simply connected case. The method converges asymptotically slow but is fast at the beginning. It works especially well for regions that are known to be difficult for other methods, including regions with corners and slits.

Komatu [144] developed a method for the mapping of a doubly-connected region to an annulus which is closely related to the Koebe method which will be described in Section 12.2.

Opfer [197] computes approximations to the module M of a ring domain by calculating the harmonic measure with difference schemes. Mizumoto and Hara [182] determine M by finite element methods using characterizations of M by extremum properties of the Dirichlet integral.

12. Multiply-connected regions

We consider multiply-connected regions of the following kind: The boundary of an unbounded region G of connectivity $m \geq 1$ consists of m Jordan curves Γ_j , $j = 1, \dots, m$. The boundary curves are parameterized by complex 2π -periodic functions $\eta_j(s)$. The orientation is clockwise, so that the region is to the left of the curves. The point ∞ is an inner point of G when considered as a subregion of the closed plane $\bar{\mathbb{C}}$ (see Example 18).

The boundary of a bounded region G of connectivity $m+1 \geq 1$ consists of $m+1$ Jordan curves Γ_j , $j = 0, 1, \dots, m$. The outer boundary curve Γ_0 is oriented counterclockwise, the inner boundaries Γ_j , $j = 1, \dots, m$, are oriented clockwise, so that also in this case the region is to the left of the curves (see Example 19).

A region H whose boundary consists only of circles C_j is called a *circular region*. The boundary circles C_j of H with centers z_j and radii R_j are parameterized by

$$\zeta_j(t) = z_j + R_j e^{-it} \quad \text{for } j = 1, \dots, m. \quad (351)$$

For a bounded region the outer circle is given by

$$\zeta_0(t) = z_0 + R_0 e^{it}. \quad (352)$$

The orientation of the circles, determined by the sign in the exponential in (351) and (352) is so that H is always to the left of C_j . For an unbounded H all circles are negatively oriented. When H is bounded, then there is a positively oriented outer circle C_0 .

It was shown by Koebe [138] that a conformal mapping $\Psi : H_1 \rightarrow H_2$ of a circular region H_1 to another circular region H_2 must be a Moebius transformation $\Psi(z) = (a + bz)/(c + dz)$. In a later paper [139] Koebe proved that, for each m -connected region G , there exists a circular region H with m boundary circles and a conformal mapping Φ from H to G . The circular region H as well as the mapping Φ are uniquely determined by G when normalization conditions are applied according to the following theorem.

THEOREM 20. (a) *For an unbounded region G with m holes there exists an unbounded circular region H and a conformal mapping $\Phi : H \rightarrow G$. Both H and Φ are uniquely determined by the region G when the hydrodynamic normalization*

$$\Phi(z) = z + O\left(\frac{1}{z}\right) \quad (353)$$

near ∞ is imposed.

(b) *For a bounded region G with m holes there exists a bounded circular region H and a conformal mapping $\Phi : H \rightarrow G$. Both H and Φ are uniquely determined by the region G when the normalization conditions are imposed:*

1. *The outer boundary C_0 of H is the unit circle.*
2. *Φ interpolates η_0 at three given points of the outer boundary, i.e.,*

$$\Phi(\zeta_0(t_j)) = \eta_0(s_j) \quad (354)$$

for prescribed parameter values $0 \leq t_1 < t_2 < t_3 < 2\pi$ and $s_1 < s_2 < s_3 < s_1 + 2\pi$.

There are other canonical regions: Each m -connected region can be conformally mapped to an unbounded region with m parallel slits. Such regions are particularly convenient for flow problems. The slits can also be radial, on concentric circles or on logarithmic spirals (see Nehari [189, Chapter VII], Courant [32, Chapter II] or Grunsky [89, Chapter 3]). One

can also require that the slits form preassigned angles α_j with the real axis (see Koebe [141] and Figure 31). A comprehensive review of results about the conformal mapping of multiply-connected regions to suitable canonical regions was given by Gaier [69].

12.1. Potential theoretic methods

Let G be a bounded region of connectivity $m + 1$ with boundary curves $\Gamma_0, \Gamma_1, \dots, \Gamma_m$ and $0 \in G$. Then there exists a conformal mapping F of G into the unit disk D in such a way that Γ_0 is mapped to the unit circle, and the Γ_j , $j = 1, \dots, m$, are mapped to circular slits of radii R_j . The mapping is unique when the conditions (61) are imposed.

The function $H = \log(F(z)/z)$ is analytic in G . The real part is a harmonic function in G with boundary values

$$u(\eta) = \log R_j - \log |\eta| \quad \text{for } \eta \in \Gamma_j. \quad (355)$$

Only $R_0 = 1$ is known in advance, all other R_j , $j = 1, \dots, m$, must be determined from the additional condition that u is the real part of a univalent analytic function in G .

The boundary value problem (355) is a special case of an RH problem, the “problem D” of Vekua [269]. It has a unique solution consisting of a harmonic function u in G and R_1, \dots, R_m (see [269, p. 264]).

If the point 0 is not in G but inside one of the inner curves, say inside Γ_1 , then one can consider a conformal mapping F of G to an annulus A_q with $m - 1$ concentric circular slits, such that Γ_0 is mapped to the unit circle, and Γ_1 to the circle with radius q . The mapping is then uniquely defined up to a factor $e^{i\alpha}$ of unit modulus (see Ellacott [51]). When $H = \log(F(z)/z)$ is formed with this mapping function F , its real part u is described by the same Dirichlet problem (355) as before, with $R_1 = q$.

One can make an ansatz for the harmonic function u as a single-layer potential and arrive at a system of integral equations with logarithmic kernel for the density σ which generalizes Symm’s equations for simply and doubly-connected regions (see Sections 3.1 and 10.1). Gaier [70] studies these equations for the case of the mapping to an annulus with circular slits. He shows that the equations have a unique solution if and only if the capacity of the outer curve Γ_0 is different from 1. The density σ is closely related to the derivative of the boundary correspondence functions in analogy to Theorem 12. The integral equations contain the radii R_j as unknown parameters. One has to impose the additional equations

$$\int_0^{2\pi} \sigma_j(s) ds = 0 \quad (356)$$

for $j = 1, \dots, m$, where σ_j is the density σ restricted to Γ_j . These conditions are derived in the same way as for the doubly-connected case (see equation (285)). One can also impose condition (356) for $j = 0$ and consider R_0 as free parameter. Then R_0 is the capacity of Γ_0 (Reichel [234]).

For the efficient numerical treatment of Symm's equations for multiply-connected bounded regions see Reichel [234].

Mikhlin [181] calls a problem of the kind (355) a *modified Dirichlet problem*. He solves it by a double-layer ansatz (79). Let $a(z, \zeta)$ denote the function which is equal to unity if the points z and ζ belong to the same internal curve Γ_j and equal to zero otherwise, and let \mathbf{A} be the integral operator with kernel a and \mathbf{K}_1 the operator with Neumann kernel (see Section 3.1). There is a unique solution μ of the integral equation

$$(\mathbf{I} + \mathbf{K}_1 - \mathbf{A})\mu = -2 \log |\eta| \quad \text{for } \eta \in \Gamma. \quad (357)$$

The double-layer potential u with this density μ satisfies (355) with

$$R_0 = 1 \quad \text{and} \quad \log R_j = \frac{1}{\pi} \int \mu(\eta_j(s)) ds \quad \text{for } j = 1, \dots, m \quad (358)$$

(see [181, p. 151]). The function H is given by the Cauchy integral

$$H(z) = \frac{1}{2\pi i} \int_{\Gamma} \frac{\mu(\eta)}{\eta - z} d\eta + \alpha i \quad (359)$$

whence $F(z) = z \exp(H(z))$ can be computed. The imaginary constant αi corresponds to a rotation of the canonical region $F(G)$.

The method of Mayo [172,173], described in Section 3.1, can be used to evaluate the mapping function in the interior of G in an efficient way.

Amano [3] solves the Dirichlet problem (355) by a charge simulation method. Inoue [127] extends his scheme (see [126]) from doubly- to multiply-connected regions. Ogata et al. [195] propose a charge simulation method for the mapping of periodic structure domains onto parallel slit domains.

Ellacott [51] considers the mapping to an annulus with circular slits. He calculates u by uniform approximation of $-\log |\eta|$ on the boundary Γ by the real part of Laurent polynomials, and of polynomials in $(z - a_j)^{-1}$ for $j = 2, \dots, m$, where the a_j are fixed points inside the curves Γ_j . The harmonic measures ω_j of Γ_j with respect to G are included for $j = 1, \dots, m$ in the set of basis functions. (Recall that the *harmonic measure* ω_j is a harmonic function in G with the boundary values $\omega_j = 1$ on Γ_j and $\omega_j = 0$ on Γ_v for $v \neq j$.) The solution of the approximation problem readily gives a rational approximation of $\log(F(z)/z)$. The coefficients of ω_j in the approximating function are estimates for $\log R_j$.

12.2. Osculation methods

Koebe's iterative method [139] determines the conformal mapping F from an unbounded m -connected region G with boundary components Γ_j to a circular region H . The mapping F is calculated as a composition of maps

$$F = \dots \circ F^{k,j} \circ \dots \circ F^{1,2} \circ F^{1,1}. \quad (360)$$

The factors are arranged from right to left in lexicographic order of the index pairs (k, j) , $k = 1, 2, \dots, j = 1, \dots, m$. If all functions $F^{l,v}$ for indices (l, v) which precede (k, j) in the lexicographic order are calculated, then the analytic function $F^{k,j}$ is determined as the conformal mapping of the exterior of the image of Γ_j under the composition of all previous mappings, to the exterior of a circle, normalized at ∞ by $F^{k,j}(z) = z + O(1/z)$. The method converges (see Gaier [65, p. 230], Henrici [107, p. 499]). The image regions become more and more circular. This is nicely illustrated by a figure in [107, p. 498], which shows the effect of the first three iterative steps on a region of connectivity 3.

Koebe's iterative method was rediscovered and applied by Halsey [96], who notes that the method converges rapidly. The region becomes nearly circular after a few iterations. The asymptotic rate of convergence is then the same as for the nearly circular region. It was shown by Wegmann [292] that this rate is the same as the rate of convergence for a “general conjugation problem” (see Section 12.4). The latter can be determined as the maximum eigenvalue of a certain matrix. The asymptotic rate of convergence depends only on the circular region H which is conformally equivalent to G .

For a doubly-connected region with module M the rate of convergence is M^{-2} (see Gaier [65, p. 216]).

A similar iterative procedure has been applied by Grötzsch [88] to construct the mapping from an unbounded m -connected region G to the plane with m parallel slits. More general iterative methods of this kind are investigated by Lind [166].

These methods occur in Gaier's book [65] under the heading “function theoretic iteration methods”. But the underlying idea is apparently closely related to that of the osculation methods, described in Section 3.3. The mapping is composed of simpler mappings which make the region locally more circular. The osculation family consists, in the case of the Koebe iteration, of all normalized conformal mappings of the exterior of a Jordan curve to the exterior of a circle.

These methods construct the conformal mapping of a multiply-connected region as an infinite composition of mappings of simply-connected regions. It is interesting to note that there even exists a representation as a finite composition. The following result was proved by Hübner [118].

THEOREM 21. *Let G be an unbounded m -connected region with boundary components Γ_j . Then each univalent function F in G can be factorized as*

$$F = F_m \circ F_{m-1} \circ \cdots \circ F_1 \quad (361)$$

with functions F_j univalent in the simply-connected region exterior to Γ_j . If F and all F_j behave like $z + O(1/z)$ near ∞ then the factors F_j are uniquely determined.

This factorization holds true in particular for the conformal mapping $F: G \rightarrow H$. This special case, announced by Erohin [54], generalizes previous results of Grunsky, Landau and Gaier. The factors F_j of the conformal map can be determined by an iterative method which is closely related to Koebe's method (see Hübner [117]).

12.3. Projection

Let H be a circular region of connectivity m . The boundary circles C_j are parameterized by ζ_j as defined in (351). Here and in what follows we denote for analytic functions F in H the values $F(\zeta_j(t))$ on the boundary circle C_j by $F|_j$. These are considered as functions of t .

An analytic function Ψ in an unbounded circular region H which vanishes at infinity can be written in a unique way as a sum

$$\Psi(z) = \sum_{j=1}^m h_j(z), \quad (362)$$

where each function h_j is analytic outside C_j and is represented by a Laurent series around the centers z_j of the circles

$$h_j(z) = \sum_{l=1}^{\infty} b_{l,j}(z - z_j)^{-l}. \quad (363)$$

Let G be an unbounded region of connectivity m as described at the beginning of Section 12. An unbounded circular region H and a conformal mapping Φ of H to G must be determined so that Φ satisfies the condition (353) near infinity. The function Φ is completely described by its boundary values. These can be represented by boundary correspondence functions $S_j(t)$. These functions have the property that $S_j(t) - t$ is 2π -periodic. The boundary correspondence equations

$$\Phi|_j = \eta_j(S_j(t)), \quad j = 1, \dots, m, \quad (364)$$

determine the functions S_j as well as the parameters z_j, R_j of the circles.

The simplest way to treat these equations is by alternating projection. Such a method was devised by Prosnak [227] and further elaborated by Klonowska and Prosnak [136]. We give here a simplified version which is closer to the method for simply-connected regions described in Section 4.2. We assume that the functions η_j are continuously differentiable with $\dot{\eta}_j \neq 0$.

In view of the normalization (353), Φ has the representation

$$\Phi(z) = z + \sum_{j=1}^m h_j(z) \quad (365)$$

with functions h_j analytic outside C_j and represented by Laurent series (363). In view of (365), (351) and (363), the boundary correspondence equation on the circle C_j takes the form

$$z_j + R_j e^{-it} + \sum_{l=1}^{\infty} \frac{b_{l,j}}{R_j^l} e^{ilt} = \eta_j(S_j(t)) - \sum_{v \neq j} h_{v|j}. \quad (366)$$

This can be used as the basis of an iterative method.

The iteration starts with estimates $z_j^{(0)}$ and $R_j^{(0)}$ for the centers and for the radii of the boundary circles of H , and with guesses $S_j^{(0)}$ for the boundary correspondence functions, and $h_j^{(0)}$ for the functions h_j in (365). One can choose $S_j^{(0)}(t) = t$ and $h_j^{(0)} = 0$.

When $z_j^{(k)}, R_j^{(k)}, S_j^{(k)}, h_j^{(k)}$ are determined for some $k \geq 0$ then the Fourier coefficients $A_{l,j}$ of the functions

$$\eta_j(S_j^{(k)}(t)) - \sum_{v \neq j} h_{v|j}^{(k)} = \sum_{l=-\infty}^{\infty} A_{l,j} e^{ilt} \quad (367)$$

are calculated. From the form (366) of the boundary correspondence equations the conditions

$$z_j^{(k+1)} + R_j^{(k+1)} e^{-it} + \sum_{l=1}^{\infty} \frac{b_{l,j}^{(k+1)}}{R_j^{(k)l}} e^{ilt} = \eta_j(S_j^{(k)}(t)) - \sum_{v \neq j} h_{v|j}^{(k)} \quad (368)$$

are obtained. Upon comparing the coefficients in the Fourier series (367) and (368) the new circle parameters and the coefficients $b_{j,l}^{(k+1)}$ of the new functions $h_j^{(k+1)}$ can be determined

$$R_j^{(k+1)} := \operatorname{Re} A_{-1,j}, \quad z_j^{(k+1)} := A_{0,j}, \quad (369)$$

$$b_{l,j}^{(k+1)} := (R_j^{(k)})^l A_{l,j} \quad \text{for } l = 1, 2, \dots \quad (370)$$

With the remaining coefficients the function

$$g_j(t) = \sum_{l=-\infty}^{-2} A_{l,j} e^{ilt} + i(\operatorname{Im} A_{-1,j}) e^{-it} \quad (371)$$

is formed which gives the change in the boundary correspondence function

$$S_j^{(k+1)}(t) := S_j^{(k)}(t) - \operatorname{Re} \frac{g_j(t)}{\dot{\eta}_j(S_j^{(k)}(t))}. \quad (372)$$

The new approximation for Φ is

$$\Phi^{(k+1)}(z) := z + \sum_{j=1}^m h_j^{(k+1)}(z), \quad (373)$$

where the functions $h_j^{(k+1)}$ are given by the Laurent series (363) with the new coefficients (370).

EXAMPLE 16. The exterior of the inverted ellipse with parameter $p = 0.4$

$$\eta_1(s) = 2 + 0.5i + 2\sqrt{1 - 0.84 \cos^2 s} e^{-is} \quad (374)$$

and ellipses

$$\eta_j := w_j + e^{i\alpha_j} (a_j \cos s + i b_j \sin s) \quad (375)$$

with $w_2 = -2.5i$, $w_3 = -1 + 0.5i$, and axes $a_2 = 1$, $b_2 = 0.8$, $a_3 = 1$, $b_3 = 1.6$ rotated by angles $\alpha_2 = 0$, $\alpha_3 = 0.5$.

Example 16 is calculated by the projection method with 128 grid points on each curve. The rate of convergence is $q = 0.88$. Figure 30 shows the images of a grid of size 0.15 in the circular region. The parameters of the circles are $z_1 = 2.0613 + 0.5837i$, $R_1 = 1.5859$, $z_2 = -0.1660 - 2.2176i$, $R_2 = 0.9586$, $z_3 = -1.2685 + 0.5544i$, $R_3 = 1.1938$.

As an indicator for convergence we take

$$\delta_k := \max_{j,t} |S_j^{(k+1)}(t) - S_j^{(k)}(t)| \quad (376)$$

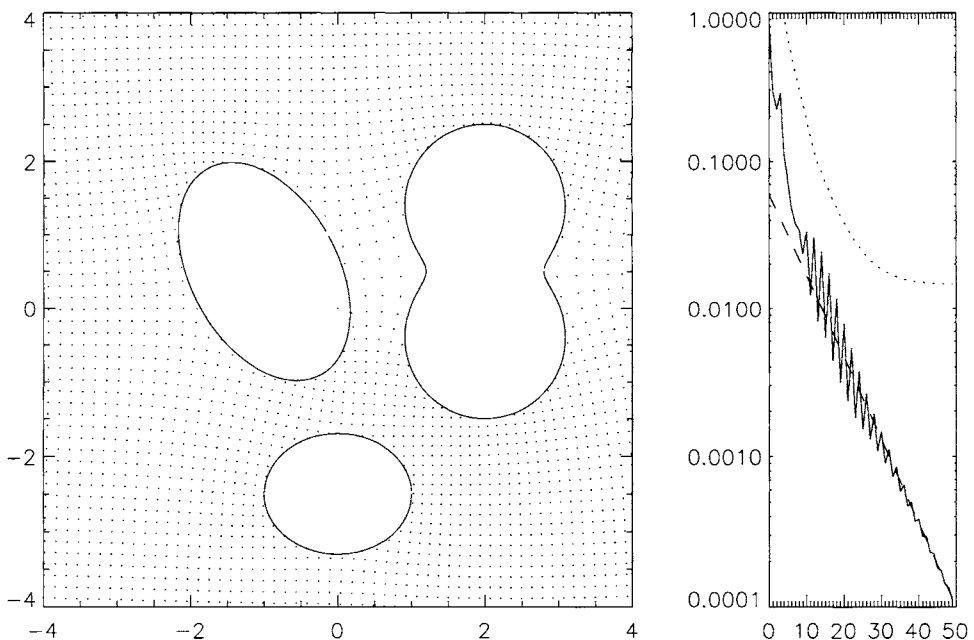


Fig. 30. Mapping to the region of Example 16 calculated by the projection method. The right panel shows the maximum change δ_k (solid) and the measure of accuracy α_k (dotted). The dashed line is proportional to 0.88^k .

and as a measure of the accuracy

$$\alpha_k := \max_j \|g_j\|_2 \quad (377)$$

with the functions g_j defined in (371) in the k th iteration.

There are several other ways of projecting $\Phi^{(k+1)}$ onto the Γ_j . Prosnak [227] studies airfoil profiles. The projection is perpendicular to a “chord”. Klonowska and Prosnak [136] associate points on the image curve of $\Phi^{(k+1)}$ with points on the curve Γ_j according to their arclength parameterization. Kosma [146] gives a version of the projection method which keeps the collocation points on the curves Γ_j fixed and varies in each iteration the preimages on the circles C_j . This method requires the solution of large systems of nonlinear equations by the Newton method. The application of this particular version of the projection method “requires a certain amount of experience” [146, p. 51].

Fil'čakova [58] extends her method of trigonometric interpolation to latticed domains whose boundaries consist of disjoint congruent continua.

12.4. Riemann–Hilbert problems

RH problems on multiply-connected regions have been studied by Vekua [269]. Krutitskii [149] investigated the relation to the directional derivative problem for harmonic functions. For the conformal mapping of multiply-connected regions, RH problems of a special kind on circular regions are needed.

Let H be an m -connected unbounded circular region with boundary circles parameterized by (351). Let l be a nonnegative integer, let λ_j be real numbers and let ψ_j be real functions. The problem of *general conjugation* asks for an analytic function Ψ in H with $\Psi(\infty) = 0$, real numbers a_{j0} and complex numbers a_{j1}, \dots, a_{jl} such that

$$\operatorname{Re}(e^{i\lambda_j} e^{ilt} \psi_{|j} + a_{jl} e^{ilt} + \dots + a_{j1} e^{it} + a_{j0}) = \psi_j \quad (378)$$

for $j = 1, \dots, m$. One can apply instead of the normalization $\Psi(\infty) = 0$ the more general condition that Ψ behaves near infinity like

$$\Psi(z) = p(z) + O(1/z) \quad (379)$$

with a given polynomial $p(z)$. When on the right-hand side of (378) the functions ψ_j are replaced by $\psi_j - \operatorname{Re}(e^{i\lambda_j} e^{ilt} p_{|j})$ this situation is reduced to the general conjugation problem (378) for the function $\tilde{\Psi} := \Psi - p$ with normalization $\tilde{\Psi}(\infty) = 0$. This covers the usual normalization condition (353) for conformal mapping functions.

Wegmann [292] introduced a method of *successive conjugation* which reduces the problem (378) to a sequence of RH problems on the circles C_j . For $l = 0$ this method was first applied by Halsey [96].

Using the representation (362) for Ψ , the equation (378) is written in the form

$$\begin{aligned} \operatorname{Re}\left(e^{i\lambda_j} e^{ilt} h_{j|j} + a_{jl} e^{ilt} + \cdots + a_{j1} e^{it} + a_{j0}\right) \\ = \psi_j - \operatorname{Re}\left(e^{i\lambda_j} \sum_{v \neq j} e^{ilt} h_{v|j}\right) =: \psi_j^*. \end{aligned} \quad (380)$$

The left-hand side of (380) contains only quantities on the circle C_j . This suggests the following iterative procedure of successive conjugation.

The iterative procedure starts with a set of functions $h_j^{(0)}$. One can choose all $h_j^{(0)} = 0$. When after the k th iterative step, functions $h_j^{(k)}$ are available, these functions are inserted into the right-hand side of (380) and new functions $h_j^{(k+1)}$ are determined successively for $j = 1, \dots, m$, from the equations

$$\begin{aligned} \operatorname{Re}\left(e^{i\lambda_j} e^{ilt} h_{j|j}^{(k+1)} + a_{jl} e^{ilt} + \cdots + a_{j1} e^{it} + a_{j0}\right) \\ = \psi_j - \operatorname{Re}\left(e^{i\lambda_j} \sum_{v < j} e^{ilt} h_{v|j}^{(k+1)}\right) - \operatorname{Re}\left(e^{i\lambda_j} \sum_{v > j} e^{ilt} h_{v|j}^{(k)}\right) =: \psi_j^*. \end{aligned} \quad (381)$$

The parameters a_{j0}, \dots, a_{jl} in (381) depend also on the iterative step $k + 1$. But they need not be updated during the iteration, since only the functions $h_j^{(k+1)}$ are needed for the next step. Therefore, it is sufficient to determine the parameters a_{j0}, \dots, a_{jl} at the end of the iteration.

The prescription by equation (381) may be considered as a Gauss-Seidel method or Einzelschrittverfahren for the system of equations (380). One can also apply a Jacobi method (Gesamtschrittverfahren) when on the right-hand side of (381) all h_v are taken from step k .

The conjugation on a single circle can be very efficiently done in Fourier space. To this aim the left-hand side of (381) must be compared with the Fourier series of the right-hand side,

$$\psi_j^*(t) = \sum_{n=-\infty}^{\infty} A_{n,j} e^{int}. \quad (382)$$

Since ψ_j^* is a real function, the coefficients satisfy $A_{-n,j} = \overline{A_{n,j}}$. In particular, $A_{0,j}$ is real. By comparing the coefficients of the left-hand side of (380) and the right-hand side of (382) we get the unique solution

$$a_{j0} = A_{0,j}, \quad a_{ji} = 2A_{i,j} \quad \text{for } i = 1, \dots, l, \quad (383)$$

for the parameters a_{ji} , and

$$b_{n,j} = 2R_j^n e^{-i\lambda_j} A_{n+l,j} \quad \text{for } n = 1, 2, \dots, \quad (384)$$

for the coefficients $b_{n,j}$ of the series (363). Wegmann [292] proved that this method converges for $l \geq 1$. Convergence is linear and the rate of convergence can be determined from an eigenvalue problem. This result gives a constructive proof for the existence of a solution of the RH problem. It follows then from the general theory of RH problems that the solution is unique. For $l = 0$ this result is well known (see, e.g., Vekua [269, p. 265]). We note this result since it will be important in Section 12.5.

THEOREM 22. *For every integer $l \geq 0$ and for any function ψ_j in W , the Riemann–Hilbert problem (378) has a unique solution consisting of an analytic function Ψ in H , normalized by $\Psi(\infty) = 0$, and of complex numbers a_{j1}, \dots, a_{jl} and real numbers a_{j0} .*

Dundučenko [48] represents the solution of the conjugation problem ((378) with $l = 0$) by a “Schwarz formula”. Sorokin [248] gives a solution of RH problems on bounded multiply connected circular regions in closed form. The formulas involve infinite series of functions which are constructed by reflection at the boundary circles. It is not quite clear how these formulas can be used for computational purposes.

Just as for simply-connected regions (see Section 4.1), for multiply-connected regions which differ only slightly from circular regions an approximation of the conformal mapping can be obtained in terms of the conjugation operator (Sorokin [248], Wegmann [292]). To be specific, let H be an unbounded circular region whose boundary consists of circles C_j with centers z_j and radii R_j , and let ψ_j be twice continuously differentiable real functions. Then one can define, for small real numbers τ , neighboring regions G_τ with boundary curves parameterized by

$$\eta_j(s) = z_j + R_j e^{-is} + \tau \psi_j(s) e^{-is}. \quad (385)$$

On the other hand, one can consider the RH problem

$$\operatorname{Re}(e^{it}\Psi_{|j} + a_{j1}e^{it} + a_{j0}) = \psi_j \quad (386)$$

as a boundary problem for an analytic function Ψ in H with $\Psi(\infty) = 0$. The region G_τ is conformally equivalent to a circular region H_τ bounded by circles $C_{\tau j}$ whose centers and radii are in first order of τ given by

$$z_{\tau j} = z_j + \tau a_{j1}, \quad R_{\tau j} = R_j + \tau a_{j0}. \quad (387)$$

The boundary values of the conformal mapping $\Phi_\tau : H_\tau \rightarrow G_\tau$ are in first order of τ ,

$$\Phi_{\tau|j} \approx z_{\tau j} + R_{\tau j} e^{-it} + \tau \Psi_{|j}. \quad (388)$$

The mapping from a circular region to a slit region can easily be calculated by means of an RH problem of the kind (378) with $l = 0$. Let α_j be fixed angles. When the boundary circles of H have centers z_j and radii R_j , $j = 1, \dots, m$, and Ψ solves the boundary problem

$$\operatorname{Re}(e^{-i\alpha_j}\Psi_{|j}) + a_{j0} = R_j \sin(t + \alpha_j), \quad (389)$$

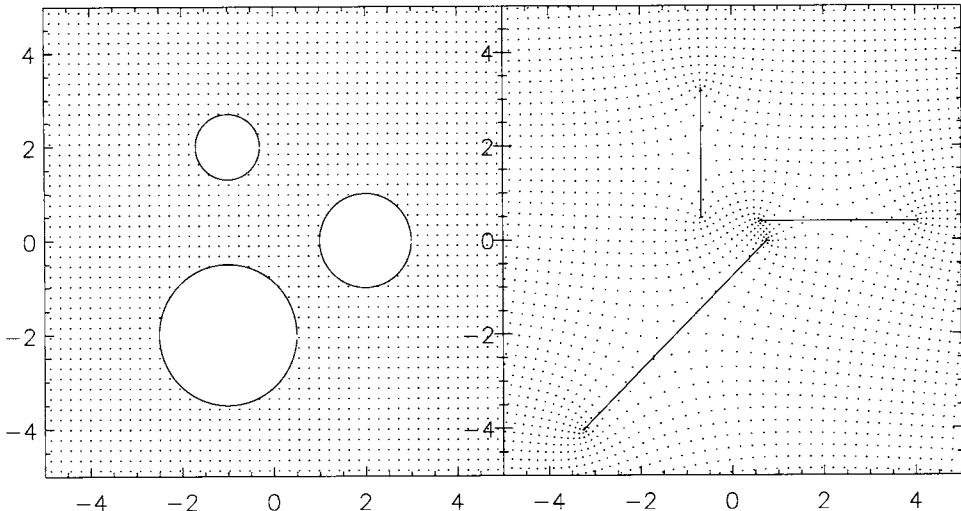


Fig. 31. Mapping of the circular region of Example 17 (left panel) to the complex plane with slits of prescribed inclination (right panel).

then the function

$$\Phi(z) = z + i\Psi(z) \quad (390)$$

maps H conformally to the complex plane with m straight slits which form the angles α_j with the real axis.

EXAMPLE 17. Circular region is bounded by circles with centers $z_1 = 2$, $z_2 = -1 - 2i$, $z_3 = -1 + 2i$ and radii $R_1 = 1$, $R_2 = 1.5$, $R_3 = 0.7$. The slits form with the real axis the angles $\alpha_1 = 0^\circ$, $\alpha_2 = 45^\circ$, $\alpha_3 = 90^\circ$.

Figure 31 shows the mapping of the circular region of Example 17 to the complex plane with slits of prescribed inclination.

12.5. The Newton method

Wegmann [293] developed a Newton method for multiply-connected regions. The procedure is quite analogous to that for simply- and doubly-connected regions as described in Sections 4.3 and 11.3. Some peculiarities must be noted, however.

A function F , analytic at ∞ , has a Laurent series representation $F(z) = b_0 + b_1/z + b_2/z^2 + \dots$. The *residue at infinity* is defined as (note the minus sign!)

$$\text{Res}_\infty F := -b_1. \quad (391)$$

Let G be an m -connected unbounded region with boundary curves Γ_j , $j = 1, \dots, m$. By linearization of the boundary correspondence equations (368) linear equations

$$\Phi_{|j} + D\Phi_{|j} + \Phi'_{|j}(Dz_j + DR_j e^{-it}) = \eta_j + \dot{\eta}_j DS_j \quad (392)$$

are obtained which connect the necessary changes $D\Phi$, Dz_j , DR_j , DS_j . These equations give the motivation for the method which will be described in the following.

The parameter functions η_j are assumed to be differentiable with Hölder continuous derivatives $\dot{\eta}_j(s) \neq 0$. The derivatives can be represented in the form

$$\dot{\eta}_j(s) = r_j(s) \exp(i\theta_j(s)) \quad (393)$$

with Hölder continuous real functions $r_j > 0$ and θ_j . When the functions S_j are Hölder continuous, the functions

$$v_j(t) := \theta_j(S_j(t)) + t + \frac{\pi}{2} = \arg[i e^{it} \dot{\eta}_j(S_j(t))] \quad (394)$$

are also Hölder continuous and 2π -periodic. There are uniquely defined Hölder continuous functions w_j , real numbers λ_j and an analytic function Y in H which has boundary values

$$Y_{|j} = w_j + i v_j + i \lambda_j \quad (395)$$

and vanishes at infinity. (See Vekua's "problem D" [269, p. 261].) The Y , w_j and λ_j satisfy the equation

$$\frac{1}{e^{i\lambda_j} \dot{\eta}_j} = i \frac{e^{w_j}}{r_j} \frac{e^{it}}{\exp(Y_{|j})}. \quad (396)$$

With w_j and λ_j the auxiliary complex functions

$$F_j := \frac{r_j}{e^{i\lambda_j} e^{w_j}} \frac{\eta_j}{\dot{\eta}_j} = \exp(-w_j - i\theta_j - i\lambda_j) \eta_j \quad (397)$$

are calculated. Then an analytic function Ξ in H , complex numbers a_j , real numbers α_j and real functions g_j are determined such that

$$e^{it} \Xi_{|j} + a_j e^{it} + \alpha_j = \operatorname{Im} F_j + i g_j \quad (398)$$

is satisfied. The function Ξ is required to behave near infinity like

$$\Xi(z) = z + O\left(\frac{1}{z}\right). \quad (399)$$

By taking the real part of equation (398) the functions g_j are eliminated and an RH problem of the kind (378) for the function Ξ remains. In view of Theorem 22, problem (398) has a unique solution Ξ , a_j , α_j and g_j .

With the numbers a_j, α_j and the functions g_j , the necessary changes in S_j, z_j and R_j are calculated by the formulas

$$DS_j = -\frac{e^{w_j}}{r_j} (g_j + \operatorname{Re} F_j) \quad (400)$$

and

$$Dz_j = a_j - \operatorname{Res}_\infty Y, \quad DR_j = \alpha_j. \quad (401)$$

Based on (400) and (401) one can devise an iterative method: When in the k th iteration functions $S_j^{(k)}$ and circle parameters $z_j^{(k)}$ and $R_j^{(k)}$ are given, insert these values into the formulas (394) etc. and calculate a shift according to (400) and (401); then change the data

$$S_j^{(k+1)} = S_j^{(k)} + DS_j, \quad z_j^{(k+1)} = z_j^{(k)} + Dz_j, \quad (402)$$

$$R_j^{(k+1)} = R_j^{(k)} + DR_j, \quad (403)$$

and perform the next step.

Wegmann [293] proved that this iteration converges to the solution of the conformal mapping problem whenever the initial functions $S_j^{(0)}$ and the circle parameters are sufficiently close to the solution. Convergence is quadratic.

The main computational effort must be spent on the solution of the boundary value problems (395) and (398). Both can be transformed into RH problems on circular regions and solved by the method of successive conjugation described in Section 12.4.

The residue term in (401) comes as a surprise. It can only be explained by the proof of convergence in [293]. On the other hand, one can convince oneself easily by numerical experiments that the method does not converge quadratically when the residue term in (401) is omitted.

Wegmann describes in [293] also how the method must be modified to deal with bounded multiply-connected regions. The outer boundary, however, requires special treatment and nonnegligible extra programming work.

EXAMPLE 18. Unbounded region bounded by three ellipses which are parameterized by (375) with $w_1 = 2i, w_2 = -2i, w_3 = -1, a_1 = 1.5, b_1 = 0.8, \alpha_1 = 0.5, a_2 = 2, b_2 = 1, \alpha_2 = -0.8, a_3 = 1.5, b_3 = 0.8, \alpha_3 = -0.5$.

The calculation for Example 18 was done with 64 grid points on each curve. It was started with $S_j^{(0)}(t) = t$ and with circle parameters $z_1 = -0.3 + 2.5i, z_2 = -0.2 - 2.5i, z_3 = -1.5, R_1 = 0.9, R_2 = 1.2, R_3 = 0.5$. At the end of the iteration the circle parameters are $z_1 = -0.13971 + 2.0470i, R_1 = 1.1214, z_2 = 0.91011 - 1.9955i, R_2 = 1.5101, z_3 = -1.2737 + 0.02541i, R_3 = 0.55958$. Figure 32 shows the image of an equidistant grid in H . The convergence, measured by δ_k defined in (376), and the accuracy α_k of the calculation are indicated on the right panel.

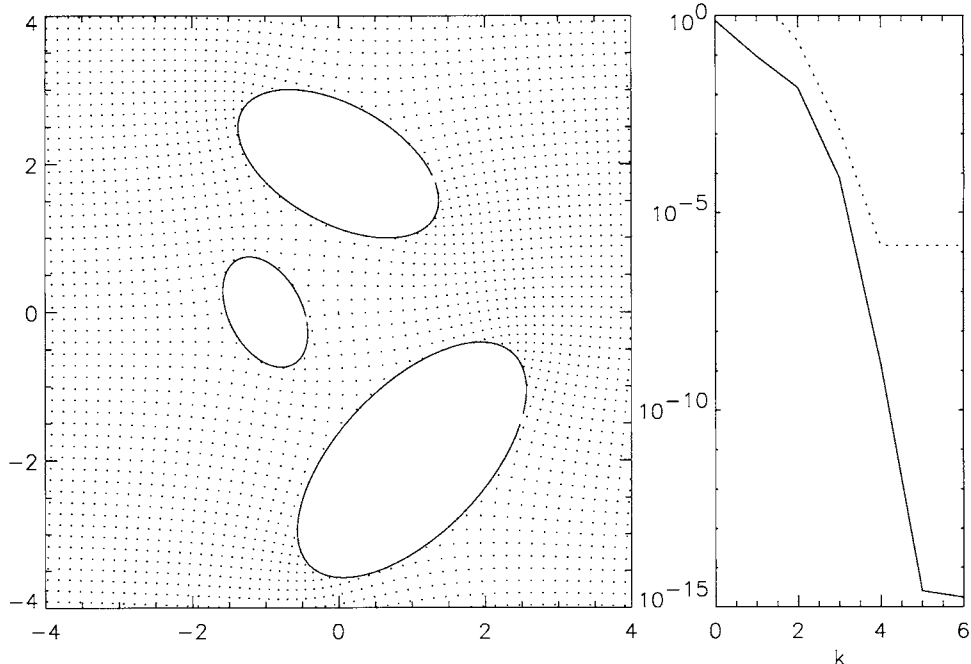


Fig. 32. Mapping of a circular region to the ellipse region of Example 18 by the Newton method. Right panel: δ_k solid, α_k dotted.

EXAMPLE 19. A region bounded from outside by an inverted ellipse which is parameterized by (162) with parameter $p = 0.5$. The inner curves are ellipses

$$\eta_j(s) = w_j + a_j \cos s + b_j i \sin s \quad (404)$$

with axes $a_1 = 0.3, b_1 = 0.2, a_2 = 0.2, b_2 = 0.4$ and centers $w_1 = -0.1 + 0.5i, w_2 = 0.1 - 0.3i$.

Example 19 is calculated with $N_j = 128$ points on each boundary. The interpolation conditions $S_0(t_1) = 0, S_0(t_{40}) = 1.9, S_0(t_{80}) = 3.6$ are applied at three of the grid points $t_k := (k - 1)2\pi/N_0$. Figure 33 shows the image of an equidistant grid in the unit circle and the convergence of the iteration. The calculated parameters of the circles are $z_1 = -0.23374 + 0.56475i, R_1 = 0.26034, z_2 = 0.10730 - 0.35282i, R_2 = 0.38068$.

12.6. Other methods

Gaier [69] gives a comprehensive survey of characterizations of slit mappings by extremal properties. Schiffer and Hawley [239] characterized the conformal mapping F of an m -connected region G to a circular region as the solution to a certain extremum problem

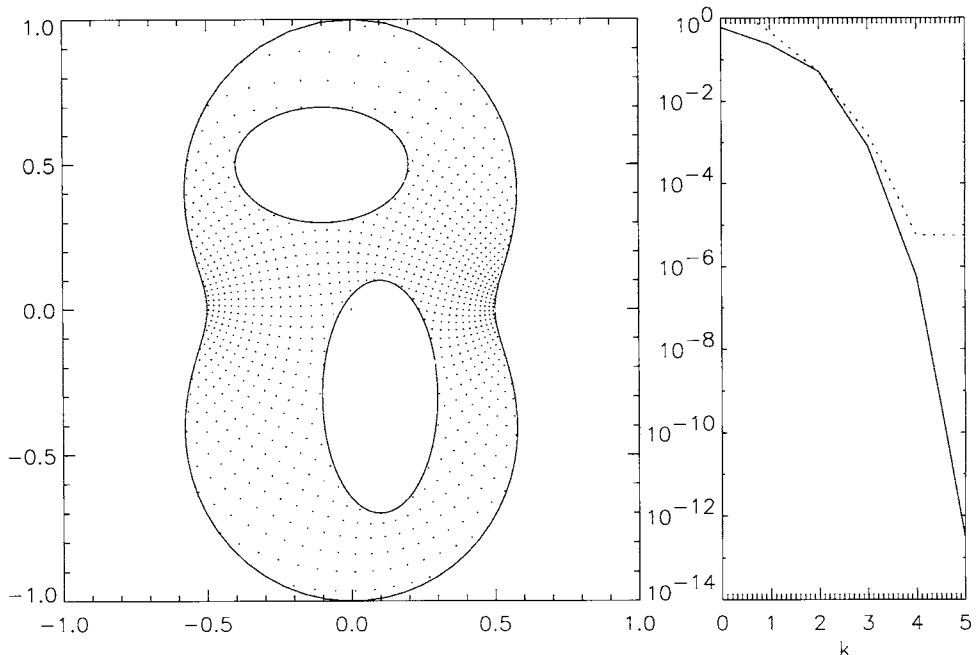


Fig. 33. Mapping of a circular region to the bounded region of Example 19 by the Newton method. Right panel: δ_k solid, α_k dotted.

which is solved by the harmonic function $\log |F'|$. This has apparently not yet been exploited for numerical calculations, but it is interesting from the theoretical point of view. It has been used by Dittmar [45] to give a new proof for the convergence of the Koebe method described in Section 12.2.

The Bergman and Szegö kernels of multiply-connected regions are discussed in great detail by Nehari [189, p. 367]. Both kernels can be built up by bilinear series of orthonormalized functions as in (93) and (105). For the Bergman kernel only analytic functions are admitted which have a single-valued integral, while for the Szegö kernel all analytic functions are admitted. A relation analogous to (109) holds between the two kernels with the modification that a linear combination of functions w_j occurs, where $\operatorname{Re} w_j = \omega_j$ is the harmonic measure of the boundary component Γ_j with respect to G . For a bounded region G a suitable set of functions for the construction of k_B by orthonormalization is given by $z^l, l = 0, 1, 2, \dots$, and $(z - a_j)^{-l}, j = 1, \dots, m, l = 2, 3, \dots$, with points a_j inside Γ_j (Gaier [65, p. 244]). Note that the omission of the terms $(z - a_j)^{-1}$ ensures that all functions have a single valued integral.

There are several ways to calculate from the kernel function k_B the conformal map from G to the complex plane with parallel slits (or the disk with circular slits) (see Gaier [65, pp. 242–243]).

Bergman and Chalmers [15] describe a procedure, based on the Bergman kernel function, for the mapping of a triply-connected domain to an annulus with a circular hole.

An orthonormalization method, quite analogous to the method described for doubly-connected regions in Section 10.2, was presented by Kokkinos et al. [143] for the construction of the mapping of a bounded multiply-connected region to an annulus with circular slits. This was extended by Kokkinos [142] to a unified method which includes several types of mappings to slit regions, in particular the mapping of an unbounded m -connected region to the exterior of a circle with $m - 1$ concentric circular slits. The boundary of G is assumed to consist of piecewise analytic Jordan curves. For a good convergence it is essential to include “singular basis functions” which reflect the behavior of the conformal mapping near the corners (see also Section 3.2).

A useful tool for multiply-connected regions is the *Ahlfors map* which is defined as follows: Let G be an m -connected bounded region with C^2 boundary and $a \in G$. Then the Ahlfors map f_a for G at a is the uniquely defined analytic function which solves the problem: f maps G into the unit disk D , is analytic in G , $f(a) = 0$, $f'(a)$ is real and $f'(a)$ is maximum. The mapping f_a is an m -to-one branched covering map of G to D . Each boundary component of G is mapped by f_a one-to-one to the unit circle (see Bell [9], Nehari [189, p. 378], Grunsky [89, p. 147]). For $m = 1$ the Ahlfors map f_a agrees with the Riemann mapping function.

Bell [9] uses a relation, discovered by Garabedian [80], between the Ahlfors map and the Szegö kernel function to compute the Ahlfors map numerically by a Kerzman–Stein method. He treats in his book [10] topics like the Riemann mapping theorem, the Ahlfors map, numerical conformal mapping, the Bergman and Szegö kernels and projections, and boundary value problems of potential theory.

The construction of the Bergman or Szegö kernels via orthonormalization of rational functions is not quite easy, and “the results of such numerical nightmares are usually disappointing” (Bell [12, p. 367]). Bell [11] points out that for an m -connected region, the Szegö kernel $S(z, w)$ is a combination of $S(z, a_j)$ at only m points a_j and the Ahlfors map f_a , i.e., of functions of a single variable only. Since the Bergman kernel can be expressed in terms of the Szegö kernel, a similar statement holds for the Bergman kernel (Chung [29]). The basic functions $S(z, a_j)$ are solutions to explicit Kerzman–Stein integral equations and as such, are easy to compute (Bell [12]). The Ahlfors map can also be calculated by this type of equations. The coefficients of the expressions $S(z, a_j)\overline{S(z, a_k)}$ are obtained by simple algebra.

DeLillo et al. [42] describe a Fornberg-type method for the mapping of an unbounded circular domain to an unbounded multiply-connected region. The formulation in [42] is asymmetric insofar as the curves Γ_1 and Γ_2 are treated differently from the other curves. The method could probably be simplified by using a symmetric formulation.

Harrington [99] proved the existence of a conformal mapping of multiply-connected regions to regions with arbitrarily specified boundary shapes. This generalizes results of Courant et al. [31] (see also Gaier [65, p. 183], Courant [32, p. 178]). Harrington’s proof in [99], based on homotopy, is constructive and has been used for the actual calculation of such mappings. But there are apparently no published results.

An asymptotic expansion for the conformal mapping of the multiply-connected domain exterior to some symmetrical thin regions to the slitted plane has been calculated by Homemcovschi [112].

References

- [1] L.V. Ahlfors, *Remarks on the Neumann–Poincaré integral equation*, Pacific J. Math. **2** (1952), 271–280.
- [2] K. Amano, *A charge simulation method for the numerical conformal mapping of interior, exterior and doubly-connected domains*, J. Comput. Appl. Math. **53** (1994), 353–370.
- [3] K. Amano, *A charge simulation method for numerical conformal mapping onto circular and radial slit domains*, SIAM J. Sci. Comput. **19** (1998), 1169–1187.
- [4] C. Anderson, S.E. Christiansen, O. Møller and H. Tornhave, *Conformal Mapping*, Selected Numerical Methods, C. Gram, ed., Regnecentralen, Copenhagen (1962).
- [5] C. Anderson and M. Dillon Daleh, *Rapid computation of the discrete Fourier transform*, SIAM J. Sci. Comput. **17** (1996), 913–919.
- [6] K.E. Atkinson, *The numerical solution of boundary integral equations*, The State of the Art in Numerical Analysis, I.S. Duff et al., eds, Oxford, Clarendon Press (1997), 223–259.
- [7] P.D. Banzuri, *On the Riemann–Hilbert-problem for doubly connected domains*, Soobshch. Akad. Nauk Gruzin. SSR (1975), 549–552 (in Russian, English summary).
- [8] R.S. Baty and P.J. Morris, *Conformal grid generation for high aspect ratio simply and doubly connected regions*, Internat. J. Numer. Methods Engrg. **38** (1995), 3817–3830.
- [9] S. Bell, *Numerical computation of the Ahlfors map of a multiply connected planar domain*, J. Math. Anal. Appl. **120** (1986), 211–217.
- [10] S.R. Bell, *The Cauchy Transform, Potential Theory, and Conformal Mapping*, CRC Press, Boca Raton, FL (1992).
- [11] S. Bell, *Complexity of the classical kernel functions of potential theory*, Indiana Univ. Math. J. **44** (1995), 1337–1369.
- [12] S. Bell, *Recipes for classical kernel functions associated to a multiply connected domain in the plane*, Complex Var. **29** (1996), 367–378.
- [13] S. Bergman(n), *Über die Entwicklung der harmonischen Funktionen der Ebene und des Raumes nach Orthogonalfunktionen*, Math. Ann. **86** (1922), 238–271.
- [14] S. Bergman, *The Kernel Function and Conformal Mapping*, Math. Surveys 5, Amer. Math. Soc., New York (1950).
- [15] S. Bergman and B. Chalmers, *A procedure for conformal mapping of triply-connected domains*, Math. Comp. **21** (1967), 527–542.
- [16] H. Bergström, *An approximation of the analytic function mapping a given domain inside or outside the unit circle*, Mém. Publ. Soc. Sci. Arts Lettr. Hainaut (1958), 193–198.
- [17] J.-P. Berrut, *A Fredholm integral equation of the second kind for conformal mapping*, J. Comput. Appl. Math. **14** (1986), 99–110.
- [18] J.-P. Berrut and M.R. Trummer, *Equivalence of Nyström's method and Fourier methods for the numerical solution of Fredholm integral equations*, Math. Comp. **48** (1987), 617–623.
- [19] G. Beylkin, *On the fast Fourier transform of functions with singularities*, Appl. Comput. Harmon. Anal. **2** (1995), 363–381.
- [20] L. Bieberbach, *Zur Theorie und Praxis der konformen Abbildung*, Rend. Circ. Mat. Palermo **38** (1914), 98–112.
- [21] F. Bissopp, *Numerical conformal mapping and analytic continuation*, Quarterly Appl. Math. **41** (1983), 125–142.
- [22] H. Braß, *Zur numerischen Berechnung konjugierter Funktionen*, Numer. Meth. Approx. Theory, Vol. 6, L. Collatz, G. Meinardus, H. Werner, eds, Birkhäuser, Basel (1982), 43–66.
- [23] J. Burbea, *A procedure, for conformal maps of simply connected domains by using the Bergman function*, Math. Comp. **24** (1970), 821–829.
- [24] J. Burbea, *A numerical determination of the modulus of doubly connected domains by using the Bergman curvature*, Math. Comp. **25** (1971), 743–756.
- [25] G.F. Carey and A. Muleshkov, *Some conformal map constructs for numerical grids*, Comm. Numer. Methods Engrg. **11** (1995), 127–135.
- [26] N.V. Challis and D.M. Burley, *A numerical method for conformal mapping*, IMA J. Numer. Anal. **2** (1982), 169–181.

- [27] S. Chakravarty and D. Anderson, *Numerical conformal mapping*, Math. Comp. **33** (1979), 953–969.
- [28] S. Christiansen, *Condition number of matrices derived from two classes of integral equations*, Math. Methods Appl. Sci. **3** (1981), 364–392.
- [29] Y.-B. Chung, *An expression of the Bergman kernel function in terms of the Szegö kernel*, J. Math. Pures Appl. **75** (1996), 1–7.
- [30] J.W. Cooley and J.W. Tukey, *An algorithm for the machine calculation of complex Fourier series*, Math. Comp. **19** (1965), 297–301.
- [31] R. Courant, B. Manel and M. Shiffman, *A general theorem on conformal mapping of multiply connected domains*, Proc. Natl. Acad. Sci. USA **26** (1940), 503–507.
- [32] R. Courant, *Dirichlet's Principle, Conformal Mapping, and Minimal Surfaces*, Interscience, New York (1950).
- [33] J.H. Curtiss, *Solution of the Dirichlet problem by interpolating harmonic polynomials*, Bull. Amer. Math. Soc. **68** (1962), 333–337.
- [34] T.K. DeLillo, *On some relations among numerical conformal mapping methods*, J. Comput. Appl. Math. **19** (1987), 363–377.
- [35] T.K. DeLillo, *A note on Rengel's inequality and the crowding phenomenon in conformal mapping*, Appl. Math. Lett. **3** (1990), 25–27.
- [36] T.K. DeLillo, *On the use of numerical conformal mapping methods in solving boundary value problems for the Laplace equation*, Adv. Comp. Methods Partial Differential Equations **7** (1992), 190–194.
- [37] T.K. DeLillo, *The accuracy of numerical conformal mapping methods: A survey of examples and results*, SIAM J. Numer. Anal. **31** (1994), 788–812.
- [38] T.K. DeLillo and A.R. Elcrat, *A comparison of some numerical conformal mapping methods for exterior regions*, SIAM J. Sci. Stat. Comput. **12** (1991), 399–422.
- [39] T.K. DeLillo and A.R. Elcrat, *A Fornberg-like conformal mapping method for slender regions*, J. Comput. Appl. Math. **46** (1993), 49–64.
- [40] T.K. DeLillo and A.R. Elcrat, *Numerical conformal mapping methods for exterior regions with corners*, J. Comput. Phys. **108** (1993), 199–208.
- [41] T.K. DeLillo, A.R. Elcrat and J.A. Pfaltzgraff, *Numerical conformal mapping methods based on Faber series*, J. Comput. Appl. Math. **83** (1997), 205–236.
- [42] T.K. DeLillo, M.A. Horn and J.A. Pfaltzgraff, *Numerical conformal mapping of multiply connected regions by Fornberg-like methods*, Numer. Math. **83** (1999), 205–230.
- [43] T.K. DeLillo and J.A. Pfaltzgraff, *Extremal distance, harmonic measure and numerical conformal mapping*, J. Comput. Appl. Math. **46** (1993), 103–113.
- [44] T.K. DeLillo and J.A. Pfaltzgraff, *Numerical conformal mapping methods for simply and doubly connected regions*, SIAM J. Sci. Comput. **19** (1998), 155–171.
- [45] B. Dittmar, *Bemerkungen zu einem Funktional von M. Schiffer und N.S. Hawley in der Theorie konformer Abbildungen*, Math. Nachr. **97** (1980), 21–37.
- [46] T.A. Driscoll, *A nonoverlapping domain decomposition method for Symm's equation for conformal mapping*, SIAM J. Numer. Anal. **36** (1999), 922–934.
- [47] T.A. Driscoll and L.N. Trefethen, *Schwarz–Christoffel Mapping*, Cambridge University Press, Cambridge (2002).
- [48] L.E. Dundučenko, *On the Riemann–Hilbert problem for a multiply connected domain*, Soviet Math. Dokl. **12** (1971), 34–37.
- [49] A. Dutt and V. Rokhlin, *Fast Fourier transforms for nonequispaced data*, SIAM J. Sci. Comput. **14** (1993), 1368–1393.
- [50] S.W. Ellacott, *A technique for approximate conformal mapping*, Multivariate Approximation (Sympos. Durham 1977), Academic Press, London (1978), 301–314.
- [51] S.W. Ellacott, *On the approximate conformal mapping of multiply connected domains*, Numer. Math. **33** (1979), 437–446.
- [52] J. Elschner and E.P. Stephan, *A discrete collocation method for Symm's integral equation on curves with corners*, J. Comput. Appl. Math. **75** (1996), 131–146.
- [53] J. Elschner and I.G. Graham, *Quadrature methods for Symm's integral equation on polygons*, IMA J. Numer. Anal. **17** (1997), 643–664.

- [54] V. Erohin, *On the theory of conformal and quasiconformal mapping of multiply connected regions*, Dokl. Akad. Nauk SSSR **127** (1959), 1155–1157 (in Russian).
- [55] M.I. Falcão, N. Papamichael and N.S. Stylianopoulos, *Curvilinear crosscuts of subdivision for a domain decomposition method in numerical conformal mapping*, J. Comput. Appl. Math. **106** (1999), 177–196.
- [56] M.I. Falcão, N. Papamichael and N.S. Stylianopoulos, *Approximating the conformal maps of elongated quadrilaterals by domain decomposition*, Constr. Approx. **17** (2001), 589–617.
- [57] P.F. Fil'čakov, *Approximate Methods of Conformal Mapping*, Naukova Dumka, Kiev (1964) (in Russian).
- [58] V.P. Fil'čakova, *Conformal Mappings of Domains of Special Type*, Naukova Dumka, Kiev (1972) (in Russian).
- [59] J.M. Floryan and C. Zemach, *Schwarz–Christoffel mappings: A general approach*, J. Comput. Phys. **72** (1987), 347–371.
- [60] J.M. Floryan and C. Zemach, *On the generalized Schwarz–Christoffel mappings and their numerical implementation*, Z. Angew. Math. Mech. **69** (1989), T75–T77.
- [61] J.M. Floryan and C. Zemach, *Schwarz–Christoffel methods for conformal mapping of regions with a periodic boundary*, J. Comput. Appl. Math. **46** (1/2) (1993), 77–102.
- [62] B. Fornberg, *A numerical method for conformal mappings*, SIAM J. Sci. Stat. Comput. **1** (1980), 386–400.
- [63] B. Fornberg, *A numerical method for conformal mapping of doubly connected regions*, SIAM J. Sci. Stat. Comput. **5** (1984), 771–783.
- [64] M.S. Friberg, *A new method for the effective determination of conformal maps*, Thesis, Univ. Minnesota (1951).
- [65] D. Gaier, *Konstruktive Methoden der konformen Abbildung*, Springer, Berlin (1964).
- [66] D. Gaier, *Ermittlung des konformen Moduls von Vierecken mit Differenzenmethoden*, Numer. Math. **19** (1972), 179–194.
- [67] D. Gaier, *Ableitungsreie Abschätzungen bei trigonometrischer Interpolation und Konjugierten-Bestimmung*, Computing **12** (1974), 145–148.
- [68] D. Gaier, *Integralgleichung erster Art und konforme Abbildung*, Math. Z. **147** (1976), 113–129.
- [69] D. Gaier, *Konforme Abbildung mehrfach zusammenhängender Gebiete*, Jahresber. Deutsch. Math.-Ver. **81** (1978), 25–44.
- [70] D. Gaier, *Das logarithmische Potential und die konforme Abbildung mehrfach zusammenhängender Gebiete*, The Influence of His Work on Mathematics and the Physical Sciences, P.L. Butzer, E.B. Christoffel and F. Feher, eds, Birkhäuser, Basel (1981), 290–303.
- [71] D. Gaier, *Numerical methods in conformal mapping*, Computational Aspects of Complex Analysis, H. Werner et al., eds, Reidel, Boston (1983), 51–78.
- [72] D. Gaier, *On a polynomial lemma of Andrievskii*, Arch. Math. **49** (1987), 119–123.
- [73] D. Gaier, *On the convergence of the Bieberbach polynomials in regions with piecewise analytic boundary*, Arch. Math. **58** (1992), 462–470.
- [74] D. Gaier, *Conformal mapping of analytic corners in a generalized sense*, Analysis **12** (1992), 187–193.
- [75] D. Gaier, *Conformal modules and their computation*, Computational Methods and Function Theory, Penang, Malaysia (1994), 159–171.
- [76] D. Gaier, *Polynomial approximation of conformal maps*, Constr. Approx. **14** (1998), 27–40.
- [77] D. Gaier and W.K. Hayman, *Modules of long quadrilaterals and thick ring domains*, Rend. Mat. Appl. **10** (1990), 809–834.
- [78] D. Gaier and W. Hayman, *On the computation of modules of long quadrilaterals*, Constr. Approx. **7** (1991), 453–467.
- [79] D. Gaier and N. Papamichael, *On the comparison of two numerical methods for conformal mapping*, IMA J. Numer. Anal. **7** (1987), 261–282.
- [80] P. Garabedian, *Schwarz's lemma and the Szegö kernel function*, Trans. Amer. Math. Soc. **67** (1949), 1–35.
- [81] I.E. Garrick, *Potential flow about arbitrary biplane wing sections*, NACA Report 542 (1936).
- [82] W. Gautschi, *Attenuation factors in practical Fourier analysis*, Numer. Math. **18** (1972), 373–400.
- [83] G. Gillot, *Calcule numérique de la transformation conforme faisant correspondre l'intérieur d'un cercle à l'intérieur d'une courbe fermée*, C. R. Acad. Sci. Paris **262** (1966), 1243–1246.
- [84] G.M. Goluzin, *Geometric Theory of Functions of a Complex Variable*, 2nd edn, Amer. Math. Soc., Providence, RI (1969).

- [85] I.G. Graham and K.E. Atkinson, *On the Sloan iteration applied to integral equations of the first kind*, IMA J. Numer. Anal. **13** (1993), 29–41.
- [86] E. Grassmann, *Numerical experiments with a method of successive approximation for conformal mapping*, J. Appl. Math. Phys. (ZAMP) **30** (1979), 873–884.
- [87] A.Z. Grinshpan and E.B. Saff, *Estimating the argument of approximate conformal mappings*, Complex Var. **26** (1994), 191–202.
- [88] H. Grötzsch, *Über das Parallelschlitztheorem der konformen Abbildung schlichter Bereiche*, Ber. Verh. Sächs. Akad. Wiss. Leipzig Math.-Phys. Kl. **84** (1932), 15–36.
- [89] H. Grunsky, *Lectures on Theory of Functions in Multiply Connected Domains*, Vandenhoeck & Ruprecht, Göttingen (1978).
- [90] M.H. Gutknecht, *Existence of a solution to the discrete Theodorsen equation for conformal mappings*, Math. Comp. **31** (1977), 478–480.
- [91] M.H. Gutknecht, *Fast algorithms for the conjugate periodic function*, Computing **22** (1979), 79–91.
- [92] M.H. Gutknecht, *Solving Theodorsen's integral equation for conformal maps with the fast Fourier transform and various nonlinear iterative methods*, Numer. Math. **36** (1981), 405–429.
- [93] M.H. Gutknecht, *On the computation of the conjugate trigonometric rational function and on a related splitting problem*, SIAM J. Numer. Anal. **20** (1983), 1198–1205.
- [94] M.H. Gutknecht, *Numerical experiments on solving Theodorsen's integral equation for conformal maps with the fast Fourier transform and various nonlinear iterative methods*, SIAM J. Sci. Stat. Comput. **4** (1983), 1–30.
- [95] M.H. Gutknecht, *Numerical conformal mapping methods based on function conjugation*, J. Comput. Appl. Math. **14** (1986), 31–77.
- [96] N.D. Halsey, *Potential flow analysis of multielement airfoils using conformal mapping*, AIAA J. **17** (1979), 1281–1288.
- [97] N.D. Halsey, *Comparison of the convergence characteristics of two conformal mapping methods*, AIAA J. **20** (1982), 724–726.
- [98] J. Hammerschick, *Über die diskrete Form der Integralgleichungen von Garrick zur konformen Abbildung von Ringgebieten*, Mitt. Math. Sem. Giessen **70** (1966).
- [99] A.N. Harrington, *Conformal mappings onto domains with arbitrarily specified boundary shapes*, J. Anal. Math. **41** (1982), 39–53.
- [100] M. Hartmann and G. Opfer, *Uniform approximation as a numerical tool for constructing conformal maps*, J. Comput. Appl. Math. **14** (1986), 193–206.
- [101] J.K. Hayes, D.K. Kahaner and R.G. Kellner, *An improved method for numerical conformal mapping*, Math. Comp. **26** (1972), 327–334.
- [102] J.K. Hayes, D.K. Kahaner and R.G. Kellner, *A numerical comparison of integral equations of the first and second kind for conformal mapping*, Math. Comp. **29** (1975), 512–521.
- [103] P. Henrici, *Einige Anwendungen der schnellen Fouriertransformation*, Int. Ser. Numer. Math. **32** (1976), 111–124.
- [104] P. Henrici, *Fast Fourier methods in computational complex analysis*, SIAM Rev. **21** (1979), 481–527.
- [105] P. Henrici, *Pointwise error estimates for trigonometric interpolation and conjugation*, J. Comput. Appl. Math. **8** (1982), 131–132.
- [106] P. Henrici, *A general theory of osculation algorithms for conformal mapping*, Linear Algebra Appl. **52/53** (1983), 361–382.
- [107] P. Henrici, *Applied and Computational Complex Analysis*, Vol. 3, Wiley, New York (1986).
- [108] R. Hofmann, *Zur punktweisen konformen Abbildung unter Verwendung des harmonischen Maßes*, Beiträge Numer. Math. **1** (1974), 57–60.
- [109] H.P. Hoidn, *Osculation methods for the conformal mapping of doubly connected regions*, J. Appl. Math. Phys. (ZAMP) **33** (1982), 640–651.
- [110] H.P. Hoidn, *A reparametrisation method to determine conformal maps*, J. Comput. Appl. Math. **14** (1986), 155–161.
- [111] D. Homemcovschi, *Conformal mapping of the domain exterior to a thin region*, SIAM J. Math. Anal. **10** (1979), 1246–1257.
- [112] D. Homemcovschi, *Conformal mapping of multiply connected domains exterior to thin regions*, Z. Angew. Math. Phys. **33** (1982), 503–511.

- [113] D.M. Hough, *User's Guide of CONFPACK*, IPS Research Report 90-11, ETH, Zürich (1990).
- [114] D.M. Hough, J. Levesley and S.N. Chandler-Wilde, *Numerical conformal mapping via Chebyshev weighted solutions of Symm's integral equation*, J. Comput. Appl. Math. **46** (1993), 29–48.
- [115] D.M. Hough and N. Papamichael, *The use of splines and singular functions in an integral equation method for conformal mapping*, Numer. Math. **37** (1981), 133–147.
- [116] D.M. Hough and N. Papamichael, *An integral equation method for the numerical conformal mapping of interior, exterior and doubly-connected domains*, Numer. Math. **41** (1983), 287–307.
- [117] O. Hübner, *Funktionentheoretische Iterationsverfahren zur konformen Abbildung ein- und mehrfach zusammenhängender Gebiete*, Mitt. Math. Sem. Giessen **63** (1964).
- [118] O. Hübner, *Die Faktorisierung konformer Abbildungen und Anwendungen*, Math. Z. **92** (1966), 95–109.
- [119] O. Hübner, *Zur Numerik der Theodorsenschen Integralgleichung in der konformen Abbildung*, Mitt. Math. Sem. Giessen **140** (1979), 1–32.
- [120] O. Hübner, *Über die Anzahl der Lösungen der diskreten Theodorsen-Gleichung*, Numer. Math. **39** (1982), 195–204.
- [121] O. Hübner, *Über die Existenz einer Lösung der diskreten Theodorsen-Gleichung in der Nähe der Restriktion der Ränderzuordnungsfunktion*, Mitt. Math. Sem. Giessen **175** (1986), 27–42.
- [122] O. Hübner, *On the fast solution of a linear system arising in numerical conformal mapping*, J. Comput. Appl. Math. **16** (1986), 381–386.
- [123] O. Hübner, *The Newton method for solving the Theodorsen integral equation*, J. Comput. Appl. Math. **14** (1986), 19–30.
- [124] T. Inoue, *Algorithm for computing an inverse function of a conformal mapping by fundamental solution method*, Trans. Inform. Process. Soc. Japan **38** (1997), 377–379.
- [125] T. Inoue, *New charge simulation method for numerical conformal mapping of ring domains*, Japan J. Industr. Appl. Math. **14** (1997), 295–301.
- [126] T. Inoue, *Theoretical consideration of charge simulation method for numerical conformal mappings in a ring domain*, Int. J. Math. Math. Sci. **21** (1998), 289–298.
- [127] T. Inoue, *Numerical conformal mappings of the domain whose outer boundary is a unit circle*, Japan J. Industr. Appl. Math. **19** (2002), 249–256.
- [128] V.I. Ivanov and M.K. Trubetskoy, *Handbook of Conformal Mapping with Computer-Aided Visualization* (with 1 IBM-PC floppy disk), CRC Press, Boca Raton, FL (1995).
- [129] D.C. Ives, *A modern look at conformal mapping including multiply connected regions*, AIAA J. **14** (1976), 1006–1011.
- [130] R.M. James, *A new look at two-dimensional incompressible airfoil theory*, Report MDC-J0918/01, Douglas Aircraft Company (1971).
- [131] A. Kaiser, *L^∞ -Konvergenz verschiedener Verfahren der sukzessiven Konjugation zur Berechnung konformer Abbildungen*, Dissertation, ETH, Zürich (1986).
- [132] L.W. Kantorowitsch and W.I. Krylow, *Approximation Methods in Higher Analysis*, Interscience, New York (1958).
- [133] N. Kerzman and E.M. Stein, *The Cauchy kernel, the Szegö kernel, and the Riemann mapping function*, Math. Ann. **236** (1978), 85–93.
- [134] N. Kerzman and M.R. Trummer, *Numerical conformal mapping via the Szegö kernel*, J. Comput. Appl. Math. **14** (1986), 111–123.
- [135] W. Kleiner, *Sur l'approximation de la représentation conforme par la méthode des points extrémaux de M. Leja*, Ann. Polon. Math. **14** (1964), 131–140.
- [136] M.E. Klonowska and W.J. Prosnak, *On an effective method for conformal mapping of multiply connected domains*, Acta Mech. **119** (1996), 35–52.
- [137] H. Kober, *Dictionary of Conformal Representations*, Pover Publication, New York (1952).
- [138] P. Koebe, *Über die konforme Abbildung mehrfach zusammenhängender ebener Bereiche, insbesondere solcher Bereiche, deren Begrenzung von Kreisen gebildet wird*, Jahresber. Deutsch. Math.-Verein. **15** (1906), 142–153.
- [139] P. Koebe, *Über die konforme Abbildung mehrfach zusammenhängender Bereiche*, Jahresber. Deutsch. Math.-Verein. **19** (1910), 339–348.
- [140] P. Koebe, *Über eine neue Methode der konformen Abbildung und Uniformisierung*, Nachr. Kgl. Ges. Wiss. Göttingen Math.-Phys. Kl. (1912), 844–848.

- [141] P. Koebe, *Abhandlung zur Theorie der konformen Abbildung: V. Abbildung mehrfach zusammenhängender schlichter Bereiche auf Schlitzbereiche*, Math. Z. **2** (1919), 198–236.
- [142] C.A. Kokkinos, *A unified orthonormalization method for the approximate conformal mapping of simply and multiply-connected domains*, Proc. CMFT Conference, Nicosia, 1997, N. Papamichael et al., eds, (1999), 327–344.
- [143] C.A. Kokkinos, N. Papamichael and A.B. Sideridis, *An orthonormalization method for the approximate conformal mapping of multiply-connected domains*, IMA J. Numer. Anal. **9** (1990), 343–359.
- [144] Y. Komatu, *Ein alternierendes Approximationsverfahren fuer konforme Abbildung von einem Ringgebiete auf einen Kreisring*, Proc. Japan Acad. **21** (1945), 146–155 (1949).
- [145] W. von Koppenfels and F. Stallmann, *Praxis der konformen Abbildung*, Springer-Verlag, Berlin-Göttingen-Heidelberg (1959).
- [146] Z. Kosma, *On an algorithm for conformal mapping of plane multiply-connected domains*, Bull. Pol. Acad. Sci. **35** (1987), 41–52.
- [147] W. Krabs und G. Opfer, *Eine Methode zur Lösung des komplexen Approximationsproblems mit einer Anwendung auf konforme Abbildungen*, Z. Angew. Math. Mech. **55** (1975), T208–T211.
- [148] R. Kreß, *Über die numerische Berechnung konjugierter Funktionen*, Computing **10** (1972), 177–187.
- [149] P.A. Krutitskii, *Equivalence of the problem of the directional derivative and the Riemann–Hilbert problem*, Differ. Equ. **28** (1992), 698–707.
- [150] R. Kühnau, *Numerische Realisierung konformer Abbildungen durch Interpolation*, Z. Angew. Math. Mech. **63** (1983), 631–637.
- [151] U. Kulisch, *Ein Iterationsverfahren zur konformen Abbildung des Einheitskreises auf einen Stern*, Z. Angew. Math. Mech. **43** (1963), 403–410.
- [152] P.K. Kythe, *Computational Conformal Mapping*, Birkhäuser, Boston (1998).
- [153] H. Lamb, *Hydrodynamics*, 6th edn, Cambridge University Press, Cambridge (1993).
- [154] L. Landweber and T. Miloh, *Elimination of corners in the mapping of a closed curve*, J. Engrg. Math. **6** (1972), 369–375.
- [155] M. Lanza de Cristoforis, *A note on conformal representation in Sobolev spaces*, Complex Var. **20** (1992), 121–133.
- [156] R. Laugesen, *Conformal mapping of long quadrilaterals and thick doubly connected domains*, Constr. Approx. **10** (1994), 523–554.
- [157] V.I. Lavrik and V.N. Savenkov, *A Handbook on Conformal Mappings*, Naukova Dumka, Kiev (1970) (in Russian).
- [158] M.A. Lawrentjew und B.W. Schabat, *Methoden der komplexen Funktionentheorie*, VEB Deutscher Verlag der Wissenschaften, Berlin (1967).
- [159] B. Lee and M.R. Trummer, *Multigrid conformal mapping via the Szegő kernel*, Electron. Trans. Numer. Anal. **2** (1994), 22–43.
- [160] R.S. Lehman, *Development of the mapping function at an analytic corner*, Pacific J. Math. **7** (1957), 1437–1449.
- [161] F. Leja, *Sur certaines suites liées aux ensembles plans et leur application à la représentation conforme*, Ann. Polon. Math. **4** (1957), 8–13.
- [162] F.D. Lesley, *Hölder continuity of conformal mappings at the boundary via the strip method*, Indiana Univ. Math. J. **31** (1982), 341–354.
- [163] J. Levesley, D.M. Hough and S.N. Chandler-Wilde, *A Chebyshev collocation method for solving Symm's integral equation for conformal mapping: A partial error analysis*, IMA J. Numer. Anal. **14** (1993), 57–79.
- [164] D. Levin, N. Papamichael and A. Sideridis, *The Bergman kernel method for the numerical conformal mapping of simply connected domains*, J. Inst. Math. App. **22** (1978), 171–187.
- [165] B.C. Li and S. Syngellakis, *Numerical conformal mapping based on the generalised conjugation operator*, Math. Comp. **67** (1998), 619–639.
- [166] I. Lind, *Some problems related to iterative methods in conformal mapping*, Ark. Mat. **7** (1967), 101–143.
- [167] M.V. Lotfullin, *A numerical method of conformal mapping of simply connected domains*, Trudy Sem. Kraev. Zadacham **22** (1985), 148–151 (in Russian).
- [168] P. Luchini and F. Manzo, *Flow around simply and multiply connected bodies: A new iterative scheme for conformal mapping*, AIAA J. **27** (1989), 345–351.

- [169] P. Luchini and F. Manzo, *A fast conformal mapping algorithm with no FFT*, J. Comput. Phys. **101** (1992), 368–374.
- [170] D.E. Marshall and S. Rohde, *The Loewner differential equation and slit mappings*, Preprint (2003).
- [171] V.V. Maymeskul, E.B. Saff and N.S. Stylianopoulos, *L^2 -approximation of power and logarithmic functions with applications to numerical conformal mapping*, Numer. Math. **91** (2002), 503–542.
- [172] A. Mayo, *The fast solution of Poisson's and the biharmonic equations on irregular regions*, SIAM J. Numer. Anal. **21** (1984), 285–299.
- [173] A. Mayo, *Rapid methods for the conformal mapping of multiply connected regions*, J. Comput. Appl. Math. **14** (1986), 143–153.
- [174] W. McLean, *A spectral Galerkin method for a boundary integral equation*, Math. Comp. **47** (1986), 597–607.
- [175] D.I. Meiron, S.A. Orszag and M. Israeli, *Applications of numerical conformal mapping*, J. Comput. Phys. **40** (1981), 345–360.
- [176] R. Menikoff and C. Zemach, *Methods for numerical conformal mapping*, J. Comput. Phys. **36** (1980), 366–410.
- [177] K. Menke, *Extremalpunkte und konforme Abbildung*, Math. Ann. **195** (1972), 292–308.
- [178] K. Menke, *Bestimmung von Näherungen für die konforme Abbildung mit Hilfe von stationären Punktsystemen*, Numer. Math. **22** (1974), 111–117.
- [179] K. Menke, *Point systems with extremal properties and conformal mapping*, Numer. Math. **54** (1988), 125–143.
- [180] K. Menke, *Conformal mapping of doubly connected regions*, Complex Var. **14** (1990), 251–260.
- [181] S.G. Mikhlin, *Integral Equations and Their Applications*, Pergamon Press, New York (1957).
- [182] H. Mizumoto and H. Hara, *Determination of the moduli of ring domains by finite element methods*, Int. J. Differential Equations Appl. **3** (2001), 325–337.
- [183] G. Monegato and L. Scuderi, *Global polynomial approximation for Symm's equation on polygons*, Numer. Math. **86** (2000), 655–683.
- [184] G. Moretti, *Orthogonal grids around difficult bodies*, AIAA J. **30** (1992), 933–938.
- [185] A.H.M. Murid, M.Z. Nashed and M.R.M. Razali, *Numerical conformal mapping for exterior regions via the Kerzman–Stein kernel*, J. Integral Equations Appl. **10** (1998), 517–532.
- [186] A.H.M. Murid, M.Z. Nashed and M.R.M. Razali, *Some integral equations related to the Riemann map*, Proc. CMFT Conference, Nicosia, 1997, N. Papamichael et al., eds, (1999), 405–419.
- [187] N.I. Muskhelishvili, *Singular Integral Equations*, Noordhoff, Groningen (1953).
- [188] S.R. Nasyrov and D.A. Fokin, *Proof of the convergence of an approximate method of conformal mapping of the exterior of an airfoil onto the exterior of a disk*, Comput. Methods. Math. Phys. **33** (1993), 1447–1457.
- [189] Z. Nehari, *Conformal Mapping*, McGraw-Hill, New York (1952).
- [190] J. von Neumann, *Functional Operators, Vol II. The Geometry of Orthogonal Spaces*, Ann. of Math. Stud., Vol. 22, Princeton Univ. Press (1950).
- [191] W. Niethammer, *Iterationsverfahren bei der konformen Abbildung*, Computing **1** (1966), 146–153.
- [192] J.L. Nieto, J. Hureau and M. Mudry, *A general method for practical conformal mapping of aerodynamic shapes*, Eur. J. Mech. B Fluids **10** (1991), 147–160.
- [193] J.A. Nitsche, *Finite-element methods for conformal mapping*, SIAM J. Numer. Anal. **26** (1989), 1525–1533.
- [194] S.T. O'Donnell and V. Rokhlin, *A fast algorithm for the numerical evaluation of conformal mappings*, SIAM J. Sci. Stat. Comput. **10** (1989), 475–487.
- [195] H. Ogata, D. Okano and K. Amano, *Numerical conformal mapping of periodic structure domains*, Japan J. Industr. Appl. Math. **19** (2002), 257–275.
- [196] D. Okano, H. Ogata and K. Amano, *A method of numerical conformal mapping of curved slit domains by the charge simulation method*, J. Comput. Appl. Math. **152** (2003), 441–450.
- [197] G. Opfer, *Die Bestimmung des Moduls zweifach zusammenhängender Gebiete mit Hilfe von Differenzverfahren*, Arch. Ration. Mech. Anal. **32** (1969), 281–297.
- [198] G. Opfer, *Über einige Approximationsprobleme im Zusammenhang mit konformen Abbildungen*, L. Collatz and G. Meinardus, eds, Numer. Meth. der Approximationstheorie **1** (1972), 93–116.
- [199] G. Opfer, *Konforme Abbildung und ihre numerische Behandlung*, Überbl. Math. **7** (1974), 33–113.

- [200] G. Opfer, *Ueber die Approximation der Identität im Komplexen*, Numer. Meth. der Approximationstheorie **2** (1975), 93–100.
- [201] G. Opfer, *New extremal properties for constructing conformal mappings*, Numer. Math. **32** (1979), 423–429.
- [202] G. Opfer, *Conformal mappings onto prescribed regions via optimization techniques*, Numer. Math. **35** (1980), 189–200.
- [203] G. Opitz, *Zur Konvergenz bei genäherter konformer Abbildung*, Z. Angew. Math. Mech. **30** (1950), 337–346.
- [204] J.M. Ortega and W.C. Rheinboldt, *Iterative Solution of Nonlinear Equations in Several Variables*, Academic Press, New York (1970).
- [205] A.M. Ostrowski, *Math. Miszellen XV: Zur konformen Abbildung einfach zusammenhängender Gebiete*, Jahresber. Deutsch. Math.-Verein. **38** (1929), 168–182.
- [206] A.M. Ostrowski, *On the convergence of Theodorsen's and Garrick's method of conformal mapping*, Nat. Bur. Standards Appl. Mat. Ser. **18** (1952), 149–163.
- [207] N. Papamichael, *Numerical conformal mapping onto a rectangle with applications to the solution of Laplacian problems*, J. Comput. Appl. Math. **28** (1989), 63–83.
- [208] N. Papamichael and C.A. Kokkinos, *Two numerical methods for the conformal mapping of simply-connected domains*, Comput. Methods Appl. Mech. Engrg. **28** (1981), 285–307.
- [209] N. Papamichael and C.A. Kokkinos, *Numerical conformal mapping of exterior domains*, Comput. Methods Appl. Mech. Engrg. **31** (1982), 189–203.
- [210] N. Papamichael and C.A. Kokkinos, *The use of singular functions for the approximate conformal mapping of doubly-connected domains*, SIAM J. Sci. Stat. Comput. **5** (1984), 684–700.
- [211] N. Papamichael, C.A. Kokkinos and M.K. Warby, *Numerical techniques for conformal mapping onto a rectangle*, J. Comput. Appl. Math. **20** (1987), 349–358.
- [212] N. Papamichael, I.E. Pritsker, E.B. Saff and N.S. Stylianopoulos, *Approximation of conformal mappings of annular regions*, Numer. Math. **76** (1997), 489–513.
- [213] N. Papamichael and E.B. Saff, *Local behaviour of the error in the Bergman kernel method for numerical conformal mapping*, J. Comput. Appl. Math. **46** (1993), 65–75.
- [214] N. Papamichael and N.S. Stylianopoulos, *A domain decomposition method for conformal mapping onto a rectangle*, Constr. Approx. **7** (1991), 349–379.
- [215] N. Papamichael and N.S. Stylianopoulos, *A domain decomposition method for approximating the conformal modules of long quadrilaterals*, Numer. Math. **62** (1992), 213–234.
- [216] N. Papamichael and N.S. Stylianopoulos, *On the theory and application of a domain decomposition method for computing conformal modules*, J. Comput. Appl. Math. **50** (1994), 33–50.
- [217] N. Papamichael and M.K. Warby, *Pole-type singularities and the numerical conformal mapping of doubly-connected domains*, J. Comput. Appl. Math. **10** (1984), 93–106.
- [218] N. Papamichael and M.K. Warby, *Stability and convergence properties of Bergman kernel methods for numerical conformal mapping*, Numer. Math. **48** (1986), 639–669.
- [219] N. Papamichael, M.K. Warby and D.M. Hough, *The determination of the poles of the mapping function and their use in numerical conformal mapping*, J. Comput. Appl. Math. **9** (1983), 155–166.
- [220] N. Papamichael, M.K. Warby and D.M. Hough, *The treatment of corner and pole-type singularities in numerical conformal mapping techniques*, J. Comput. Appl. Math. **14** (1986), 163–191.
- [221] C. Pommerenke, *Polynome und konforme Abbildung*, Monatsh. Math. **69** (1965), 58–61.
- [222] C. Pommerenke, *Über die Verteilung der Fekete-Punkte*, Math. Ann. **168** (1967), 111–127.
- [223] C. Pommerenke, *Über die Verteilung der Fekete-Punkte, II*, Math. Ann. **179** (1969), 212–218.
- [224] C. Pommerenke, *Boundary Behaviour of Conformal Maps*, Springer, Berlin (1992).
- [225] R.M. Porter, *An interpolating polynomial method for numerical conformal mapping*, SIAM J. Sci. Comput. **23** (2001), 1027–1041.
- [226] I.I. Priwalow, *Randeigenschaften analytischer Funktionen*, 2. Auflage, VEB Deutscher Verlag der Wissenschaften, Berlin (1956).
- [227] W.J. Prosnak, *Conformal representation of arbitrary multiconnected airfoil sections*, Bull. Acad. Pol. Sci. **25** (1977), 25–36.
- [228] B.I. Rabinovich and Yu.V. Tyurin, *A recursive numerical method in the conformal mapping of doubly connected regions onto a circular annulus*, Soviet Math. Dokl. **28** (1983), 447–450.

- [229] B.I. Rabinovich and Yu.V. Tyurin, *On a recursive numerical method in conformal mapping*, Soviet Math. Dokl. **28** (1983), 415–418.
- [230] B.I. Rabinovich, Yu.V. Tyurin, A.A. Livshits and A.S. Leviant, *Recursive numerical algorithm for conformal mapping in two-dimensional hydrodynamics*, AIAA J. **34** (1996), 2014–2020.
- [231] M.R.M. Razali, M.Z. Nashed and A.H.M. Murid, *Numerical conformal mapping via the Bergman kernel* J. Comput. Appl. Math. **82** (1997), 333–350.
- [232] M.R.M. Razali, M.Z. Nashed and A.H.M. Murid, *Numerical conformal mapping via the Bergman kernel using the generalized minimum residual method*, Comput. Math. Appl. **40** (2000), 157–164.
- [233] L. Reichel, *On polynomial approximation in the complex plane with application to conformal mapping*, Math. Comp. **44** (1985), 425–433.
- [234] L. Reichel, *A fast method for solving certain integral equations of the first kind with application to conformal mapping*, J. Comput. Appl. Math. **14** (1986), 125–142.
- [235] B. Riemann, *Grundlagen für eine allgemeine Theorie der Functionen einer veränderlichen complexen Grösse*, Gesammelter mathematische Werke und wissenschaftlicher Nachlaß, R. Dedekind und H. Weber, eds, Teubner, Leipzig (1876).
- [236] E.V. Sallinen, *Approximate determination of conformal mappings by means of methods of continuation and the Newton–Raphson method*, Latv. Mat. Ezhegodnik **29** (1985), 236–242 (in Russian).
- [237] S.B. Samli, *Über die Konstruktion von Polynomen, die ein gegebenes Gebiet näherungsweise auf einen Kreis abbilden*, Z. Angew. Math. Mech. **43** (1963), T32–T35.
- [238] J. Saranen and G. Vainikko, *Two-grid solution of Symm's integral equation*, Math. Nachr. **177** (1996), 265–279.
- [239] M. Schiffer and N.S. Hawley, *Connections and conformal mapping*, Acta Math. **107** (1962), 175–274.
- [240] R. Schinzinger and P.A.A. Laura, *Conformal Mapping: Methods and Applications*, Elsevier, Amsterdam (1991).
- [241] A. Seidl and H. Klose, *Numerical conformal mapping of a towel-shaped region onto a rectangle*, SIAM J. Sci. Stat. Comput. **6** (1985), 833–842.
- [242] S. Semmes, *Nonlinear Fourier analysis*, Bull. Amer. Math. Soc. **20** (1989), 1–18.
- [243] M. Skwarczyński, *A general description of the Bergman projection*, Ann. Polon. Math. **46** (1985), 311–315.
- [244] M. Skwarczyński, *Alternating projections in complex analysis*, Compl. Anal. Appl., Varna, 1983, Sofia (1985), 192–199.
- [245] E.J. Song, *Methods for solving Theodorsen's equation in numerical conformal mapping*, Master thesis, Nagoya Univ. (1988).
- [246] E. Song and H. Sugiura, *Automatic numerical conformal mapping based on the Wegmann's method*, Trans. Inform. Proc. Soc. Japan **35** (1994), 309–312 (in Japanese).
- [247] E. Song, H. Sugiura and T. Sakurai, *Analysis of instability and stabilization on Wegmann's method for conformal mapping*, Trans. Inform. Proc. Soc. Japan **32** (1991), 126–132 (in Japanese).
- [248] A.S. Sorokin, *The variational method of M.A. Lavrent'ev and the Hilbert problem for multiply connected circular domains*, Dokl. Math. **54** (1996), 547–550.
- [249] G. Steidl, *A note on fast Fourier transforms for nonequispaced grids*, Adv. Comput. Math. **9** (1998), 337–352.
- [250] F. Stenger and R. Schmidlein, *Conformal maps via Sinc methods*, Proc. CMFT Conf., Nicosia, 1997, N. Papamichael et al., eds, (1999), 505–549.
- [251] H. Sugiura and T. Torii, *Real fast Fourier transform on quasi-equidistant sample points*, J. Inform. Process. **15** (1992), 460–465.
- [252] H. Švecová, *On the Bauer's scaled condition number of matrices arising from approximate conformal mapping*, Numer. Math. **14** (1970), 495–507.
- [253] G.T. Symm, *An integral equation method in conformal mapping*, Numer. Math. **9** (1966), 250–258.
- [254] G.T. Symm, *Numerical mapping of exterior domains*, Numer. Math. **10** (1967), 437–445.
- [255] G.T. Symm, *Conformal mapping of doubly-connected domains*, Numer. Math. **13** (1969), 448–457.
- [256] G. Szegő, *Über orthogonale Polynome, die zu einer gegebenen Kurve der komplexen Ebene gehören*, Math. Z. **9** (1921), 218–270.
- [257] G. Szegő, *On conjugate trigonometric polynomials*, Amer. J. Math. **65** (1943), 532–536.
- [258] T. Theodorsen, *Theory of wing sections of arbitrary shape*, NACA Report 411 (1931).

- [259] T. Theodorsen and I.E. Garrick, *General potential theory of arbitrary wing sections*, NACA Report 452 (1933).
- [260] A.D. Thomas, *Conformal mapping of nonsmooth domains via the Kerzman–Stein integral equation*, J. Math. Anal. Appl. **200** (1996), 162–181.
- [261] J.F. Thompson, Z.U.A. Warsi and C.W. Mastin, *Boundary fitted coordinate systems for numerical solution of partial differential equations – A review*, J. Comput. Phys. **47** (1982), 1–108.
- [262] J.F. Thompson, Z.U.A. Warsi and C.W. Mastin, *Numerical Grid Generation*, North-Holland, Amsterdam (1985).
- [263] R. Timman, *The direct and the inverse problem of airfoil theory: A method to obtain numerical solutions*, Report F 16, Nat. Luchtv. Labor., Amsterdam (1951).
- [264] L.N. Trefethen, *Numerical computation of the Schwarz–Christoffel transformation*, SIAM J. Sci. Stat. Comput. **1** (1980), 82–102.
- [265] L.N. Trefethen, ed., *Numerical Conformal Mapping*, Elsevier, New York (1986).
- [266] M.R. Trummer, *An efficient implementation of a conformal mapping method based on the Szegő kernel*, SIAM J. Numer. Anal. **23** (1986), 853–872.
- [267] A.G. Ugodčikov, *Construction of Functions Yielding Conformal Mappings, by Means of Electro-Modelling and the Lagrange Interpolation Polynomials*, Naukova Dumka, Kiev (1966) (in Russian).
- [268] P.N. Vabishchevich and S.I. Pulatov, *A numerical algorithm for conformal mapping*, Mat. Model. **1** (1989), 132–139 (in Russian).
- [269] I.N. Vekua, *Generalized Analytic Functions*, Pergamon Press, London (1992).
- [270] B.A. Vertgeim, *Approximate construction of some conformal mappings*, Dokl. Akad. Nauk SSSR **119** (1958), 12–14 (in Russian).
- [271] E.A. Volkov, *Block method for solving the Laplace equation and for constructing conformal mappings*, CRC Press, Boca Raton, FL (1994).
- [272] A. Wahl, *Konforme Abbildung durch gebrochene rationale Funktionen*, Z. Angew. Math. Mech. **44** (1964), 397–399.
- [273] S.E. Warschawski, *Über einen Satz von O.D. Kellogg*, Nachr. Ges. Wiss. Gött. **25** (1932), 73–86.
- [274] S.E. Warschawski, *On the higher derivatives at the boundary in conformal mapping*, Trans. Amer. Math. Soc. **38** (1935), 310–340.
- [275] S.E. Warschawski, *On conformal mapping of variable regions*, Nat. Bur. Standards **18** (1952), 175–187.
- [276] S.E. Warschawski, *On a theorem of L. Lichtenstein*, Pacific J. Math. **5** (1955), 835–839.
- [277] S.E. Warschawski, *On the solution of the Lichtenstein–Gershgorin integral equation in conformal mapping: I. Theory*, Nat. Bur. Standards Appl. Math. Ser. **42** (1955), 7–29.
- [278] S.E. Warschawski, *On Hölder continuity at the boundary in conformal maps*, J. Math. Mech. **18** (1968–1969), 423–427.
- [279] E. Wegert, *An iterative method for solving nonlinear Riemann–Hilbert problems*, J. Comput. Appl. Math. **29** (1990), 311–327.
- [280] E. Wegert, *Iterative methods for discrete nonlinear Riemann–Hilbert problems*, J. Comput. Appl. Math. **46** (1993), 143–163.
- [281] E. Wegert, *Nonlinear Riemann–Hilbert problems – history and perspectives*, Proc. CMFT Conf., Nicosia, 1997, N. Papamichael et al., eds, (1999), 583–615.
- [282] R. Wegmann, *Convergence proofs and error estimates for an iterative method for conformal mapping*, Numer. Math. **44** (1984), 435–461.
- [283] R. Wegmann, *Ein Iterationsverfahren zur konformen Abbildung*, Numer. Math. **30** (1978), 453–466; as: *An iterative method for conformal mapping*, Numerical Conformal Mapping, L.N. Trefethen, ed., North-Holland, Amsterdam (1986), 7–18.
- [284] R. Wegmann, *On Fornberg's numerical method for conformal mapping*, SIAM J. Numer. Anal. **23** (1986), 1199–1213.
- [285] R. Wegmann, *An iterative method for the conformal mapping of doubly connected regions*, J. Comput. Appl. Math. **14** (1986), 79–98.
- [286] R. Wegmann, *Discrete Riemann–Hilbert problems, interpolation of simply closed curves, and numerical conformal mapping*, J. Comput. Appl. Math. **23** (1988), 323–352.
- [287] R. Wegmann, *Conformal mapping by the method of alternating projections*, Numer. Math. **56** (1989), 291–307.

- [288] R. Wegmann, *Discretized versions of Newton type iterative methods for conformal mapping*, J. Comput. Appl. Math. **29** (1990), 207–224.
- [289] R. Wegmann, *An estimate for crowding in conformal mapping to elongated regions*, Complex Var. **18** (1992), 193–199.
- [290] R. Wegmann, *Crowding for analytic functions with elongated range*, Constr. Approx. **10** (1994), 179–186.
- [291] R. Wegmann, *Fast conformal mapping of an ellipse to a simply connected region*, J. Comput. Appl. Math. **72** (1996), 101–126.
- [292] R. Wegmann, *Constructive solution of a certain class of Riemann–Hilbert problems on multiply connected circular regions*, J. Comput. Appl. Math. **130** (2001), 139–161.
- [293] R. Wegmann, *Fast conformal mapping of multiply connected regions*, J. Comput. Appl. Math. **130** (2001), 119–138.
- [294] L. von Wolfersdorf, *Zur Unität der Lösung der Theodorsenschen Integralgleichung der konformen Abbildung*, Z. Anal. Anwendg. **3** (1984), 523–526.
- [295] Y. Yan and I.H. Sloan, *On integral equations of the first kind with logarithmic kernels*, J. Integral Equations Appl. **1** (1988), 549–579.
- [296] H. Yoshikawa, *On the conformal mapping of nearly circular domains*, J. Math. Soc. Japan **12** (1960), 174–186.
- [297] C. Zemach, *A conformal map formula for difficult cases*, J. Comput. Appl. Math. **14** (1986), 207–215.